STUDENT REPORT

JUNE 1994

STUDREP.94.030

LONG TERM STATISTICS OF EXTREME ENVIRONMENTAL LOADS ON FIXED OFFSHORE STRUCTURES
Effects of strongly directional currents

by
M. BLOEMSMA
(DELFT UNIVERSITY OF TECHNOLOGY)

This report is intended to document student work.

M. Bloemsma

Afstudeerrapport

Long term statistics of extreme environmental loads on fixed offshore structures

Uitgeleend aan:

Naam:	Datum:	Telnr:
Christian Verhaert	24/06/94	121070.
Bernadette Weber	10/8/94	NB123041

Student Report May 1994

LONG TERM STATISTICS OF EXTREME ENVIRONMENTAL LOADS ON FIXED OFFSHORE STRUCTURES

Effects of strongly directional currents

by

M. Bloemsma

Delft University of Technology
Department of Civil Engineering

KONINKLIJKE/SHELL EXPLORATIE EN PRODUKTIE LABORATORIUM
RIJSWIJK, THE NETHERLANDS

ACKNOWLEDGEMENT

This report is the result of student thesis work performed at Koninklijke/Shell Exploratie and Produktie Laboratorium in Rijswijk.

I found working at KSEPL a very stimulating and interesting experience. I am therefore very pleased to have had this opportunity.

Special thanks should go to my mentors at KSEPL, dr. P.S. Tromans and dr. L. Vanderschuren for the time they spent and effort they took to assist me. Also, I would like to thank the members of the steering committee, prof. dr. ir. J.A. Battjes (chairman of the committee who arranged the first contact with KSEPL), prof. dr. ir. J.H. Vugts and W.W. Massie MSc. P.E. for their support and comments on the draft version of this report.

Last but not least thanks should go to the fellow students with whom I shared an office at KSEPL, Leon "Jackdyn" Harland and Jelle "Gnuplot" van Dam who made the sometimes long working days also good fun.

Mark Bloemsma,

Rijswijk, April 1994.

SUMMARY

The design and re-assessment of fixed offshore structures for operation in the harsh conditions of the North Sea is largely determined by extreme environmental loading. The ability to predict accurately the extreme storm load remains an important factor in the continued safe and economic exploitation of the hydrocarbon reserves in this area.

The problem of specifying met-ocean design conditions (MDC) is one of estimating the environmental variables corresponding to some return period, typically 100 years, on the basis of measured or hindcast time series extending over a relatively short period, say 5 or 25 years.

A new method for deriving met-ocean design conditions has been developed at KSEPL. Statistics are calculated for the whole storm rather than for three-hour intervals. By combining a model, for translating a set of environmental conditions into a structural load, and the environmental parameters for a sea state, statistics can be generated for loads rather than for single environmental parameters. These load statistics are then used in an extrapolation process to extrapolate to rare events. Once an extreme load is derived, a characteristic set of environmental parameters (joint met-ocean conditions) which could have generated this load can be derived via "back calculation". This set of environmental parameters can be used as an input for a more detailed calculation of the distribution of the extreme load over the structure. The new method avoids the shortcomings of existing approaches and is distinguished from them by being equally applicable to the prediction of extreme waves, long term load statistics and joint met-ocean conditions.

Environmental conditions and long term load statistics are directionally sensitive. To account for this phenomenon, the met-ocean data for a location must be divided into sectors, containing the directions from which severe storms are coming. So far, for the North Sea, these sectors have been chosen on the basis of wave height. The resulting sectors are reasonably wide. From the NESS data base, sectors containing severe storms include around 100 storms (sufficient for the subsequent statistical analysis). Storms in a wide sector are assumed to have a uniform distribution over this sector. However, (tidal) current can be much more sensitive to direction than significant wave height, and can influence loads. To resolve the (tidal) current correctly, we would have to reduce sector sizes so much that the number of storms would be too small for a reliable statistical analysis.

It is possible to increase artificially the sample size, by treating the angle between mean wave direction and (tidal) current direction as a parameter that can be varied. All the storms in the wide sectors (based on wave height) can then be used to generate load statistics in narrower sectors (based on current speed). This idea has been implemented within KSEPL methodology in this work. The effects of strongly directional current and artificially increased sample size on load statistics and on a structural reliability are investigated. The data base used for this purpose contains all the relevant environmental parameters for a location in the southern North Sea for a hindcasting period of 25 years. The southern North Sea is selected, because of its relatively high (tidal) current speeds, compared to other areas in the North Sea.

For the example considered the derived extreme met-ocean design conditions and calculated structural reliability are not very sensitive to the effects of a strongly directional current. The extra effort necessary to account for the effect of those strongly directional currents seems therefore, based on the calculations as carried out in this report, not justified. Moreover, since the southern North Sea is the sector of the North Sea with the strongest and most directional currents, it is likely that this result pertains to the whole of the North Sea. However, further work (e.g. calculations for other grid points) may be required to generalise this conclusion.

KEYWORDS

long term load statistics, met-ocean design conditions, strongly directional currents

CONTENTS **Page**

Fig. 1.1; Example of a fixed space frame structure.

1. INTRODUCTION

The design and re-assessment of fixed offshore structures for operation in the harsh conditions of the North Sea is largely determined by extreme environmental loading. The ability to predict accurately the extreme storm load remains an important factor in the continued safe and economic exploitation of the hydrocarbon reserves in this area.

1.1. Offshore structures and extreme loads

Offshore technology has experienced a remarkable growth since the late 1940's, when offshore drilling platforms were first used in the Gulf of Mexico. Nowadays a wide variety of offshore structures is being used. By far the most common type however, is the type of fixed, tubular, space frame structures as illustrated in figure 1.1.

Offshore structures are mainly used for oil and gas recovery, but are also used in other applications such as harbour engineering, ocean energy extraction and so on. Difficulties in design and construction have always challenged the offshore industry, particularly as structures are being located in ever increasing water depths and in extremely hostile environmental conditions. Recent decreases of the oil price and the ever smaller recoverable reserves in newly discovered fields present new challenges to the industry. New structures will have to be designed as cost effective as possible. The fact that many of the new field discoveries are in well developed areas, as the North Sea, allows several of them to be produced as satellite fields. Improvements in the exploitation of hydrocarbon reservoirs have tended to lengthen a field's economic life. To handle with existing infrastructure the oil and gas production from new fields and extended production from fields already producing, old platforms have to be equipped with additional facilities and kept operational beyond their originally intended service life. Careful assessment of the integrity of offshore platforms is of prime importance to maintain safe and economic operations. The environmental load on the structure arises from a combination of waves, currents and wind, though waves are, in general, the dominant factor. The specification of the loads induced in extreme storms is crucial in the design and re-assessment of offshore structures.

1.2. Design conditions

The difficulty in the specification of design values for the met-ocean (meteorological and oceanographic) variables, wave, wind and current, is the major source of uncertainty and conservatism in the present methods of predicting extreme storm loads.

Conventional design practice is still largely empirical. It is based on historical experience, especially that gained in the Gulf of Mexico from 1950 onwards. Figure 1.2 [1] shows the traditional, deterministic approach to the design and re-assessment of offshore structures. A data base containing meteorological and oceanographic conditions (i.e. a "met-ocean" data base) is used to generate separate values for 100 year return period waves and currents. These statistics are used in conjunction with

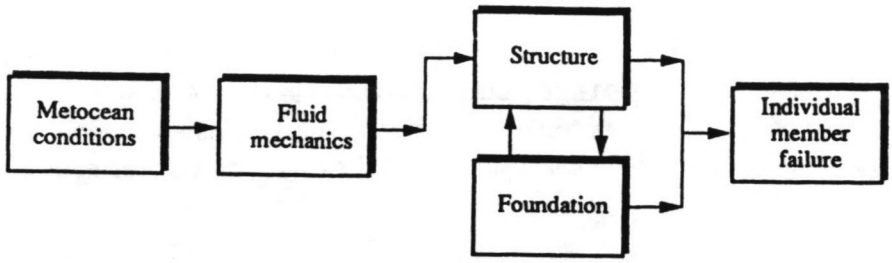

Fig. 1.2; Traditional approach.

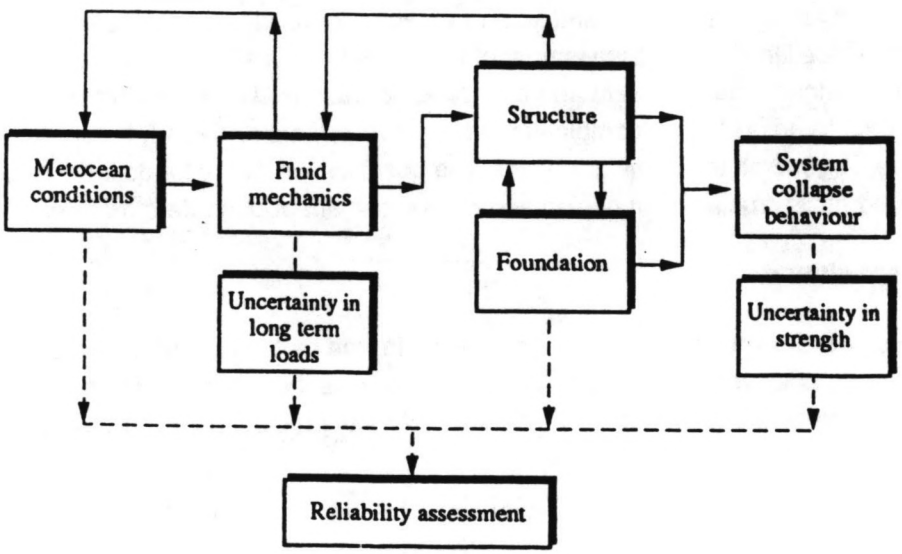

Fig. 1.3; Realistic physical interactions.

regular wave theories to define loads. No account is taken of non-coincidence of extreme waves and currents or the random nature of surface elevation.

A more rational and realistic approach is indicated in figure 1.3 [1]; the full complexity of the real relationships between the boxes involves additional, "feedback"-type interactions. For example, the environment generating the 100 year response of the structure is probably not the combination of 100 year wave and 100 year current, since they are most unlikely to coincide. Rather it must be obtained from the statistics of the extreme response of interest. This depends not only on the environmental conditions but also on the type of structure considered and its behaviour. "State of the art" models for the detailed processes are required in all the boxes in figure 1.3. For loading these are [1]:

- Joint met-ocean conditions. Hindcast (i.e. numerical simulations of) storms in combination with theories for the statistics of the joint occurrence of extreme waves and currents are required to evaluate the joint met-ocean conditions which generate an extreme response.

- Accurate wave and current kinematics. New models have been developed to describe accurately the extreme wave crests and associated kinematics which occur during the random process of a storm in the open sea, and the blockage of current by the structure.

- Realistic force coefficients in Morison's equation, used in determining the environmental load on a structure.

This student thesis will address issues in the first of the above categories, and will concern the inclusion of the directional aspects of (tidal) currents in a procedure, developed at KSEPL, for deriving long term load statistics and joint met-ocean design conditions.

KSEPL, Koninklijke/Shell Exploratie en Produktie Laboratorium, is Shell's exploration and production laboratory in Rijswijk, Holland.

The adoption of revised environmental loading models, as part of a design practice for the North Sea, must not result in the elimination of "perceived" conservatisms that may balance other unknown aspects. Thus, it is necessary to validate the revised practice by assessing its consequence for the "true" probability of structural failure, and ensuring that it is acceptable.

The problem of specifying met-ocean design conditions (MDC) is one of estimating the environmental variables corresponding to some return period, typically 100 years, on the basis of measured or hindcast time series extending over a relatively short period, say 5 or 25 years. The time series typically contain three-hourly values for significant wave height, wave period, current speed (both tidal and residual) and wind speeds, and their directional properties. In the conventional practice for predicting extreme design waves for northern European seas, a probability distribution is fitted to the entire time series of significant wave height. Thereby, the data is extrapolated to rare events to obtain the 100 year significant wave height. This value is multiplied by an appropriate factor to specify the 100 year individual wave in terms either of its height or its crest elevation. In this process, both the correlation between the significant wave heights of successive three hour sea states and the uncertainty in

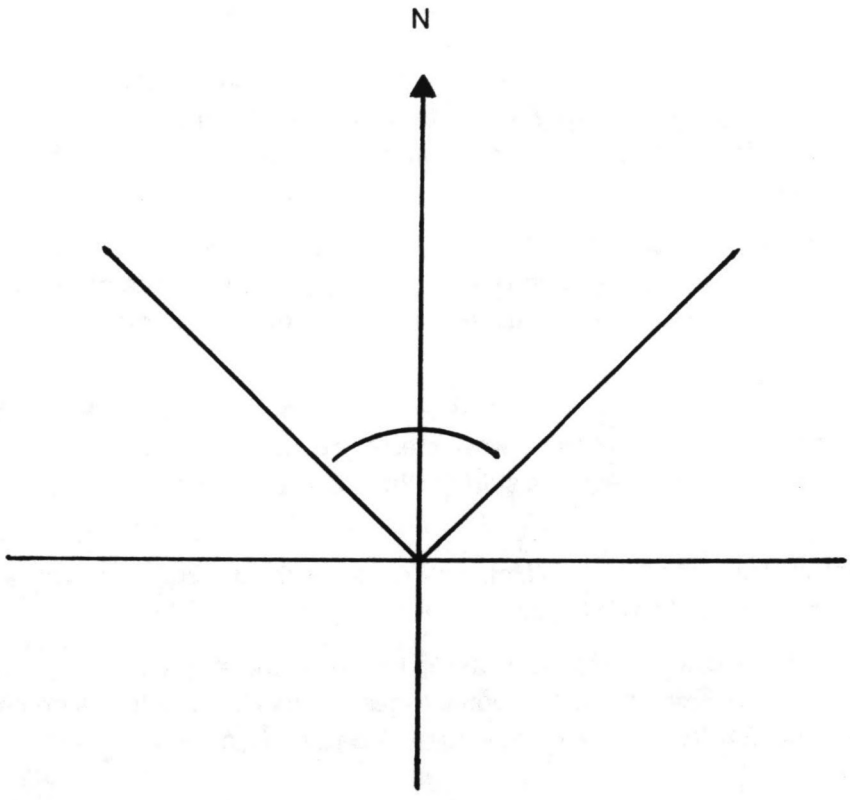

Fig. 1.4; Wide sector.

the extreme wave within a sea state are neglected. In fact, these effects approximately cancel one another. Similar methods are used to estimate, independently, design current and wind speeds, leading to conservative values. Moreover, the consequent "100 year" wind, wave and current combination, used in generating an extreme load, will be even more conservative. This is because extreme winds, waves and currents do not necessarily occur simultaneously or act in the same direction.

The completion of the Northern European Storm Study (NESS), a high quality hindcast study, provides an opportunity to develop and apply new approaches to the prediction of extreme met-ocean conditions. Such a new method has been developed at KSEPL. Statistics are calculated for the whole storm rather than for three hour intervals. A storm is a period of severe sea involving a development phase, a peak and a subsequent decay. A novel feature is the use made of some self-similar properties of storm statistics. That is, we assume that the probability distribution functions of a variable (e.g. wave height) within all storms are similar and can be characterised by their most probable extreme value. By combining a model, for translating a set of environmental conditions into a structural load, and the environmental parameters for a sea state, statistics can be generated for loads rather than for single environmental parameters. Once an extreme load is derived, a set of environmental parameters which could have generated this load can be derived via "back calculation". This set of environmental parameters can be used as input in a more detailed calculation of the distribution of the extreme load over the structure. The new method avoids the shortcomings of existing approaches and is distinguished from them by being equally applicable to the prediction of extreme waves, long term load statistics and joint met-ocean conditions.

1.3. Problem description

Environmental conditions and long term load statistics are directionally sensitive. To account for this phenomenon, the met-ocean data for a location must be divided into sectors, containing the directions from which severe storms are coming. So far, for the North Sea, these sectors have been chosen on the basis of wave height. The resulting sectors are reasonably wide (fig 1.4), around 90 degrees. Sectors containing severe storms include around 100 storms (sufficient for the subsequent statistical analysis). Long term statistics are derived for each of the sectors containing storms of similar severity. These statistics are then used in an extrapolation process to generate values for extreme wave heights and loads beyond the 25 year of hindcasting. Typically return values associated with a 100 year return period are calculated. However, (tidal) current can be much more sensitive to direction than significant wave height, and (at least in the southern North Sea, with current speeds up to well above 1 m/s) can influence loads. To resolve the (tidal) current correctly, we would have to reduce sector sizes so much that the number of storms would be too small for a reliable statistical analysis.

It has been proposed by KSEPL that it may be possible to increase artificially the sample size, by treating the angle between mean wave direction and (tidal) current direction as a parameter that can be varied. All the storms in the wide (based on wave height) sectors can then be used to generate load statistics in narrower (based

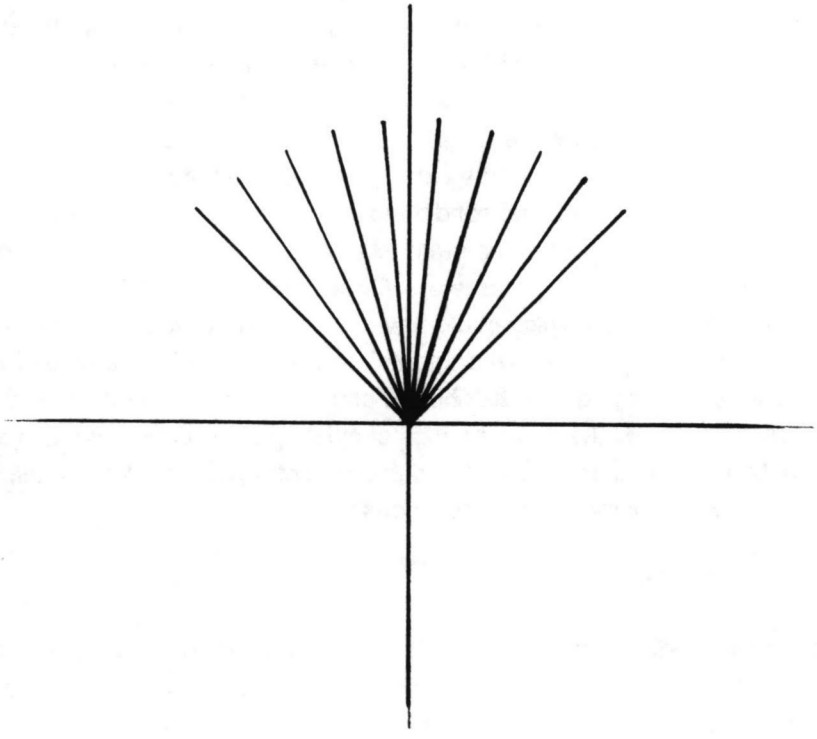

Fig. 1.5; Narrow sectors.

on current speed) (fig 1.5) sectors. This thesis will concern the implementation of this idea within KSEPL methodology. The effects of strongly directional current and artificially increased sample size on load statistics will be investigated. The data base used for this purpose contains all the relevant environmental parameters for a location in the southern North Sea for a hindcasting period of 25 years. The southern North Sea is selected, because of its relatively high (tidal) current speeds, compared to other areas in the North Sea.

1.4. Outline of the report

In section 2 an outline will be given of the methodology for deriving met-ocean design conditions, as developed at KSEPL. Section 3 will discuss how a strongly directional (tidal) current can be implemented in the present methodology. An analysis of the parameters in the data base used for this project will be given in section 4. Section 5 will highlight the implementation of the suggested changes in the integrated procedure, and section 6 the results obtained from using it. In section 7 an outline is given of a structural reliability analysis. The effects of accounting for a strongly directional current on the results of a structural reliability analysis will be investigated in section 8. Finally section 9 is used to put the used procedures, their results and this student thesis work in a somewhat broader perspective.

2. THE MET-OCEAN DESIGN CONDITIONS PROCEDURE

2.1. Outline of the theory

In this section the theory of the met-ocean design conditions (MDC) procedure will be outlined. Consider a variable X, which may represent crest elevation, wave height or a global load such as total horizontal force or overturning moment on a structure. Let X represent the global load on a structure. A generic load model (GLM) can then be used to predict values of X from sets of environmental parameters (waves, current speed and wind speed) for sea states from a data base. Using this load model, it is very easy to transform the statistics of extreme waves, within a sea state, into statistics of extreme loads. Statistics for individual sea states are used to derive statistics of extremes for a storm. These statistics for a storm are called the short time scale statistics. The long time scale statistics are described by the probability density of storms. Combining the short time scale with the long time scale statistics, results in a so called random storm formula. This random storm formula gives the cumulative probability of (a value of) X within a random storm. This random storm formula, in combination with the arrival rate of storms, will be used to extrapolate to rare events. Combinations of environmental variables (e.g. wave height and current speed) capable of generating the global load, found by extrapolating to rare events, can be derived. This back calculation uses the same load model, however inverted. The following sections discuss in turn:

- the derivation of the load model.
- the data base.
- the identification of storms and directional sectors.
- the statistics.
- the derivation of the extreme environment.
- the integrated procedure for deriving met-ocean design conditions.

2.2. The load model

When X is a global load, it is calculated from the met-ocean data using algebraic expressions obtained with a generic load model or GLM of the structure. These algebraic expressions also allow the statistics of the extreme wave of a sea state to be very easily transformed into statistics of extreme load. In this section the derivation of the load model is outlined, a more detailed discussion of the load model and its derivation is given by Tromans et al. [3] and Kraneveld [2].

2.2.1. Morison's equation

Many space frame structures can be analysed for extreme responses assuming a quasi-static structural behaviour. Frequencies of extreme waves are then assumed to be outside the range of the natural frequencies of the structure. A model is developed for global loading on a single column (stick). The analytical model gives a relation

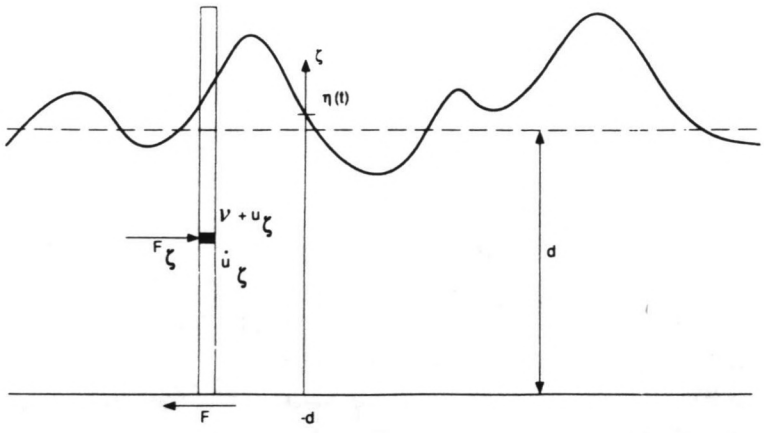

Fig. 2.1; Single pile under wave and current loading.

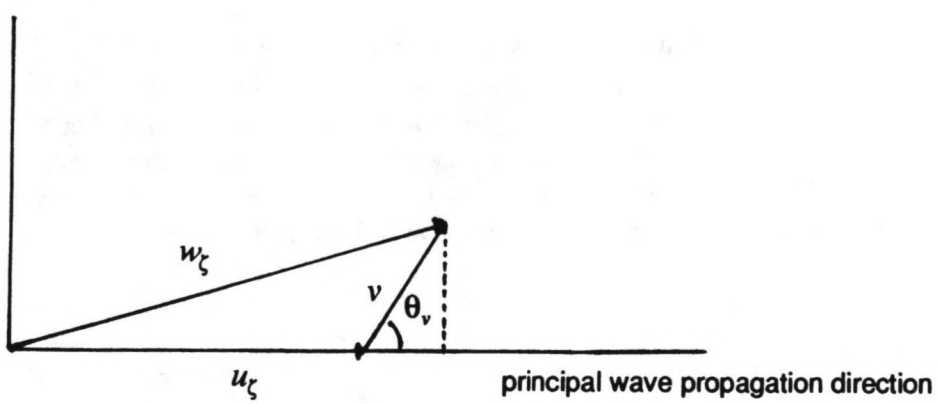

Fig. 2.2; Wave induced velocity, u_ζ, and current speed, v, as vectors and their vector sum w_ζ.

between global load and the environmental parameters, such as crest elevation, current speed and wave period.

Forces on an element of an offshore structure due to waves and currents, are usually obtained from Morison's equation (2.1). Equation (2.1) gives the resultant horizontal hydrodynamic force per unit length on a vertical member with a constant diameter, D, see figure 2.1.

$$F_\zeta = A_\zeta \cdot \dot{u}_\zeta + B_\zeta \cdot (v + u_\zeta) \cdot \left| (v + u_\zeta) \right| \tag{2.1}$$

$$A_\zeta = \left(C_m \cdot \rho \cdot \frac{\pi}{4} \cdot D^2 \right)_\zeta \tag{2.1a}$$

$$B_\zeta = \left(C_D \cdot \rho \cdot \frac{1}{2} \cdot D \right)_\zeta \tag{2.1b}$$

in which:
A_ζ = inertia factor
u_ζ = amplitude of wave induced horizontal water particle acceleration
B_ζ = drag factor
v = depth averaged current speed
$\dot{u}_\zeta$ = amplitude of wave induced horizontal water particle velocity
C_m = inertia coefficient
ρ = density of (sea) water
D = diameter
C_D = drag coefficient

Since some variables, such as the amplitude of water particle velocities in a wave, u_ζ, are not constant over depth, the subscript ζ is used to denote that the values of those variables are related to a certain water depth, ζ.

The first term on the r.h.s. of equation 2.1 represents the contribution of inertia to the hydrodynamic force on the member, and the second term represents the drag force.

In order to be able to account for an angle between wave and current directions in the horizontal plane, $(v+u_\zeta)\cdot|(v+u_\zeta)|$ in (2.1) is replaced by w_ζ^2 which is the modulus of the vector sum of wave induced velocity, u_ζ, and a depth-independent current speed, v, see figure 2.2.

$$w_\zeta^{\,2} = u_\zeta^{\,2} + 2 \cdot u_\zeta \cdot v \cdot \cos\theta_v + v^2 \tag{2.2}$$

in which θ_v represents the angle of the current speed relative to the wave direction.

Submerged structures suffer from fouling by marine life. A layer of marine growth on members of the structure below the water line changes the diameter and roughness of these individual members. Different inertia and drag coefficients, in Morison's equation, are used above and below mean sea level. Typical values used for the drag coefficient, C_D, are 0.65 above and 1.2 below mean sea level.

The total horizontal force, F, can be found by integrating the equation for F_ζ over the submerged part of the column, using a vertical coordinate ζ which has its origin at mean sea level. The instantaneous water level is represented by η and the level of the sea bed by $-d$.

$$F = \int_{-d}^{\eta} F_\zeta \cdot d\zeta \tag{2.3}$$

2.2.2. *Wave kinematics*

In the linear wave theory the amplitude of horizontal particle velocity at a certain water depth, u_ζ, in a wave, can be expressed as a function of the vertical coordinate, ζ [4].

$$u_\zeta = u_0 \cdot \frac{\cosh(k \cdot (d + \zeta))}{\sinh(k \cdot d)} \tag{2.4}$$

in which u_0 represents the amplitude of vertical particle velocity in the wave at mean sea level:

$$u_0 = a \cdot \omega \tag{2.5}$$

expressed in terms of the crest height, a, and the angular wave frequency, ω. The wave number, k, is defined as:

$$k = \frac{2 \cdot \pi}{L} \tag{2.6}$$

in which L represents the wave length.

A similar relation is found for the amplitude of particle acceleration in the wave. Assuming the water depth to be large relative to wave length, i.e. $k \cdot d$ to be large, the expressions for particle speed and acceleration can be simplified.

$$u_\zeta = u_0 \cdot e^{k \cdot \zeta} \tag{2.7a}$$

$$\dot{u}_\zeta = u_0 \cdot \omega \cdot e^{k \cdot \zeta} \tag{2.7b}$$

Using these deep water approximations for the water particle velocity and acceleration will highly facilitate the (analytical) integrating of Morison's equation over the submerged depth.

For large-amplitude waves, that are most likely to generate the extreme loads, these formulas (2.7a and b) overpredict the particle velocities and accelerations in the wave crest. A technique known as delta-stretching [5] provides a simple empirical correction. The technique involves a linear transformation of the ζ coordinate over a part of the ζ axis in the linear wave theory. If $\zeta > -D_s$ it will be replaced by ζ_s (2.8).

$$\zeta_s = (\zeta + D_s) \cdot \frac{\eta \cdot \nabla + D_s}{\eta + D_s} - D_s \tag{2.8}$$

The stretching depth, D_s, is usually set to one half of the significant wave height. The stretching parameter, ∇, typically equals 0.3.

Since extreme global loads of interest, i.e. total horizontal force and overturning moment, tend to be drag dominated for steel space frame structures, the inertia term, in Morison's equation, is omitted. Justification for this omission will be given in appendix A.

Now, in order to derive a model for total horizontal force, only the drag term has to be integrated over the submerged length of the column:

$$F = \int_{-d}^{\eta} B_\zeta \cdot w_\zeta^2 \cdot d\zeta \tag{2.9}$$

The derivation of the load model, also including inertia, is discussed in more detail by Tromans et al. [3] and Kraneveld [2].

2.2.3. *Effects of directional spreading of waves*

Until now the directional spreading of wave propagation has not been discussed. The directional spreading of waves leads to a reduction in the variance of the velocity and acceleration in the mean direction of wave propagation. The reduction of particle velocities and accelerations in the mean direction of wave propagation leads to a reduction in the wave induced loads in this direction. A reduction factor, φ, is applied to the horizontal particle velocities (and accelerations) to account for the effect of directional spreading, i.e. in the calculations u is replaced by $\varphi \cdot u$. The directional spreading of wave energy is assumed to follow a normal distribution. In the NESS data base the root mean square (or standard deviation, σ_θ) of the directional spreading within a sea state is given as a parameter. The reduction factor, φ, is then easily calculated from equation (2.10), which is derived from the ratio of the variance of the velocity in the mean wave direction in a uni-directional sea and a sea with directional spreading [2].

$$\varphi = \sqrt{\left(1 - \sigma_\theta^2 + \sigma_\theta^4\right)} \tag{2.10}$$

A typical value for φ, for the North Sea, is 0.88.

2.2.4. *The generic load model*

Assuming a quasi static response and omitting the inertia term, the maximum wave load on a stick will occur during the passage of the wave crest. Integrating (2.9) over depth (and simplifying it, by making some linearisations around mean water line) results in an algebraic relationship [2,3] for total horizontal force. The process of integrating the Morison equation over the entire submerged column length will be discussed in more detail in section 3.2, where also some new terms will be included to account for the directional effects of currents, and in appendix B.

The algebraic relationship (2.11) expresses the total horizontal force, F, on a vertical column in terms of crest height, a, current velocity, v, and (peak)period, T. A similar

relationship can be derived for overturning moment, M. The functional forms of the load models for total horizontal force and overturning moment are identical.

$$X = A_1 \cdot v^2 + A_2 \cdot v \cdot \varphi \cdot a \cdot T \cdot \cos\theta_v + A_3 \cdot \varphi^2 \cdot a^2 + A_4 \cdot \frac{v \cdot a^2}{T} \cdot \varphi \cdot \cos\theta_v + A_5 \cdot \varphi^2 \cdot \frac{a^3}{T^2} \tag{2.11}$$

A_1 to A_5 are the constants for a particular variable X for a given application. The values of the A's depend on e.g. whether the load model is used for total horizontal force or overturning moment, the configuration of the structure and the values of the drag coefficients used in Morison's equation.

Inclusion of inertial effects will not radically alter the functional form of the load model; one extra term is introduced in the load model to account for inertia [2,3].

The constants in the load model are calibrated against the load derived from a numerical loading model, for representative data in storm conditions from the data base. At KSEPL a computer program (LOAD) is in use, which calculates the fluid load on vertical piles, by numerical integration over depth. LOAD and the calibration of the constants in the generic load model are discussed in more detail in appendix C. The computer program does not include wind induced forces and reduced current speeds due to the presence of the structure; these effects are incorporated in the load model afterwards. The same procedure as for a single pile can be used for a space frame structure, approximating it by a group of closely spaced columns.

Using the deep water approximations for the wave kinematics (2.7a and 2.7b) highly facilitates the integrating of Morison's equation over the submerged depth. Using these approximations does not imply that the load model is not applicable in case the deep water requirements are not met. The constants in the load model are calibrated against the results from the LOAD program which accounts for a finite water depth, in which case the constants can compensate for a certain level of inadequacy of the load model. In appendix C a scatter plot is given of the results of the generic load model against the results of the LOAD program for different sets of environmental conditions and a 30 metre water depth. The scatter plot shows the good agreement between results from the generic load model and the LOAD program. The good agreement can be explained from the fact that in intermediate water depth wave and current load will still be roughly proportional to respectively wave height and current speed squared which are correctly represented in the load model. In appendix C also a load model is given with some empirically derived extra terms in it which is known to give extremely good results in case of intermediate water depth conditions.

2.2.5 *Inclusion of wind and current blockage effects*

The drag force exerted by the wind on the structure is included in the load model by adding the following extra term:

$$F_w = C_w \cdot W^2 \cdot \cos(\theta_w) \tag{2.12}$$

in which:

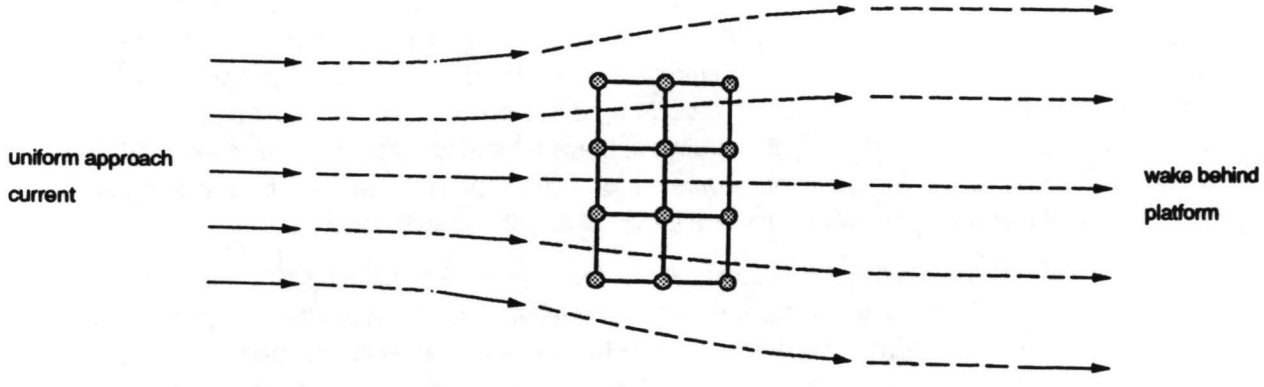

Fig. 2.3; The blockage of current by a structure.

$$C_w = \frac{1}{2} \cdot \rho_a \cdot S \cdot C_D \tag{2.12a}$$

Here, W represents an averaged wind speed, θ_w the direction of the wind relative to the waves, ρ_a density of air, S a representative area of the topside and C_w a drag coefficient. C_w can be calculated from ρ_a, S etc. For modelling purposes however it is often adequate to choose C_w such that the wind force contributes from 10 to 15% of the total global load.

When analysing a space frame structure (modelled as a group of closely spaced columns) a reduction factor for the current speed is introduced. The current speeds from the data base represent speeds in open sea. However, the flow of the current is influenced by the presence of the structure (fig 2.3). Current speeds will be reduced, locally, within the structure and its wake. Not all the columns in a space frame structure will experience the same level of current load. A so called current blockage factor [6] (which can be implemented easily in the load model) accounts for the effect of the reduced current speeds within the structure on the global loads. The current speed, v, is then replaced by a reduced current speed, v_s.

$$v_s = v \cdot \left(\frac{1}{1 + C_d \cdot \frac{A}{4 \cdot A_c}} \right) \tag{2.13}$$

A represents the projected area of the structural elements, as used in the Morison equation (i.e. the sum of the column diameters) and A_c the area normal to the direction of the flow enclosed by the cross-section of the space frame structure (essentially width times height of the structure). A typical value for the reduction factor due to current blockage is 0.77, derived from a ratio of A/A_c of 1 and a value of C_d of 1.2.

The load model for variable X, including the effects of wind load and current blockage is thus easily derived from a load model omitting these effects.

$$X = A_1 \cdot {v_s}^2 + A_2 \cdot v_s \cdot \varphi \cdot a \cdot T \cdot \cos\theta_v + A_3 \cdot \varphi^2 \cdot a^2 + A_4 \cdot \frac{v_s \cdot a^2}{T} \cdot \varphi \cdot \cos\theta_v + A_5 \cdot \frac{\varphi^2 \cdot a^3}{T^2} + A_6 \cdot W^2 \cdot \cos\theta_w \tag{2.14}$$

The origin of the terms in the generic load model (2.14) are discussed briefly below. Each term in the load model is identified by its constant.

A_1 : current speed squared
A_2 : cross term between wave induced velocity and current speed, below mean sea level
A_3 : wave induced velocity squared, below mean sea level
A_4 : cross term between wave induced velocity and current speed, above mean sea level
A_5 : wave induced velocity squared, above mean sea level
A_6 : force exerted by the wind

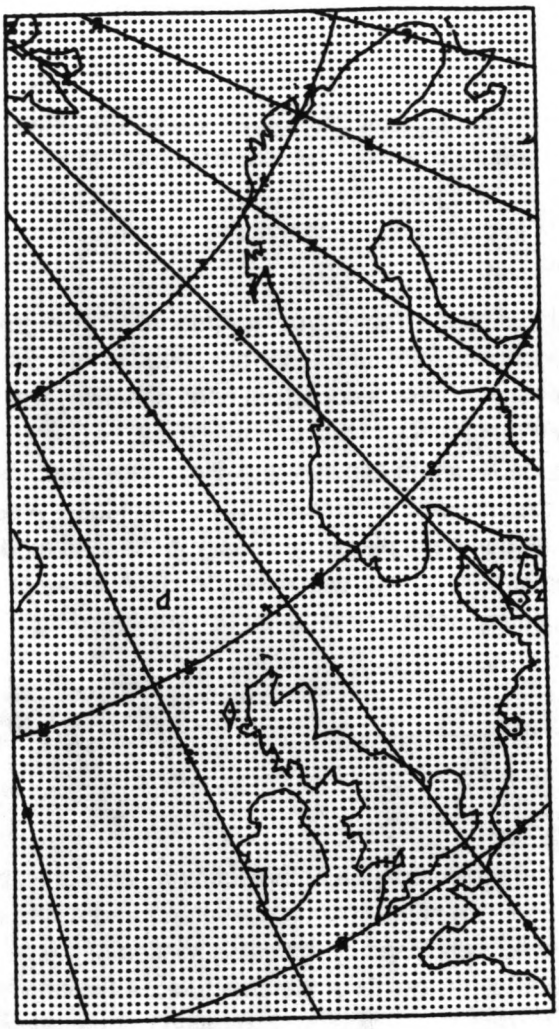

Fig. 2.4; The NESS grid.

2.3. The data base

The environmental parameters for sea states, which are input into the load model, come from a met-ocean (hindcast) data base. A hindcast in essence provides over a long period, typically 25 years, met ocean data as derived from numerical simulation of atmospheric pressure and wind patterns in combination with models describing how energy of the wind is converted into waves and currents. The used models are calibrated against measurements of currents and waves.

The met-ocean data base used in the MDC procedure for the North Sea is the result of the North European Storm Study (NESS) [7]. NESS was initiated in order to produce a high quality hindcast database of winds, waves, storm surges and depth-integrated currents for the North European continental shelf (see figure 2.4). The project was funded by eleven participants (nine oil companies, and two government departments) and the work was carried out by meteorological and oceanographic institutes in five European countries. The project took more than five years to complete at a cost of over £2.1 million. Oceanographic and meteorological data gathered from many of the countries over the geographic extent of the study area, as well as from archives of the oil industry in combination with models and numerical simulations has resulted in a database containing simulated wave, wind, surge, and current conditions for grid points in the studied area. The NESS data base covers a period of 25 years, 1963-1988. Information in the data base consists of average sea state statistics for 3-hour intervals, for the periods October to March. For the remainder of each year, average sea state statistics are given only for periods when storm conditions exist. A sea state is a period of time in which the environmental statistics (e.g. significant wave height) are assumed to be stationary; three hours is a commonly used length for this period.

The data base contains data on significant wave height, H_s. Significant wave height was originally defined as the average of the highest third of the wave heights. When the waves can be considered as a Gaussian process with a narrow energy spectrum, H_s can also be defined as four times the standard deviation of ocean surface elevation within a record. The latter definition is used in the data base.

2.4. The identification of storms and directional sectors

Since waves dominate the extreme load on an offshore structure, storms, to be used in the subsequent statistical analysis, are selected from the data base according to the values of significant wave height. A storm is a period of severe sea involving a development phase, a peak and a subsequent decay. Though storms are easily defined in a time series of significant wave height, their temporal and spatial boundaries are not well defined [8]. In the prediction of extreme conditions, moderate seas play no role and all time intervals in the data base with a significant wave height less than a certain fraction of the largest value within the data base can be discarded. This is done in the analysis by introducing a threshold level for wave height, $H_{threshold}$. Records with a significant wave height below this level are not considered in the calculations for extreme environmental conditions. The threshold level lies typically at 30 to 40% of the maximum significant wave height found in the data base, keeping in

mind that one needs a certain amount of storms, e.g. more than 100, for the subsequent statistical analysis to work properly. Introducing this threshold level both reduces the data to a more manageable quantity and breaks the data base into storm periods.

However, a few of the resulting storm periods will have twin peaks and it is debatable as to whether these should be split into two separate storms. Since sea-states with a significant wave height lower than a certain fraction, typically 0.8, of the maximum significant wave height in that storm do not contribute in the probability distribution of the maximum values, a set of simple rules have been adopted [2,8]:

- When the two peaks are less than 12 hours apart, the event is described as a single storm.
- When the two peaks are more than 12 hours and less than 24 hours apart:
  - If the valley in significant wave height between the two peaks is higher than 80% of the lowest of the two peaks, the event is described as a single storm.
  - If the valley in significant wave height between the two peaks is less than 80% of the lowest of the two peaks, the storm period is broken at the valley to form two storms.
- When the time interval between the two peaks exceeds 24 hours, two storms are derived, regardless of the minimum H_s values between them.

The probability distributions of parameters in storms with a relatively small maximum significant wave height ($0.8 \cdot H_{s,max} < H_{threshold}$) are influenced by sea states below the threshold level. Since the records for sea states with a significant wave height below the threshold level are not considered in the calculations, the probability distributions of parameters in those storms will be influenced by the threshold level and are therefore omitted from further calculations [2].

Application of the above suggested steps for a grid point in NESS should produce a few hundred storms coming from all directions.

The sea states associated with the thus derived storms will come from many different directions. The direction of a storm is defined as the principal wave direction associated with the peak significant wave height within this storm. Some directions correspond to longer fetches and deeper waters and produce the most severe seas. When long time scale statistics are considered, it is both worthwhile and necessary to divide the storm directions into sectors. The sectors can be selected, based on severity, from a polar plot of the peak significant wave height (or most probable extreme wave heights, after short time scale statistics are derived) against direction of the storms, i.e. sectors are chosen from which the highest waves are coming. The directions bounding the chosen sectors should be checked against (hydrographic) charts to confirm consistency with fetch limits and water depths.

2.5. The statistics

The complete description of the statistics for a variable X, e.g. wave height or total horizontal force, involves a combination of "long time scale" and "short time scale" models. Short time scale statistics describe the probabilistic behaviour of the extreme

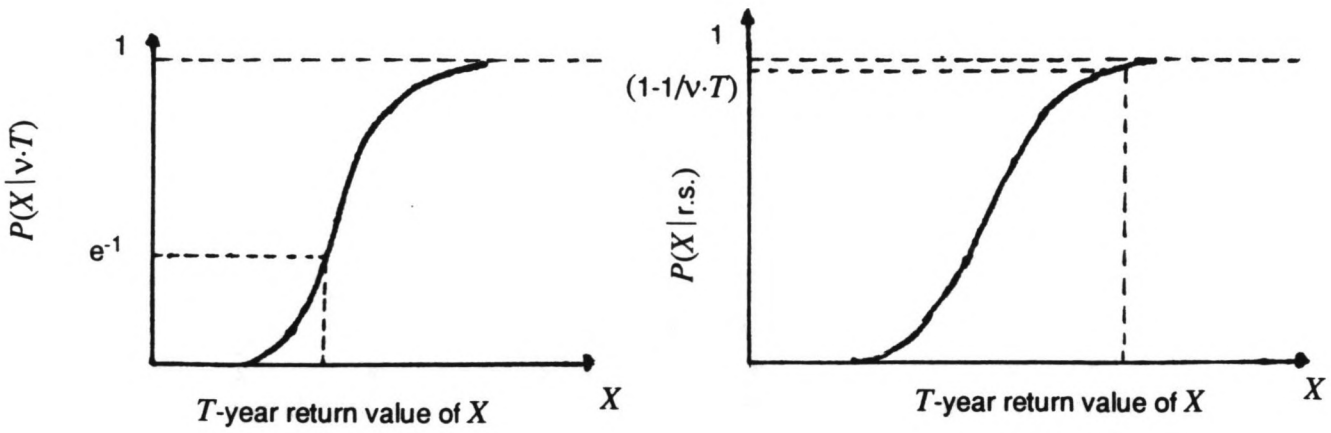

Fig. 2.5; Derivation of T-year return values.

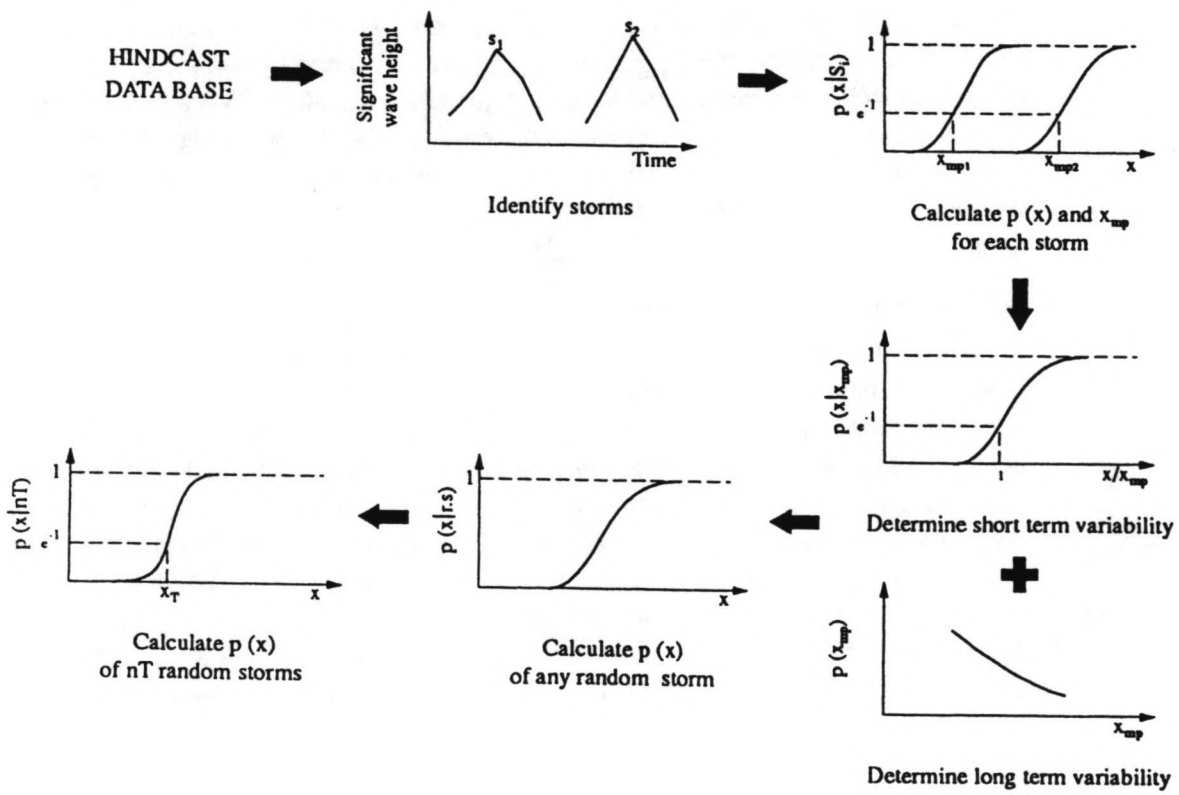

Fig. 2.6; Logic of the evaluation of the extreme response.

value of X within a time interval. In the present theory this interval is a storm. Once a directional sector containing the most severe storms (i.e. with the highest peaks in significant wave height) is selected, the statistics of the extreme value of X in a storm, within this sector, are conditional on and completely defined by its most probable value in that storm. This arises from the self-similar properties of storm statistics (the self-similarity has been proven theoretically at KSEPL and can be demonstrated by the analysis of storm histories [8]). Thus, the cumulative probability of the extreme value of X in a storm characterised by a most probable extreme value, X_{mp}, is $P(X|X_{mp})$.

The long term statistics describe the variation in storm severity, in terms of the probability density of their X_{mp} values. Let $p(X_{mp})$ be this probability density function of X_{mp}. The probability distribution of the extreme value of X in a random storm (of unknown X_{mp}) is then:

$$P(X|r.s.) = \int P(X|X_{mp}) \cdot p(X_{mp}) \cdot dX_{mp} \qquad (2.15)$$

This is called the random storm formula. Storms arrive randomly at some average rate, ν, per year. This ν is called the arrival rate. For periods longer than a year the arrivals can be modelled as a Poisson process (appendix D and [2]). Thus the probability distribution of the extreme value of X in some long interval T, e.g. 25 or typically 100 years is:

$$P(X|\nu \cdot T) = [P(X|r.s.)]^{\nu \cdot T} \qquad (2.16)$$

The T year return value of X is the most probable maximum of the T year distribution of X. This is almost exactly the value of X corresponding to a probability of non-exceeding, in T years, of e^{-1}. This value of X will be exceeded on the average once in T years. Since the arrivals can be modelled as a Poisson process, the T year return value can also be read from the probability distribution of X in a random storm (with $P(X|r.s.)=1-1/\nu \cdot T$) (fig. 2.5).

The specification of $P(X|X_{mp})$, $p(X_{mp})$ and ν can be deduced from a time series (like NESS) of significant wave height, wind, current and their directional properties. The logic is shown diagramatically in figure 2.6.

Once a directional sector is selected, the steps involved are:

1. Identify the storms.

2. By combining data for the three-hour intervals of each storm, calculate the distribution, $P(X)$, of the extreme value of X for each storm and identify the most probable maximum of X, X_{mp}, in each storm.

3. Re-normalise (by dividing by the value of X_{mp}) all the distributions to obtain the short term variability, $P(X|X_{mp})$. The short term variability can now be represented for all the storms by a similar probability distribution function conditional on the X_{mp} in a storm:

$$P(X|X_{mp}) = e^{-e^{\left(\beta\left(1-\frac{X}{X_{mp}}\right)\right)}} \qquad (2.17)$$

in which β is a constant describing the time scale of the storm This formula (2.17) is discussed in more detail in appendix E.

4. Take the X_{mp} values of the most severe storms (i.e. the ones with highest X_{mp} values) from a chosen directional sector and fit a probability density function, $p(X_{mp})$ [2,9]. The number of storms used in the fitting is chosen based on minimising the mean square error (MSE) of the estimate of the index of variation, γ, between the fitted curve and data points of X_{mp} calculated for the storms from the data base. The value of v is now the number of storms used in the fitting of the probability density function $p(X_{mp})$ (or rather $1\text{-}P(X_{mp})$) divided by the duration of the complete time series. The fitted curve can be represented by:

$$p(X_{mp}) = \frac{\xi}{\gamma} \cdot \left(1 + \xi \cdot \left(X_{mp} - X_0\right)\right)^{-\frac{1}{\gamma}-1} \tag{2.18}$$

which, also, will be the subject of a more detailed explanation in appendix E.

5. Equations (2.15) and (2.16) are used to obtain the probability distribution of the extreme value of X in a long time interval T. The desired return value, say a 100 year value, can be read from the distribution.

Steps 1 to 5 can be repeated for a number of variables such as crest elevation or wave height, overturning moment and total horizontal force. From all the storms in the data base, only a number of the largest is used for fitting of the probability density function ($p(X_{mp})$). Therefore this probability density function can only be used to derive for values of X_{mp} greater than the value associated with the least severe storm (X_0) used in the fitting. Normally, the fitted curve will be used to extrapolate to rare events, and this lower bound will be of no importance.

Global loads can be transformed back into a suitable combination of design wave, in-line current and wind speed generating this load, for use as design conditions, via "back calculation" (section 2.6).

2.6. The derivation of an extreme environment as design conditions

Once the probability distribution for extreme global loading on a structure is derived, as discussed in the previous section, one can select a loading level from it corresponding to a certain return period. Typically the return values corresponding to a 100 year return period will be calculated. The extreme loading on this structure can be determined accurately when one knows the met-ocean conditions that in combination with each other will result in this level of global load. Possible combinations of joint met-ocean conditions, which yield the extreme load, can be derived from the load model using it in an inverse manner.

Once the, say 100 year, return values are derived from the statistics, combinations of environmental parameters generating this load can be calculated. If all environmental parameters, apart from crest height and current speed, are held constant (at representative values) in the load model, then a relation can be derived between an extreme global load (e.g. a 100 year return value for total horizontal force omitting wind) and crest height and in-line current speed. The global load can thus be given as a function of crest height and in-line current speed.

Using as input e.g. the 100 year return values of total horizontal force and wave height, the associated current speed required to generate this value of total horizontal

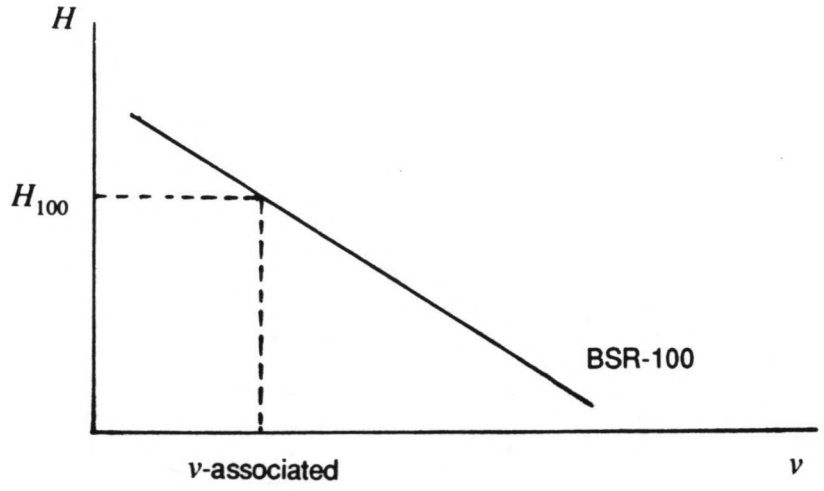

Fig. 2.7; Joint met-ocean conditions, H_{100} and an associated current.

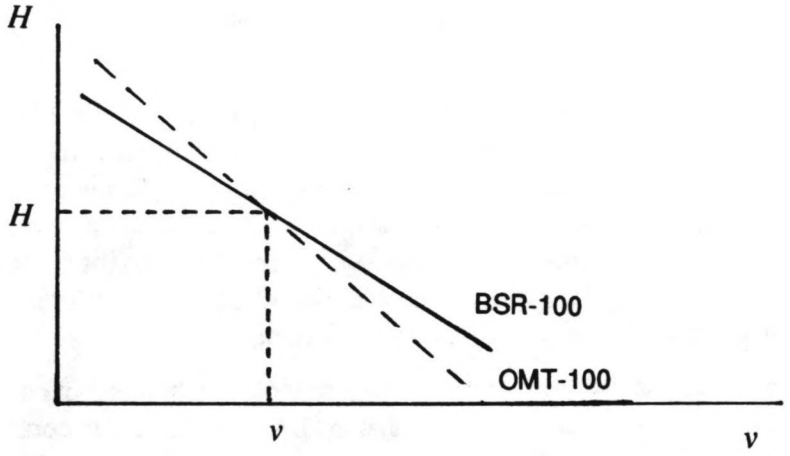

Fig. 2.8; Joint met-ocean conditions.

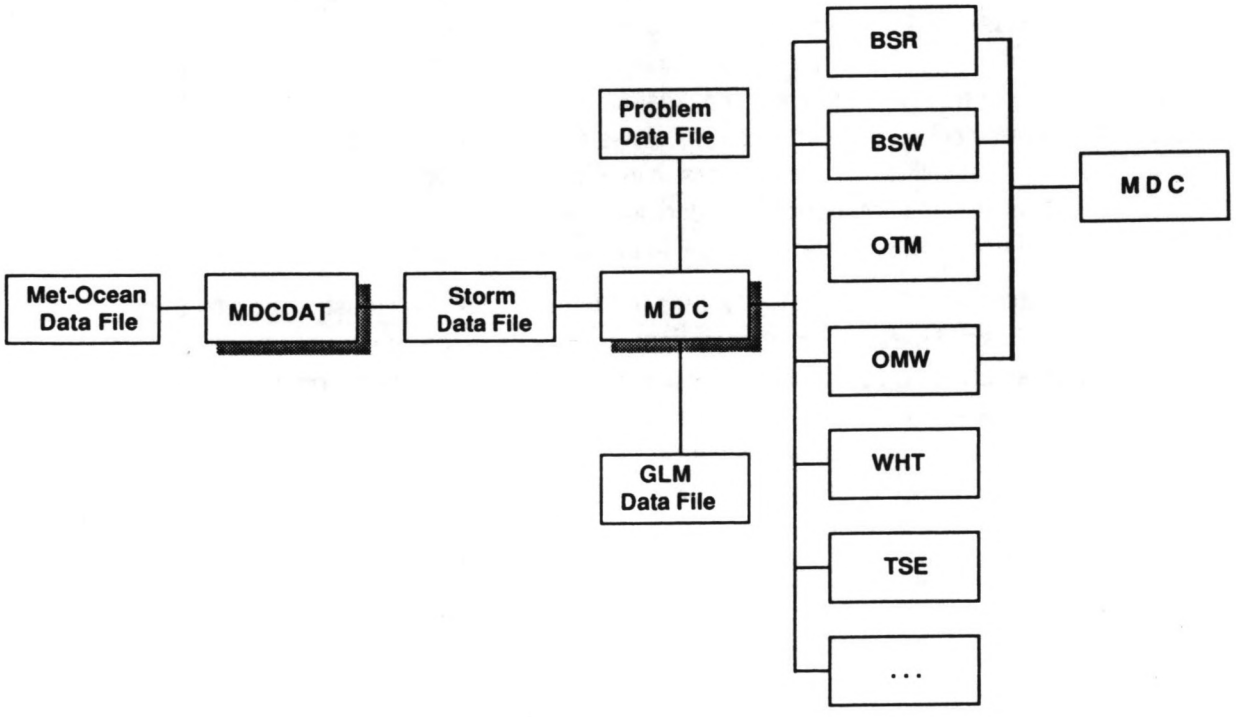

Fig. 2.9; Integrated MDC procedure.

force (fig. 2.7) can be derived. The derived associated current speed is not the 100 year return value of the current speed, i.e. the 100 year current speed may well occur in combination with a lower wave height. This displays the difference with the traditional method of deriving design conditions, where in the determination of the 100 year return value of a load the 100 year return values of wave height and current speed are considered to coincide.

There is another method for deriving joint met-ocean conditions which can be used. Write both total horizontal force and overturning moment for the desired return period as a function of crest height and in-line current speed. Plotting the two functions in one graph, the point of intersection of the functions gives the joint wave and current speed generating both the total horizontal force and overturning moment return values (fig. 2.8). (Once the joint wave and current conditions are derived the associated wind speed can be calculated from these wave and current conditions combined with the return values found for total horizontal force or overturning moment including wind.)

The distribution of extreme loading on a particular structure can be calculated accurately from the met-ocean conditions that together result in the level of global loading. The derived joint met-ocean conditions can therefore be used as design conditions in the design and re-assessment of offshore structures.

2.7. Met-ocean Design Conditions, the integrated procedure

Since the met-ocean data files are large (in the order of mega-bytes) and the computations involved are numerous and laborious, an integrated computer procedure has been developed at KSEPL. Figure 2.9 shows diagramatically the outline of the procedure to go from a met-ocean data file to Met-ocean Design Conditions (MDC). X is the variable of interest. Starting from a data file containing wave, wind and current parameters for a certain location (e.g. from NESS), the procedure will generate the short time scale probability distribution (statistics over single storms, $P(X \mid X_{mp})$) and the long time scale statistics ($p(X_{mp})$) which are used to calculate return values and (via back calculation) joint wave and current values generating these return values. The procedure uses, in addition to the data file, one input file which contains information about the location and the calculations that should be executed (the problem data file) and a second which contains the constants in the load model for the different variables (the GLM data file). The procedure can be used for various variables:

- wave height (WHT).
- crest height (CHT).
- total surface elevation (TSE), crest height plus tidal and surge elevation.
- total horizontal (hydrodynamic) force on the construction (sometimes referred to in literature as base shear, BSR).
- total horizontal force including force exerted by wind (BSW).
- overturning moment (OMT), total moment on the construction at the sea bed (mud line).

- overturning moment including force exerted by wind (OMW).

Results (e.g. short and long term probability distributions) can be shown graphically.

The MDCDAT code reads the met-ocean data file, determines the storm periods and outputs to a storm file. The latter contains, among other things:

- the data for the sea states in those storms.
- the number of complete and incomplete records.
- maximum and minimum values of the environmental variables over the complete record period.

In further calculations the direction from which a storm comes is defined as the wave direction associated with the maximum value of significant wave height in a storm. The MDCDAT code prompts the user for a threshold value for the significant wave height for a storm, and a cut-off-factor. The cut-off-factor is used for separating adjacent storms. This storm separation is based on the fact that sea states with a significant wave height lower then a certain fraction, typically 0.8, of the maximum significant wave height in a storm do not contribute in the probability distribution of the maximum values [2,8]. The same factor is used in rejecting storms with a relatively small maximum significant wave height, as discussed in more detail in section 2.4. Not all the three-hourly records in the NESS data base are complete. During (most of the) summer storms no data on currents and combined tidal and surge elevation are available, because they were not hindcast. The code checks whether the records are complete.

The MDC code needs as input the storm data file, pre-processed by MDCDAT, a problem data file and a generic load model (GLM) data file. The problem data file specifies information relevant to the variables (X) for which the code should do the MDC calculations (e.g. sector size, return periods, variables (wave height, total horizontal force, etc.), back calculation etc.). The GLM data file contains, as stated earlier, values of the constants in the load models for the different variables for which the procedure is used, for a specific structure. The MDC code has the option to generate a relationship between the most probable value of two variables. In this way a storm which lacks data (e.g. on current) to do the calculations for one of these variables still can be used. Using the storms with complete records on all data, a correlation rule (2.19) between the most probable extremes of variable X (e.g. total horizontal force or overturning moment) and wave height is derived [2]. The correlation rule is based on the fact that for a drag dominated problem, a global load is roughly proportional to the wave height squared.

$$X_{mp} = \alpha \cdot \left(\mathrm{WHT}_{mp}\right)^2 \tag{2.19}$$

This relation is used to generate estimated (or "bogus") values for X_{mp} in incomplete storms, which can be used in the subsequent statistical analysis of X. However, one should be cautious not to add too great a number of "bogus" storms.

The output files contain information on the variables for which the procedure is executed. Amongst other things, this information consists of:

- the most probable maximum values of the variables in each storm.

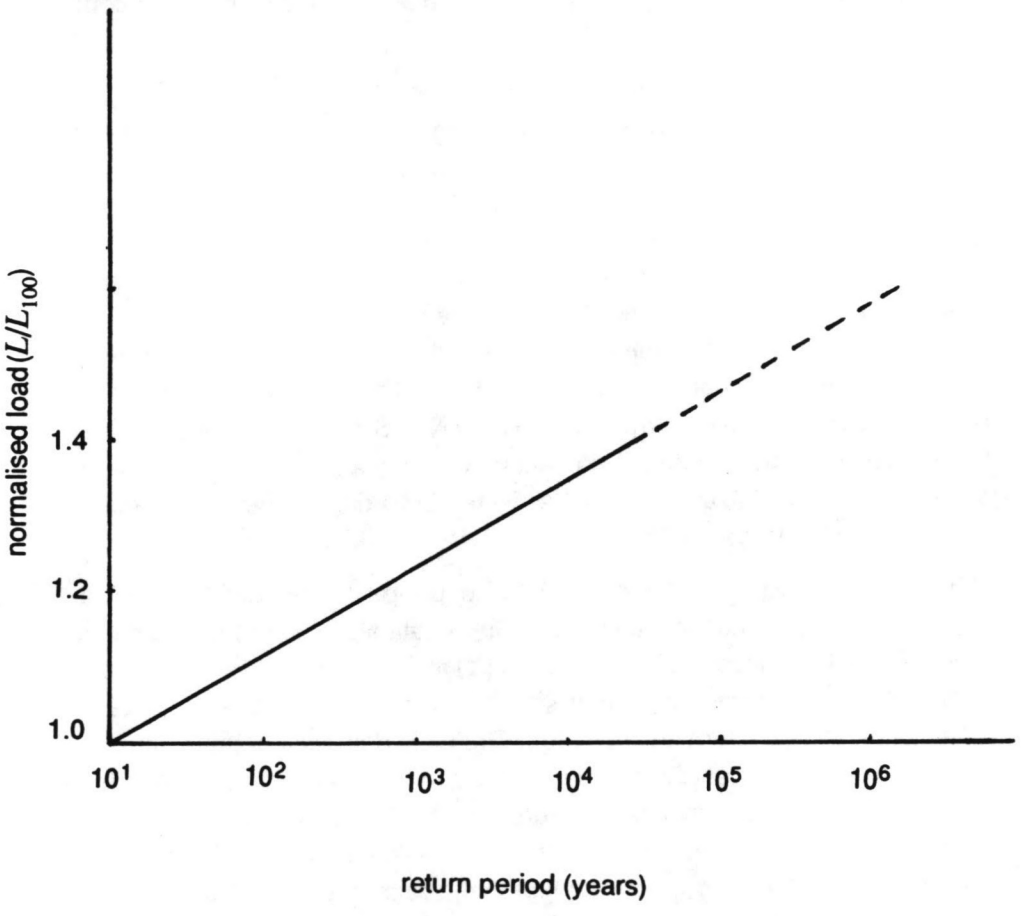

Fig. 2.10; Normalised load versus return period.

- return values associated with given return periods.
- the coefficients in the fitting of a function which should represent the probability density function of the most probable extremes over the storms ($p(X_{mp})$).

2.8. Extreme global loads and return period

A relation between return period and return value can be derived (2.20) from a pair of return values for a variable generated by the code. The return value for a variable (i.e. total horizontal force or overturning moment) is assumed to vary linearly with the logarithm of return period (fig. 2.10). This line represents the long time scale distribution of extreme loads. Because of physical limitations (e.g. wave height will be influenced by a limited water depth), the return values associated with large return periods will tend to fall below this line. The assumption of the return value to vary linearly with the logarithm of return period appears to be valid for return periods shorter than about 10^4 years.

In the graph of return value, on the vertical axis versus logarithm of return period on the horizontal axis (fig 2.10), the return values, L_{rp}, are normalised to a 100 year level by dividing them by the 100 year return value, L_{100}.

$$Q_{rp} = A \cdot e^{\left(-\frac{L}{\delta}\right)} \tag{2.20}$$

in which:

$$L = \frac{L_{rp}}{L_{100}} \tag{2.20a}$$

The value of δ depends on the slope of the line (fig. 2.10). The slope of the line is typical for a certain sea area. The environmental conditions in the southern North Sea are not as severe as the conditions in the northern North Sea. The slope for a location in the northern North Sea will therefore be higher. The long time scale distribution of extreme global loads is therefore highly dependable on the geographical area.

When structural strength is expressed as the 100-year level of loading multiplied by a certain factor (section 7.3 and 8.2), the above relation (2.20) can be used to calculate the return period ($1/ Q_{rp}$) associated with the structural strength.

Rewriting expression (2.20) a relation can be derived from which the load can be calculated associated with a given return period (section 3.4):

$$L_{rp} = -\delta \cdot L_{100} \cdot \ln\left(\frac{Q_{rp}}{A}\right) \tag{2.21}$$

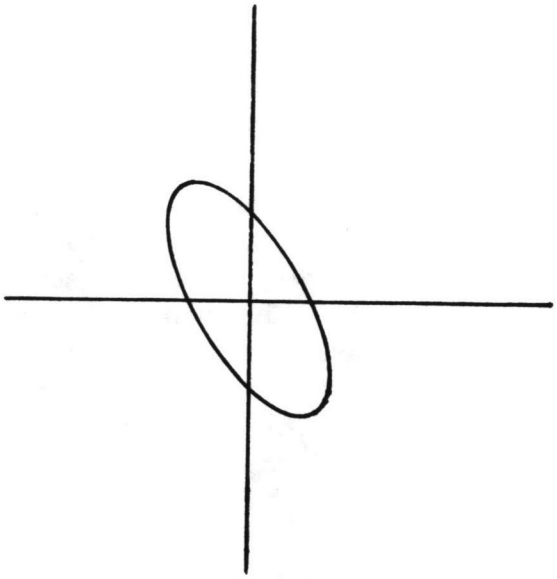

Fig. 3.1; Ellipse of tidal current.

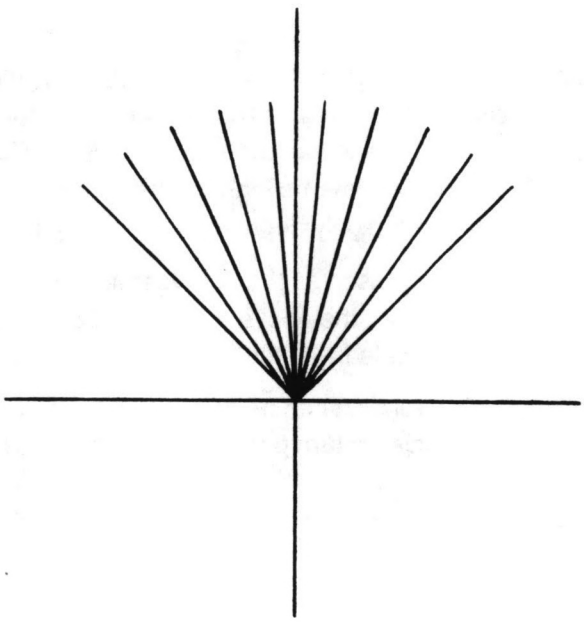

Fig. 3.2; Narrow sectors

3. INCLUSION OF STRONGLY DIRECTIONAL CURRENTS

3.1. Introduction

In the method for calculating met-ocean design conditions, developed at KSEPL, load statistics are assumed to be similar over a relatively wide sector, typically around 100 degrees. Currents however can be highly anisotropic, i.e. there may be a major axis along which the highest current speeds occur. E.g., when the velocity vector of the tidal current describes an ellipse over one tidal cycle (fig 3.1). When, as in the southern North Sea, the (tidal) currents have a significant influence on the global load, the assumption of similarity of the load statistics in the wide sector may be inappropriate. The significance of the contribution of the current to the global load, in this area, arises because (tidal) current speeds are high (due to the bathymetry between the continent and the UK) and waves are small, relative to other parts of the North Sea. The directionality of the (tidal) current may have an influence on the load statistics within the wide sector. To resolve the effect of this strongly directional (tidal) current correctly, the wide sector should be divided into several (e.g. 8) narrower sectors. These narrow sectors are based on dividing the ellipse of (tidal) current speeds into a number sectors, of equal width, in which the (tidal) current speeds are assumed to be of similar magnitude.

Normally around 100 storms are found in the data base for the wide sector. This number of storms is just sufficient for the statistical analysis to work properly. When dividing such a wide sector in narrow sectors, a narrow sector will not contain enough storms for reliable statistical analyses.

When the (tidal) current speed and direction has no correlation with the wave height and direction, i.e. these two parameters are independent, any current direction can occur with any wave direction. Thus any of the wave directions found in the data base can be associated with any of the current directions. At KSEPL the idea exists that this principle presents a possibility to overcome the problem of not having enough storms in each of the narrow sectors by treating the angle between mean wave direction and (tidal) current direction (or major (tidal) current axis) as a parameter that can be varied. All the storms found in the wide sector (based on wave height) can then be used to generate load statistics in narrower sectors (based on (tidal) current speed) (fig. 3.2). The idea is that inclusion of the effect of directionality of the current will result in a different distribution of the load statistics (i.e. return values and met-ocean design conditions) within the wide sector, e.g. higher return values of load in the directions that coincide with the major current axis. Treating the (tidal) current (speed and direction) as a separate environmental parameter requires some modifications in the load model. Also the larger storm sample size will have effects on the statistics. The changes to the load model and the statistics are the subjects of investigation in the next sections.

3.2. The load model

For the generic load model which could be used to account for the effect of strongly directional currents two distinctive cases are considered:

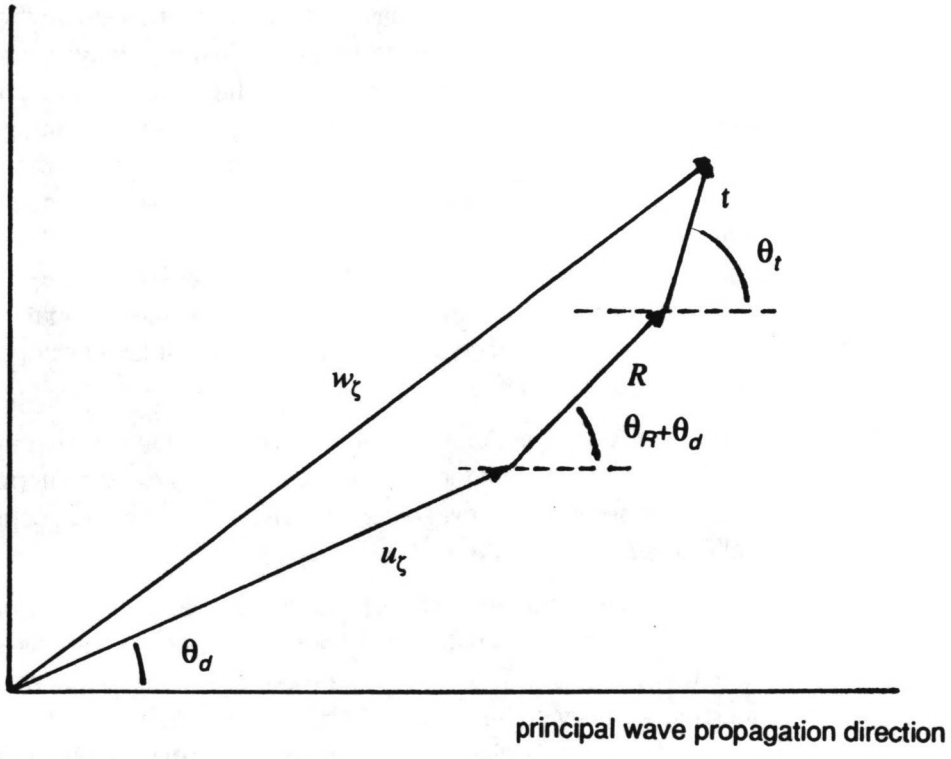

Fig. 3.3; Wave induced velocity, u_ζ, residual current speed, R, and tidal current speed, t, as vectors and their vector sum w_ζ.

- The (direction of the) residual current, defined as total current minus tidal current, is highly correlated to the (direction of the) waves, i.e. is mainly driven by the wind and waves. In this case the angle between the mean wave direction and the *tidal* current direction is used as a parameter which can be varied. The derivation of a load model including the extra parameters is given below in section 3.2.1.
- The (direction of the) residual current shows (hardly any or) no correlation with the local (direction of) the waves, e.g. because it is dominated by effects acting over a wider area. The total current, however, can be considered as being strongly directional. Then the angle between the mean wave direction and the *total* current direction is incorporated into the load model as a parameter which can be varied. The derivation of such a load model is analogue to the one in section 2.2, and is discussed briefly in section 3.2.2.

3.2.1. A load model for a strongly directional tidal current

In order to incorporate directional aspects of tidal current, the wide sector of wave heights will be divided into 7 or 8 narrower sectors based on the magnitude of the tidal current speed. All the storms within the wide sector are put into each narrow sector by replacing the wave direction with the central direction of each narrow sector. Now all the (say 100) storms are within each of the narrower sectors. The angle between the wind and wave direction is held fixed. A version of the generic load model was formulated such that, if required, the angle between the residual current and the wave direction could also be fixed, leaving the direction between the tidal current direction and the wave direction as a parameter that can be varied.

Current speeds are no longer (as in section 2.2) specified by one vector but by two, a tidal and a residual current speed vector (see figure 3.3). Tidal current speed, t, is the current speed as generated by the astronomical tides, i.e. a combination of centrifugal and gravitational forces of the earth, sun and moon on the water in the oceans. Residual current speed, R, is defined as total current speed minus tidal current speed, t. The central direction (i.e. the middle) of a narrow sector is called θ_d. The angles θ_R and θ_t are the directions of the residual current and tidal current relative to the original direction of wave propagation. The water (particle) velocity squared, w_ζ^2, as used in the drag term of the Morison equation in the derivation of a load model will now be:

$$w_\zeta^2 = u_\zeta^2 + 2\cdot u_\zeta \cdot R\cdot\cos\theta_R + R^2 + 2\cdot R\cdot t\cdot\cos(\theta_R + \theta_d - \theta_t) + t^2 + 2\cdot u_\zeta\cdot t\cdot\cos(\theta_d - \theta_t) \qquad (3.1)$$

The inertia term is omitted, for the same reasons as in section 2.2. In order to derive the total horizontal force on a structure, the drag term of Morison's equation should be integrated over the entire submerged length:

$$F = \int_{-d}^{\eta} B_\zeta \cdot w_\zeta^2 \cdot d\zeta \qquad (2.9)$$

Here, as in section 2.2, the load model is initially derived for total horizontal force. The same functional form, with different constants, is valid for overturning moment.

The same formulae, as in section 2.2, are used for the decrease of the amplitude of particle velocity under a wave with depth:

$$u_\zeta = u_0 \cdot e^{k\cdot\zeta} \tag{2.7a}$$

for the different drag coefficients above and below mean sea level:

$$\zeta \le 0 \quad \Rightarrow B_\zeta = B$$
$$\zeta > 0 \quad \Rightarrow B_\zeta = B_s$$

and for delta stretching:

$$\zeta > -D_s \;\Rightarrow\; \zeta_s = (\zeta + D_s)\cdot\frac{\eta\cdot\nabla + D_s}{\eta + D_s} - D_s \tag{2.8}$$

Since $w_\zeta{}^2$ contains 6 terms which should be integrated over the entire submerged length of the column, the global load, F, can be written as the summation of 6 independent integrals:

$$F = \sum_{i=1}^{6} F_i \tag{3.2}$$

in which the individual integrals are:

$$F_1 = \int_{-d}^{\eta} B_\zeta \cdot u_\zeta^2 \cdot d\zeta \tag{3.3a}$$

$$F_2 = \int_{-d}^{\eta} 2\cdot B_\zeta \cdot u_\zeta \cdot R\cdot\cos\theta_R \cdot d\zeta \tag{3.3b}$$

$$F_3 = \int_{-d}^{\eta} B_\zeta \cdot R^2 \cdot d\zeta \tag{3.3c}$$

etc.

In appendix B a detailed solution of the integral for F_1 is given. If all the 6 integrals are evaluated properly and the influences of wind and directional spreading are included, a new load model can be obtained:

$$\begin{aligned} X = {} & A_1\cdot\varphi^2\cdot a^2 + A_2\cdot\frac{\varphi^2\cdot a^3}{T^2} + A_3\cdot T\cdot\varphi\cdot a\cdot R\cdot\cos\theta_R \\ & + A_4\cdot\varphi\cdot a^2\cdot R\cdot\cos\theta_R + A_5\cdot R^2 + A_6\cdot R\cdot t\cdot\cos(\theta_R + \theta_d - \theta_t) \\ & + A_7\cdot t^2 + A_8\cdot T\cdot\varphi\cdot a\cdot t\cdot\cos(\theta_d - \theta_t) \\ & + A_9\cdot\frac{\varphi\cdot a^2\cdot t}{T}\cdot\cos(\theta_d - \theta_t) + C_w\cdot W^2\cdot\cos(\theta_w) \end{aligned} \tag{3.4}$$

A_1 to A_9 are constants associated with the variable X in a particular application. The inclusion of current blockage is simple and can be done by means of multiplying the

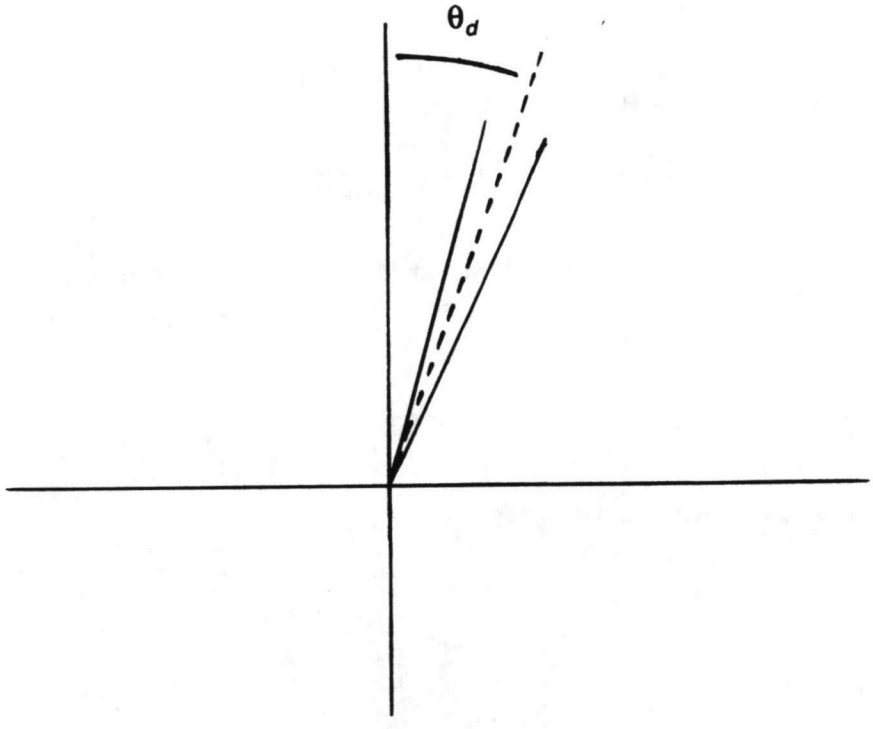

Fig. 3.4; A narrow sector and it's middle.

current speeds (i.e. R and t) in the equation by the current blockage factor (see section 2.2.5).

3.2.2. A load model for a strongly directional total current

When the total current is strongly directional, the angle between the total current and the mean wave direction can be included in the generic load model as a parameter which can be varied. The load model in this case will become:

$$X = A_1 \cdot v^2 + A_2 \cdot v \cdot \phi \cdot a \cdot T \cdot \cos(\theta_d - \theta_v) + A_3 \cdot \phi^2 \cdot a^2 + A_4 \cdot \frac{v \cdot a^2}{T} \cdot \phi \cdot \cos(\theta_d - \theta_v) + A_5 \cdot \frac{\phi^2 \cdot a^3}{T^2} + A_6 \cdot W^2 \cdot \cos\theta_w \quad (3.5)$$

which is similar to the load model derived in section 2.2.5. In the above formula θ_v represents the direction of the total current while θ_d represents the direction of the middle of the narrow sector considered (see fig. 3.4).

3.3. The statistics

Since all the storms from the wide sector are put into narrow sectors, the increased sample size allows the statistical analysis to be performed properly in each of the narrow sectors. The steps involved, for one of the narrow sectors, are now (see section 2.5 for the "normal" method);

1. Identify a wide sector of assumed storm similarity.

2. Divide this wide sector in a number (n) narrow sectors (determined by (tidal) current speed).

3. Put all the storms from a wide sector in a narrow sector by changing the directions of the storms to the middle of the narrow sector.

4. By combining the data for three-hour intervals of each storm, and using the generic load model that allows one for treating the tidal current as a parameter that can be varied, calculate the distribution, $P(X)$, of the extreme value of X for each of those storms in the narrow sector.

5. Re-normalise all the distributions (by dividing by the value of X_{mp}) to obtain the short term variability, $P(X \mid X_{mp})$. The short term variability can now be represented for all the storms by a similar probability distribution function being only conditional on the X_{mp} in a storm.

6. Take the X_{mp} values of the largest storms from a chosen directional sector and fit a density function, $p(X_{mp})$ [2,9]. The number of storms used in the fitting is chosen based on minimising the mean square error (MSE) of the parameter defining the fitted curve. The value of ν is the number of storms used to fit the probability density function, $p(X_{mp})$, divided by the duration of the complete time series.

7. Equations (2.15) and (2.16) are used, again, to obtain the probability distribution of the extreme value of X in a long time interval T.

$$P(X|r.s.) = \int P\left(X\middle|X_{mp}\right) \cdot p\left(X_{mp}\right) \cdot dX_{mp} \tag{2.15}$$

$$P(X|\nu \cdot \mathrm{T}) = \left[P(X|r.s.)\right]^{\nu \cdot \mathrm{T}} \tag{2.16}$$

The desired return value, say a 100 year value, can be read from the distribution.

Steps 3 to 7 can be repeated for all the narrow sectors and for different variables of interest.

Except for dividing the wide sector into a number of narrow ones, and putting all the storms into one of those narrow sectors, no changes are made to the procedure for deriving the (load) statistics. Joint met-ocean conditions, for a narrow sector, can be derived from the return values of total applied horizontal force (total horizontal force) and overturning moment.

3.4. Combined statistics over narrow sectors

The results for the return values of variables such as total horizontal force and joint wave and current values in narrow sectors are derived using all the storms in the wide sectors for the calculations in this sector. In doing so the arrival rates of the storms in the small sectors are assumed to be the same as the arrival rate in the wide sector. This is obviously not true, a narrow sector will contain fewer storms and thus have a smaller arrival rate. Consider the wide sector to be divided into N narrower sectors; by putting all the storms in a narrow sector with a size $1/N$ of the original size and assuming that the storms have a uniform distribution over the wide sector, the arrival rate in the sector is artificially increased N times. So strictly speaking, the y-year return values derived for a narrow sector represent the y·N-year return value.

In further calculations in this section, N represents the total number of narrow sectors, n the sector number and f_n the fraction of the number of storms used in the fitting, of $p(X_{mp})$, originally in a narrow sector n, i.e. as found in the data base before the concentrating of all the storms in this narrow sector. E.g., assuming a uniform distribution of the storms over the wide sector and N narrow sectors, f_n equals $1/N$.

Formula (2.20) as derived in section 2.8, is used here to relate the return periods (or rather one over return period, Q, the annual probability of exceedance) for the wide sector to those derived for the narrow sectors.

$$Q_{rp} = \frac{1}{\text{Return Period}} \tag{3.5}$$

$$Q_{rp} = A \cdot e^{\left(-\frac{L}{\delta}\right)} \tag{2.20}$$

$$L = \frac{L_{rp}}{L_{100}} \tag{2.20a}$$

The constants A and δ, in formula 2.20, are derived from the 100 and 1,000 year return values from the "normal" met-ocean design conditions (MDC) procedure. The "normal" MDC procedure refers here to the procedure as used at KSEPL for a wide

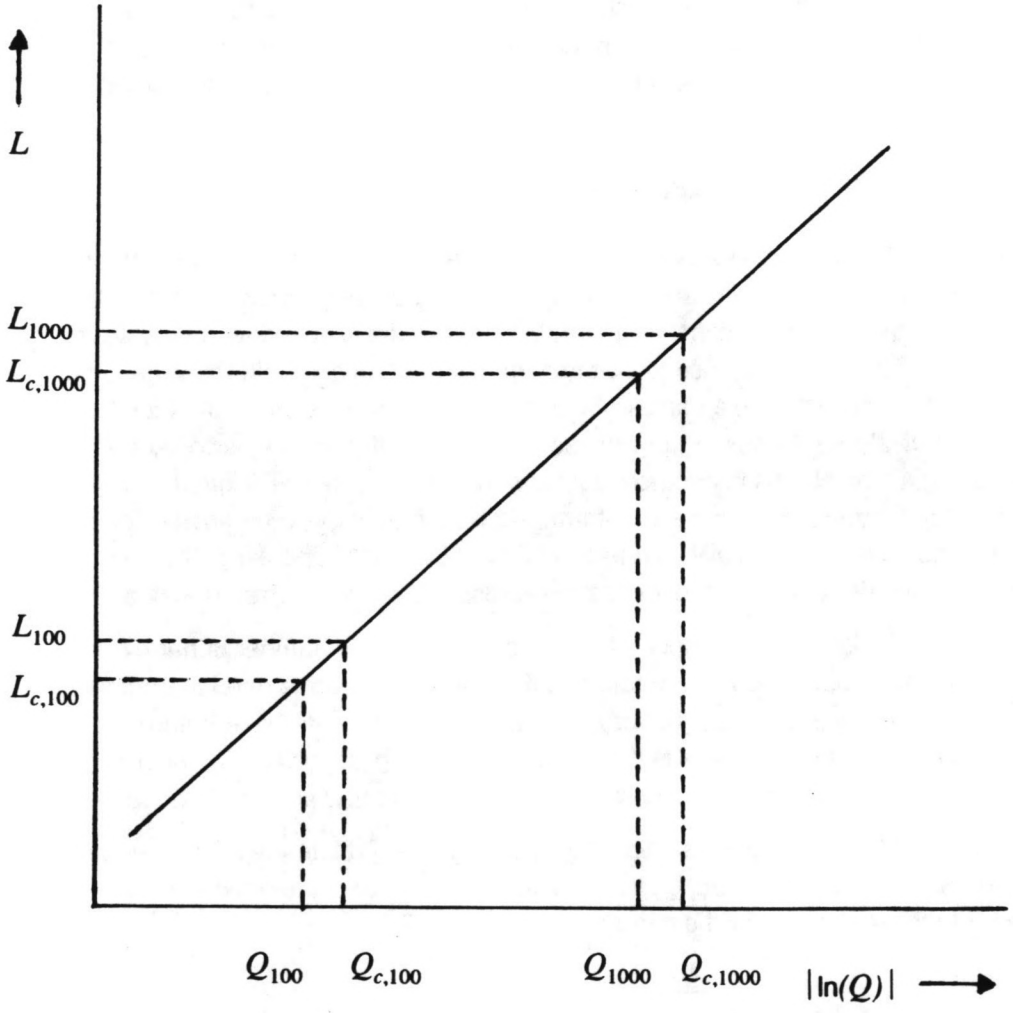

Fig. 3.5; Deriving return values for the combined sectors.

sector and a generic load model as discussed in section 2.2, i.e. without any of the changes suggested in this report.

The results for the return values derived from the MDC procedure for all the n narrow sectors are used to derive values of Q for all the narrow sectors, i.e. $Q_{\text{sector } n}$.

The values of Q for each sector are derived from formula 3.6, where L_{100} represents the 100 year return value for the global load L from the "normal" MDC procedure and $L_{100,\text{sector } n}$ the "100 year return" value for a narrow sector n.

$$Q_{\text{sector } n} = f_n \cdot A \cdot e^{\left(\frac{-L_{100}}{L_{100,\text{ sector } n} \cdot \delta}\right)} \tag{3.6}$$

The values of Q from each of the sectors are combined to derive a probability of exceedance for the wide sector, Q_c:

$$1 - Q_c = \prod_{n=1}^{N} (1 - Q_{\text{sector } n}) \tag{3.7}$$

For small values of $Q_{\text{sector } n}$ and Q_c this can be simplified to:

$$Q_c = \sum_{n=1}^{N} Q_{\text{sector } n} \tag{3.8}$$

The results for Q_c are used to derive return values for the wide sector by combining the statistic of the narrow sectors. The calculations are carried out for the "100 year" and the "1,000 year" return values as derived from the MDC procedure for the narrow sectors.

Summation of the values found of $Q_{\text{sector } n}$ associated with the 100 year return value in all the narrow sectors, N, from formula 3.6 gives one the $Q_{c,100}$. Analogously, a $Q_{c,1000}$ can be derived by replacing $L_{100,\text{ sector } n}$ by $L_{1000,\text{ sector } n}$ in formula 3.6 and using the results derived for the 1,000 year return values in all the narrow sectors.

These values of $Q_{c,100}$ and $Q_{c,1000}$ are associated with the 100 and 1,000 year return values as derived from a "normal" procedure. A line can be plotted through these points in a load versus annual probability of exceedance graph (fig. 3.5).

In order to derive an approximation of the 100 and 1,000 year return values for the combined sectors, values associated with an annual probability of exceedance, Q, of 0.01 and 0.001 can be read from figure 3.5.

The results of the statistical analysis in the narrow sectors can be combined to derive statistics for the wide sector. Differences found for the wide sector between the results from a "normal" procedure and from a combination of the results of the narrow sectors show the influence of the (strongly directional) current on the load statistics over the wide sector.

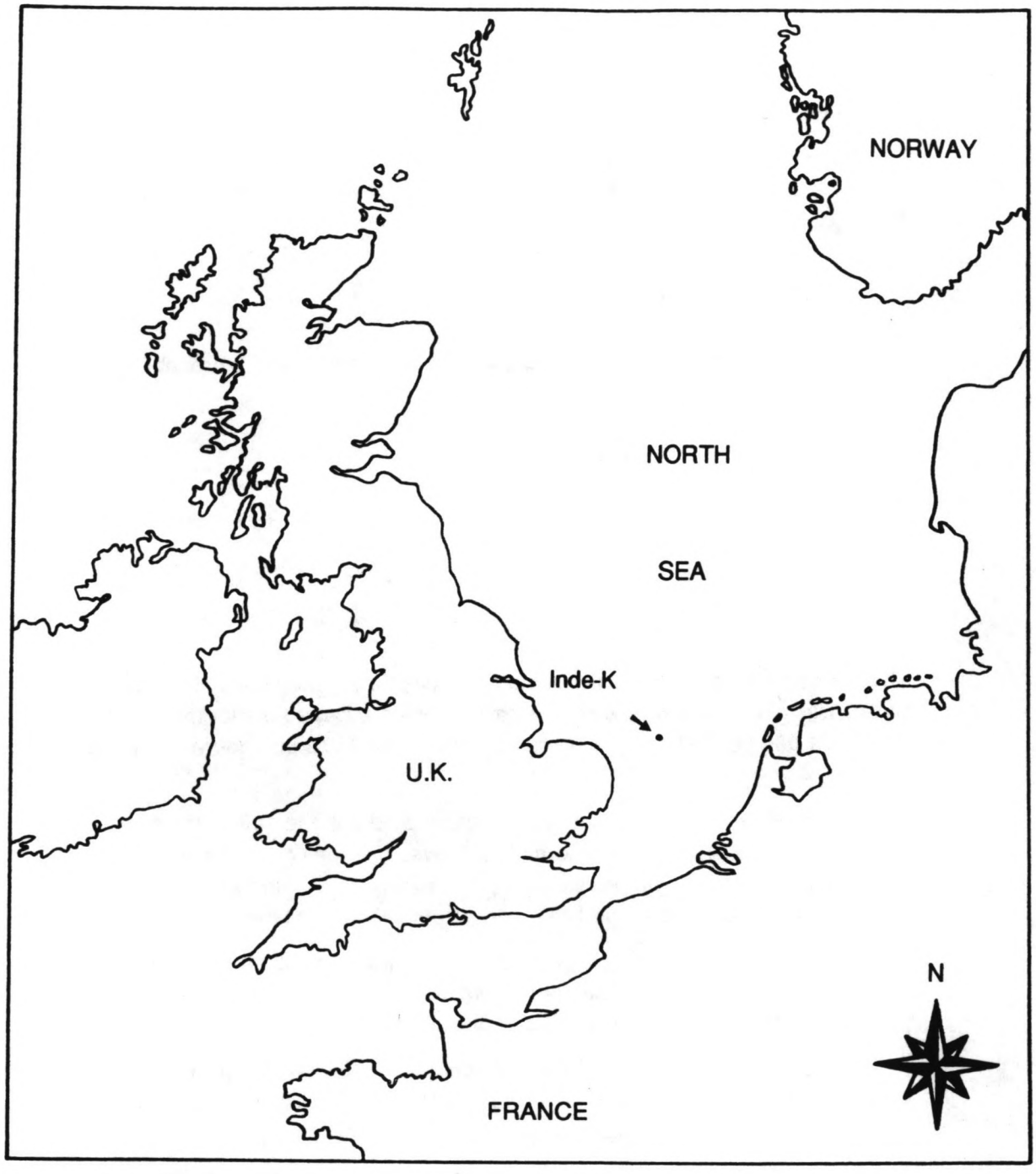

Fig. 4.1; Location of INDE-K.

4. ANALYSIS OF THE DATA BASE

4.1. The data base used in this project

In this project NESS hindcast data are used for a grid point at the location of the production platform INDE-K in the natural gas field Indefatigable. INDE-K stands in about 30 metres of water in the southern North Sea (SNS) (fig. 4.1) in the British sector. Over a period of 25.5 years the NESS data give information about the date, time and 11 environmental parameters at three-hourly intervals:

- average direction of sea state (deg.)
- significant wave height (m.)
- root mean square directional spreading (deg.)
- zero crossing period (sec.)
- mean wind direction (deg.)
- mean wind speed (m/s.)
- mean total current direction (deg.)
- mean total current speed (m/s.)
- mean residual current direction (deg.)
- mean residual current speed (m/s.)
- combined tide and surge elevation (m.)

This data base contains, instead of previously used ones, two current vectors. Residual current is defined as total current minus tidal current. Directions are given clockwise from North, current directions are given "pointing towards" while wave and wind directions are given "coming from". Special attention should also be paid to the wave period which is given in terms of the zero crossing period, while it is often (i.e. in other databases) given as peak period. The relation between peak period, T_p, and zero crossing period, T_z, depends on the wave spectrum. For the North Sea, the JONSWAP (JOint North Sea WAve Project, Hasselmann et al., 1973) spectrum is often assumed. For a JONSWAP spectrum the relation $T_z \approx 0.78 \cdot T_p$ is valid. Since the integrated procedure uses T_p in its calculations, the T_z found in the data base is converted in the code to T_p by multiplying it by 1.28.

4.2. Analysis of the data

Before the NESS data base is used in the met-ocean design conditions (MDC) procedure, the environmental parameters in it are subjected to an analysis. This is done in order to get more insight in the (directional) properties of the environmental parameters, e.g. how directional is the (tidal) current. Only the data during storm periods are used in the met-ocean design condition procedure. It seems therefore logical to analyse only the records in the storm intervals. The storms are selected from the data base by a pre-processor, MDCDAT, as used in the integrated procedure. The integrated procedure in use at KSEPL (see section 2.7) has been

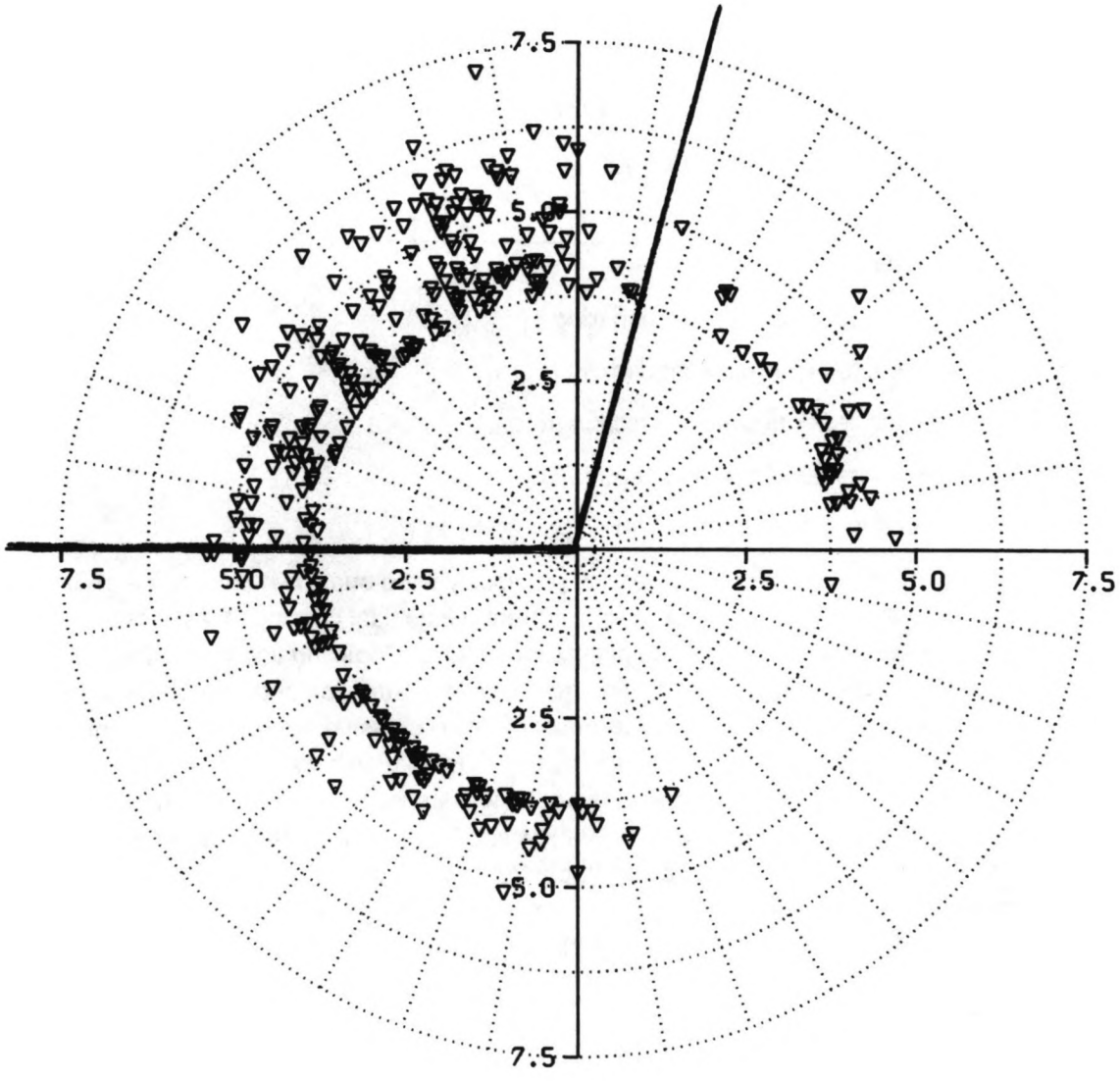

Fig. 4.2; Polar plot of peak H_s.

used previously for data files containing a single, only the total, current speed vector. The programs in the procedure were not designed to read and process the extra current data which are in the data file used in this project. Changes were made to the MDCDAT code in order to make it able to read , process (e.g. to be able to calculate the tidal current, speed and direction, from the total current and residual current) and write all the environmental parameters.

To check whether the tidal current has the expected main current axis, and to look at other properties and correlation structures of the environmental parameters in the storm data file, the data file is loaded into a spreadsheet program. In creating the storm file a threshold level of 3 meters for significant wave height is used. This threshold is chosen, keeping in mind that one needs more than 100 storms, in the wide sector, to perform the subsequent statistical analysis properly. The three meter threshold results in somewhat more than 300 storms coming from all directions and will result in about 200 storms for wave height statistics and about 100 storms for global load statistics for a 100 degree wide directional sector containing the most severe storms. In this section three-hour intervals from all directions are considered. Omitting the incomplete records (i.e. records without current and tidal and surge elevation information) leaves about two thousand complete three-hour records which can be used in the analysis of the parameters from the data base.

Scatter plots have been made of the distributions of wave height, current speeds over the directions and several other (combinations of the) data on the environmental parameters from the data base.

KSEPL has developed software for plotting directly from the output files from the MDC procedure. A polar plot made from the storm data file shows that the most severe storms, i.e. the storms with the highest peaks in significant wave height, H_s, came from a sector from 270 to 15 degrees (fig. 4.2).

The total current shows a major axis along which the highest current speeds occur. The highest current speeds are found to point to approximately 330 and 150 degrees clockwise from North, see figure 4.3.

The speed versus direction graph of the tidal current, shows very clearly a major axis along which the highest speeds occur (fig. 4.4).

Since some component of the residual current should be (at least partially) wave and wind driven, we may expect a correlation between the directions of residual current and waves. In contrast with what was anticipated, the graph of residual current direction versus wave direction (fig. 4.5) shows no obvious relation. This may be explained by the location of INDE-K in the relatively sheltered southern North Sea; the residual currents in this area may well be dominated by forces acting over a wide area of the North Sea.

A scatter plot of the directions of the tidal current versus the directions of the residual current (fig. 4.6) shows a relation where the residual current has a difference in direction of about 120 degrees to the residual current, while graphs of residual current speeds and tidal current speeds (fig. 4.7 and 4.8) show the same order of magnitude for the speeds of tidal and residual current. Because of the way tidal and residual current are defined, this was again unlike what one would expect. After extensive checking, no errors were observed in the, changed MDCDAT, code or in the way the

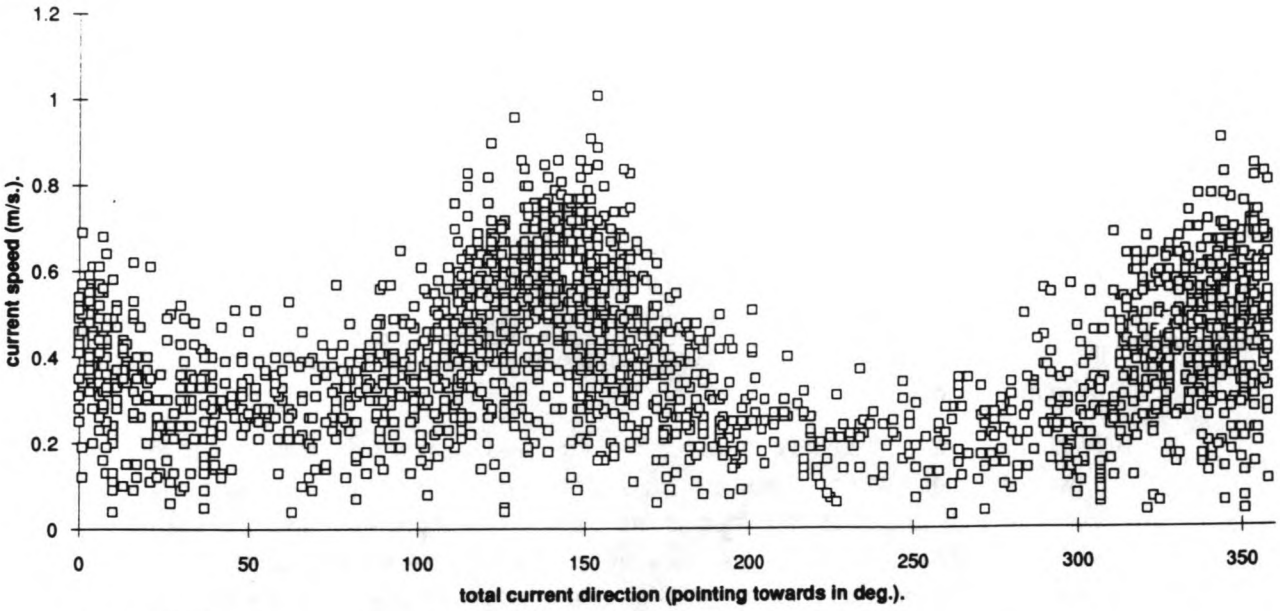

Fig. 4.3; Total current direction vs. speed.

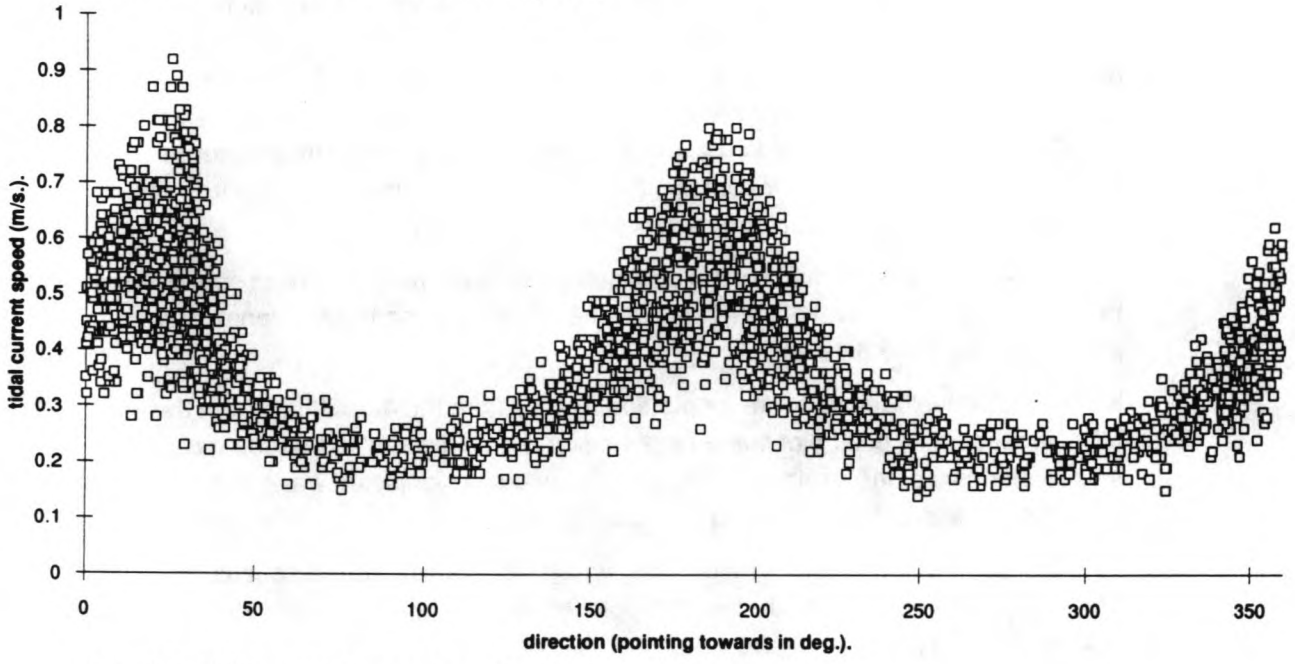

Fig. 4.4; Tidal current speed vs. direction.

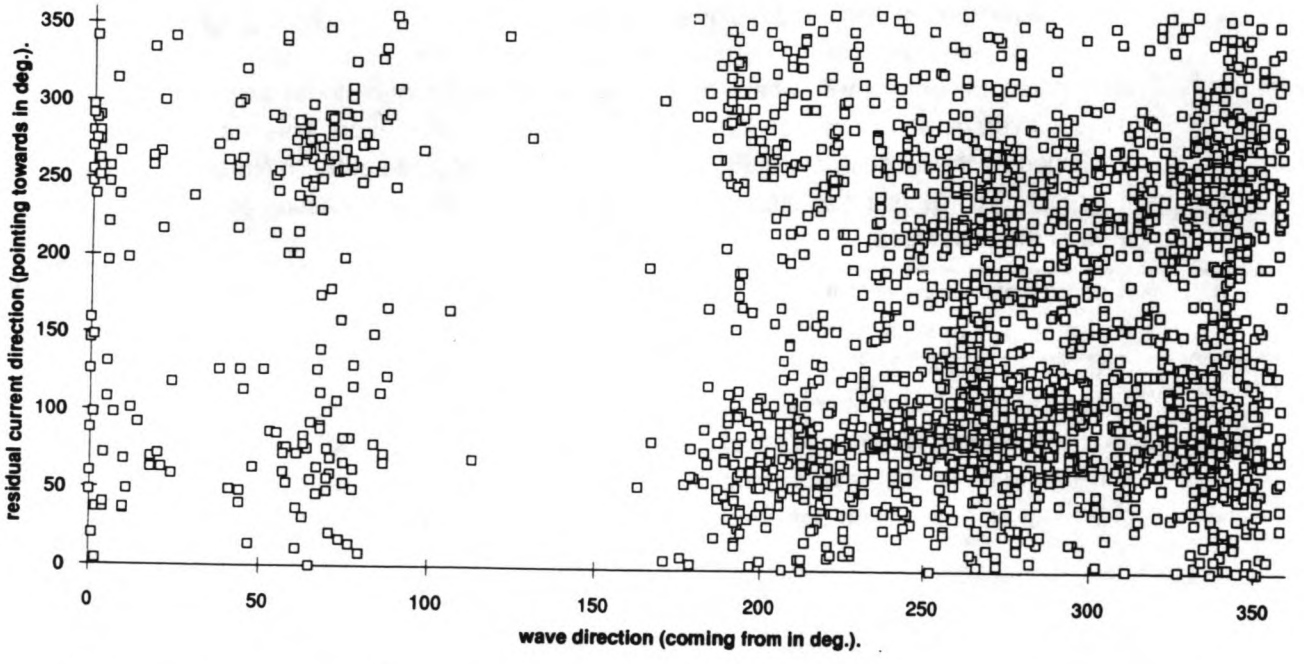

Fig. 4.5; Residual current direction vs. wave direction.

data were treated in them. It seems, therefore, as if the data on residual current and maybe also on tidal current in the data base might not be correct. One way of explaining the observed relation is that in generating the data base there are still tidal components left in the residual current after the harmonic analysis of the currents. At a later stage during the thesis work this supposition was confirmed by SIPM (Shell Internationale Petroleum Maatschappij); the data on total current are believed to be correct, however, the software for resolving tidal and residual current separately did not work properly. Therefore no confidence should be placed in the data on tidal and residual current in the data base. Since, at the time this data base was generated, there was no particular interest in separate data on tidal and residual current, no action was undertaken to improve the software.

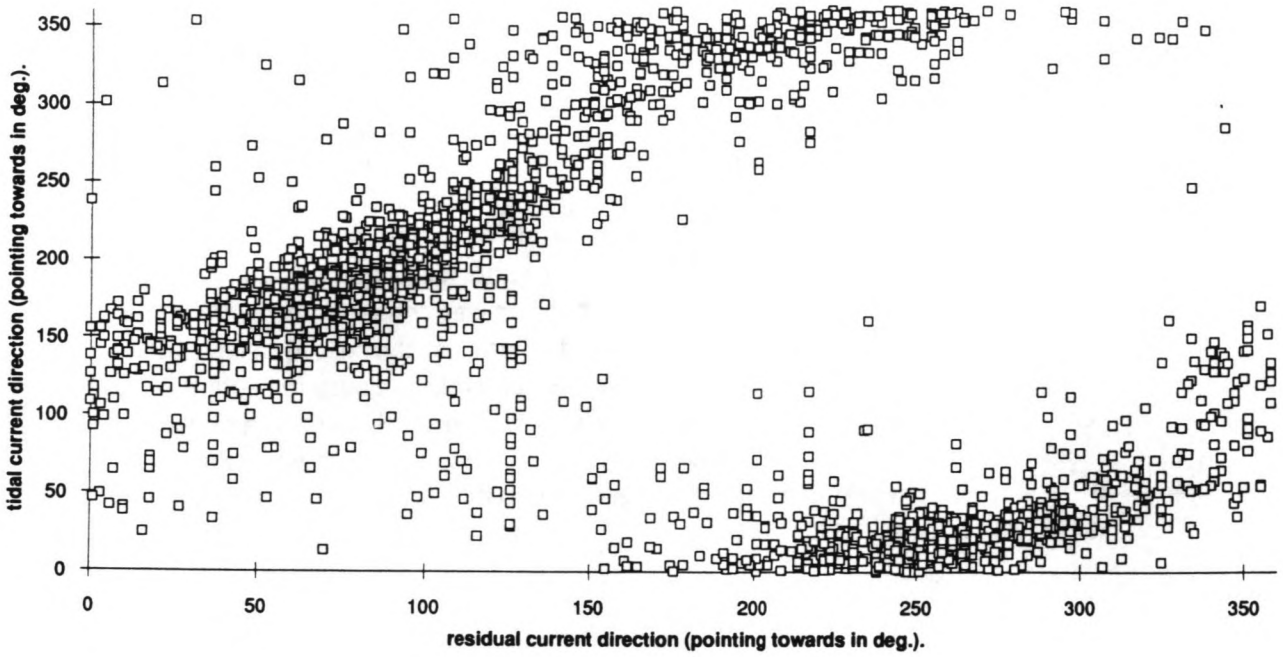

Fig. 4.6; Tidal current direction vs. residual current direction.

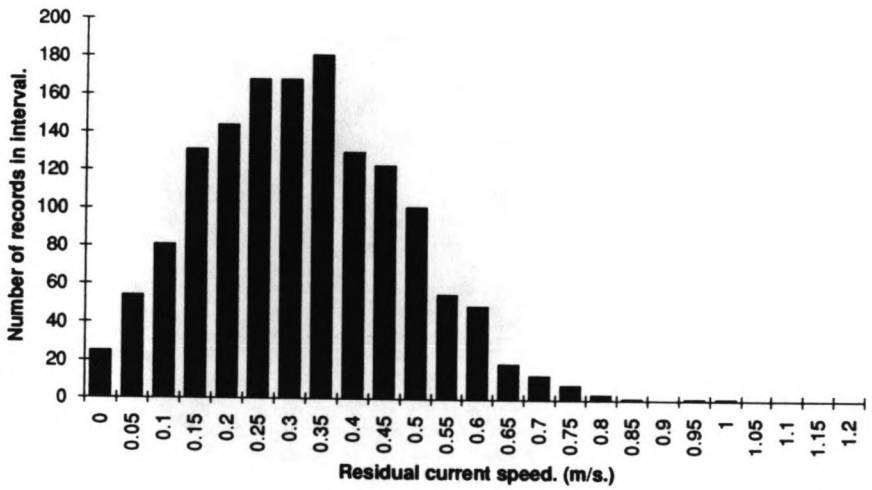

Fig. 4.8; Tidal current speeds.

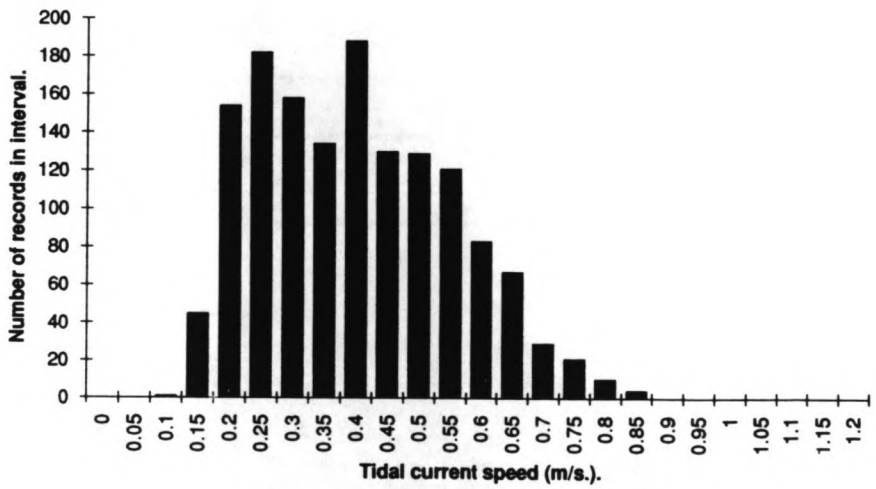

Fig. 4.7; Residual current speeds.

5. IMPLEMENTATION OF THE NEW APPROACH IN THE INTEGRATED PROCEDURE

The computer programs and problem data files of the integrated procedure for deriving met-ocean design conditions are adjusted to read and process the extra parameters as used in thesis work. The outline of the integrated procedure is given in section 2.7.

Since the narrow sectors are chosen to be typically 10 to 15 degrees wide, it seems justifiable not to spread all the storms over this small sector but simply concentrate them in the middle of it.

In analyses of the data base as discussed in the previous section (4.2), the total current appeared to be strongly directional and both the data in the NESS data base on tidal current and residual current seemed to be unreliable. The wave direction showed no correlation with the total current direction (fig. 5.1) and the total current showed to have an axis along which the highest current speeds occurred (fig. 4.3). Therefore, the suggested idea of treating the relative angle between wave direction and current direction as a parameter that can be varied is carried through. Hence, all the storms from the wide sector are now concentrated in narrow (total) current sectors. The second load model (3.5) as derived in section 3.2.2 is used in further calculations. The load model for a strongly directional total current:

$$X = A_1 \cdot v^2 + A_2 \cdot v \cdot \phi \cdot a \cdot T \cdot \cos(\theta_d - \theta_v) + A_3 \cdot \phi^2 \cdot a^2 + A_4 \cdot \frac{v \cdot a^2}{T} \cdot \phi \cdot \cos(\theta_d - \theta_v) + A_5 \cdot \frac{\phi^2 \cdot a^3}{T^2} + A_6 \cdot W^2 \cdot \cos\theta_w \qquad (3.5)$$

which is similar to the load model already used in the "normal" met-ocean design conditions procedure at KSEPL except for the current related cosine terms. Thus the constants in an existing load model used previously at KSEPL for the location of INDE-K can be used.

A generic load model (GLM) data file for a single pile with a diameter of 1 meter at the location of INDE-K generated at KSEPL and which is known to give good results is used unchanged. As stated above, the values for the constants in the generic load model, generated at KSEPL, are still valid. Therefore, no new calibration of the constants in the load model was necessary, and was consequently not performed.

The water depth at the location of INDE-K is about 30 metres and wave lengths associated with the extreme wave heights are about 100 metres. Under these circumstances the assumption of a relatively large water depth compared to the wave length, i.e. deep water conditions, no longer holds. A load model has been derived at KSEPL which is known to give more accurate results in intermediate water depths. This load model is used in further calculations and differs slightly from the one suggested before in this section:

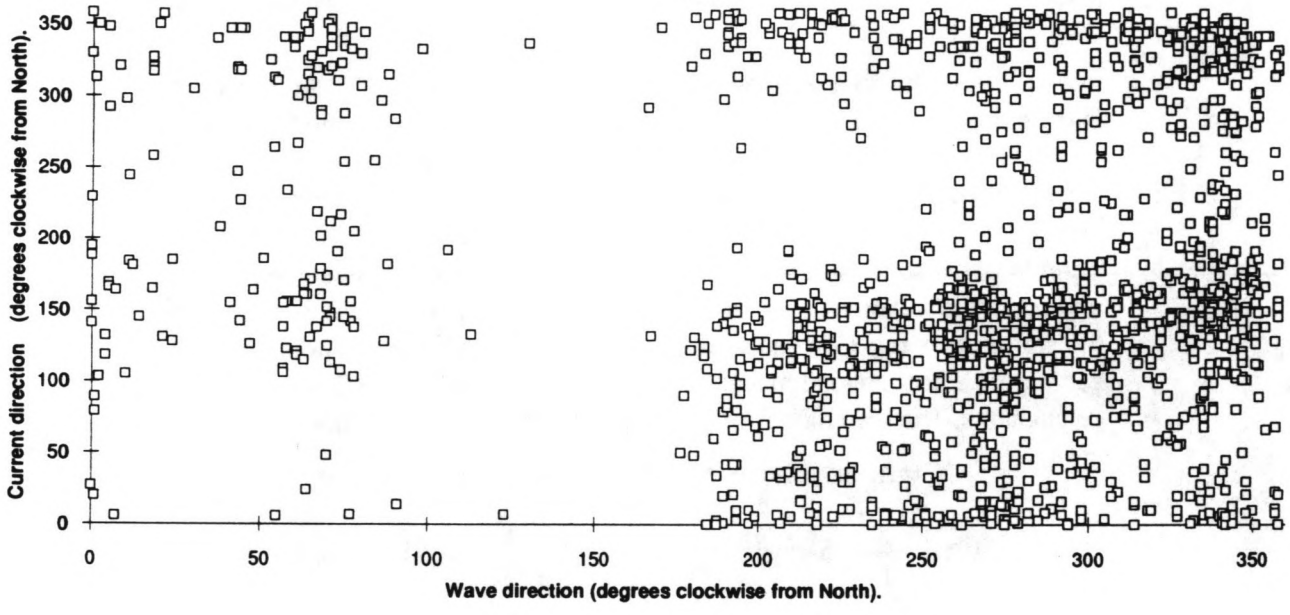

Fig. 5.1; Wave direction vs. current direction.

$$X = A_1 \cdot v^2 + A_2 \cdot v \cdot \phi \cdot a \cdot T \cdot \cos(\theta_d - \theta_v) + A_3 \cdot \phi^2 \cdot a^2$$
$$+A_4 \cdot \frac{v \cdot a^2}{T} \cdot \phi \cdot \cos(\theta_d - \theta_v) + A_5 \cdot \frac{\phi^2 \cdot a^3}{T^2} + A_6 \cdot v \cdot \phi \cdot a \cdot T^2 \cdot \cos(\theta_d - \theta_v)$$
$$+A_7 \cdot \phi^2 \cdot a^2 \cdot T + A_8 \cdot v \cdot a^2 \cdot \phi \cdot \cos(\theta_d - \theta_v) + A_9 \cdot \frac{\phi^2 \cdot a^3}{T} \qquad (5.1)$$
$$+A_{10} \cdot W^2 \cdot \cos\theta_w$$

The terms with constants A_6 to A_9 arise from a linearisation of the terms including wave influences, according to a Taylor series. In appendix C this load model is discussed in more detail. A similar model, i.e. without the parameter θ_d, has been used before at KSEPL for the location of INDE-K.

The MDC code was changed by adjusting the load model in it to the one given above (5.1), i.e. the parameter θ_d is incorporated in the load model for intermediate water depth. Some extra lines were also added to the code to read and write the direction of the middle of the narrow sector in which all the storms are concentrated and to convert T_z into T_p.

The MDC calculations can now be performed for a series of narrow sectors, one at a time. The following section gives the results of using the procedure for a series of narrow sectors at the location of INDE-K.

6. APPLICATION OF THE INTEGRATED MDC PROCEDURE

In order to investigate the results from the MDC procedure and the effect of the changes made to it on the results, a number of runs with the MDC procedure (with and without the suggested changes) were made, changing parameters like sector size and the direction of the small sectors. The influence of the wind is not included in (most of) the calculations, for reasons of simplicity.

6.1. Return values

As suggested in section 4.2, the directional sector from which the most severe storms are coming covers the range from 270 to 15 degrees. Over this wide sector the long time scale statistics of wave height are assumed to be homogeneous. Also some calculations were performed for slightly different sectors (i.e. 270-0, 255-15 etc.). The 100 year return values for wave height found for different wide sectors do not show much difference. This indicates the robustness of the method. The results also show good agreement with results derived earlier at KSEPL for this location.

From the plots discussed in section 4.2, the directions from which the strongest currents are coming are found to be 150 and 330 degrees. The computations, in the MDC procedure, involve significant computer processing time. Therefore, a limited number of narrow sectors, for which the calculations are performed, is chosen. The 105° wide sector is divided into seven narrow sectors of equal width. Table 6.1 shows some of the properties of the seven narrow sectors.

Table 6.1; The sector numbers, directions and sizes.

sector number n	bearings (degrees)	middle of sector (degrees)	width (degrees)
1	270-285	277.5	15
2	285-300	292.5	15
3	300-315	307.5	15
4	315-330	322.5	15
5	330-345	337.5	15
6	345-360	352.5	15
7	360-15	7.5	15
		width of the wide sector:	105

The option is used to generate estimated (or "bogus") most probable extreme values of global loads for storms with data on wave height but without current records (see section 2.7). Using the complete storms a correlation rule (2.19) between the most probable extreme values of both total horizontal force and overturning moment and wave height is derived.

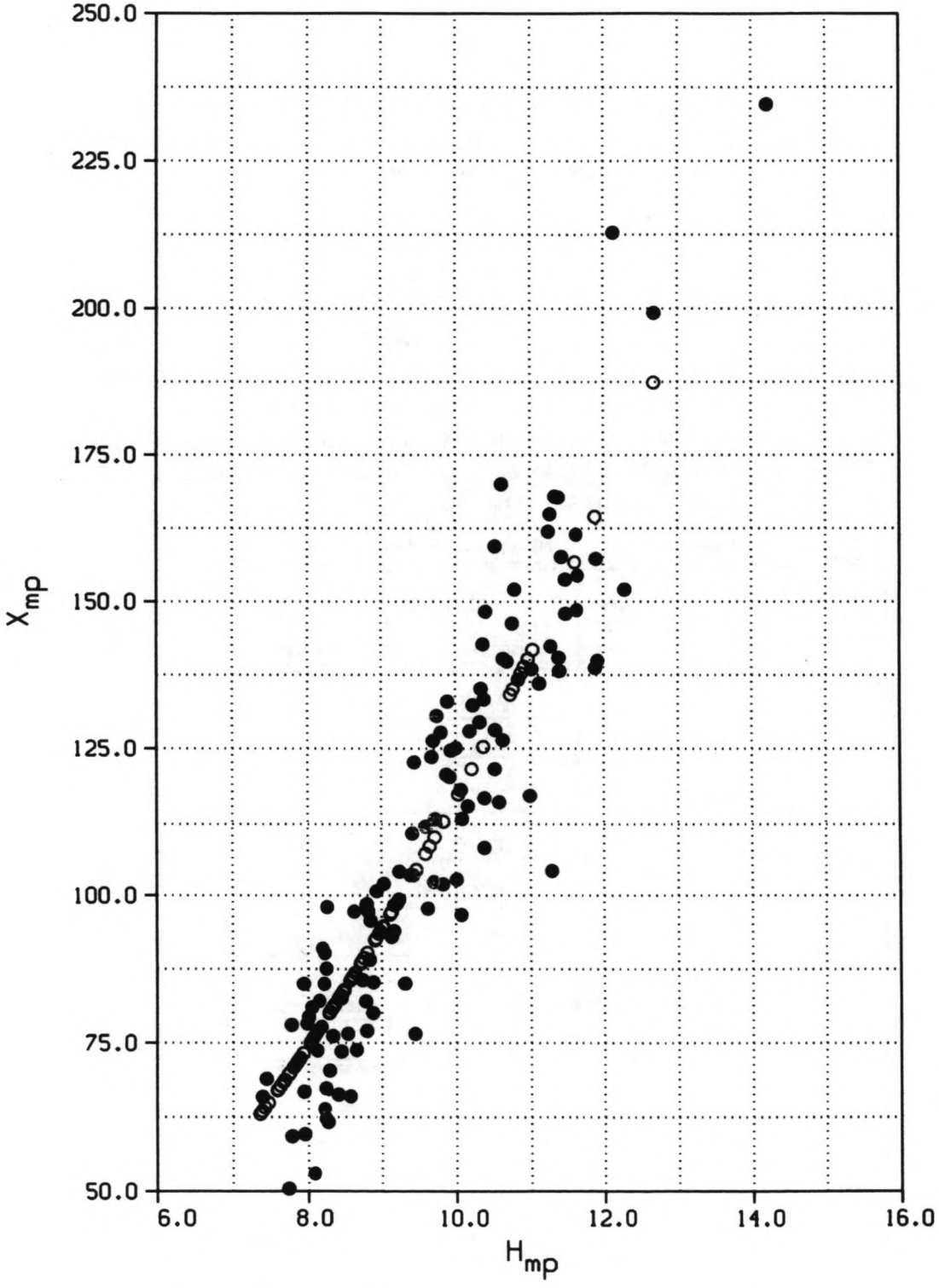

Fig. 6.1; Example of the results of the correlation rule for total horizontal force.

$$X_{mp} = \alpha \cdot \left(\mathrm{WHT}_{mp}\right)^2 \tag{2.19}$$

Figure 6.1 shows, as an example, the most probable extreme values for total horizontal force versus those for wave height. The white dots represent the most probable values derived via the correlation rule, for one of the narrow sectors.

This relation is used to generate "bogus" values for the variables in those storms for which the most probable maximum of wave height is known but not that for the variable of interest. This allows more storms to be used in the subsequent statistical analysis. However, one should be cautious not to add too great a number of "bogus" storms. Here some 100 "bogus" values were derived of a total of about 210. Since the fitting of 1-$P(X_{mp})$ is done over an optimum number of storms not all the ("bogus") storms will be used in the fitting (e.g. about 180 of the 210). Comparing results derived with and without the use of the correlation rule showed that the fits made including "bogus" storms were much better. The correlation rule is used in further calculations.

For reasons of comparison, some "normal" runs were also made. "Normal" here refers to the standard method developed in KSEPL, although it is, itself, unconventional compared with the traditional methods of the European offshore industry. This was done by using the MDC procedure for the wide sector and with the load model (2.14), without any of the changes suggested in this report, as given in section 2.2.5. Runs were made with and without wind and without both wind and current. Wind and current are omitted from the calculations simply by setting the constants of the terms including wind or current in the GLM data file to zero. As expected, the return values derived by doing a "normal" run are between the minimum and maximum values derived from the changed code, see table 6.2. The difference found between the 100 year total horizontal force return values from the "normal" procedure when including and omitting current is approximately 16%.

To get an impression of the differences in return values for different narrow sectors and the performance of the MDC procedure, a start was made by performing the procedure for a few of the narrow sectors. Considering the return values for total horizontal force and overturning moment, for four of the seven narrow sectors, showed the presence of a trend over the wide sector. However, maximum return values were not necessarily found for the narrow sector containing the highest current speeds. Comparing the way the fittings were done in the procedure for different sectors pointed out that this could be the cause of not finding the highest return values for total horizontal force and overturning moment in the most severe sector. The shape of the fitted curve for the different sectors showed some variety. This may be due to the scarcity of data points in the "tail" (i.e. amongst the most severe storms) of 1-$P(X_{mp})$.

A random number generator is used in the procedure for fitting a probability distribution of the most probable extremes for storms ($p(X_{mp})$), see section 2.5, to estimate the index of variation between the fitted curve and the data points for X_{mp}. This random number generator needs a seed to generate a first random number; a different seed can result in a different optimum number of X_{mp} values used for fitting a curve, which in turn results in a different fit. A different fit will result in different return values for X. Different values for the seed have been tried. Although the

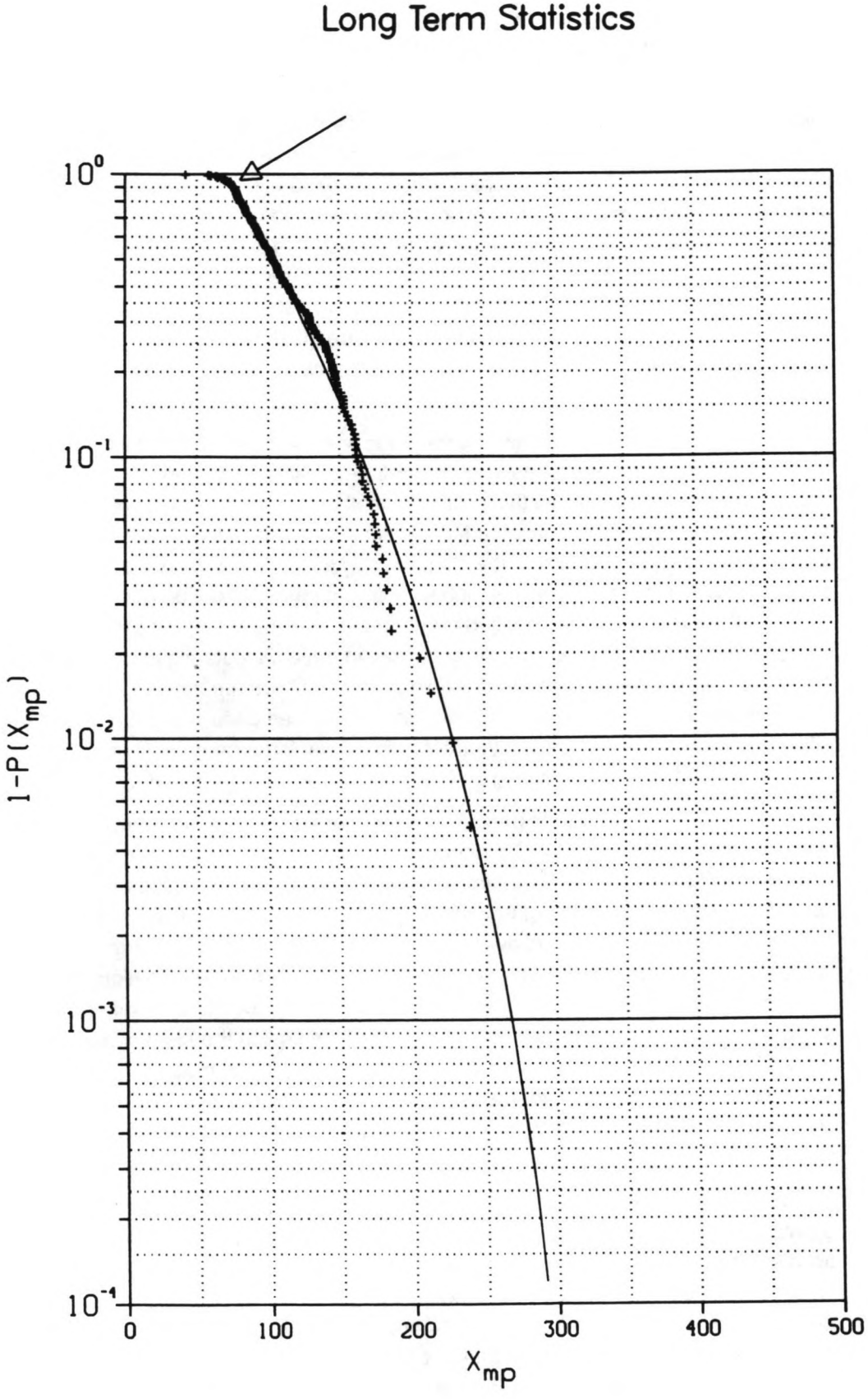

Fig. 6.2; Example of the fitting of (1-$P(X_{mp})$)

different seeds were found to have some effect on the number of storms used in the fitting and thus on the shape of the fitted curve, again for different sectors rather different fits were found. This shows that the fitting procedure, although not leading to completely unrealistic answers, was not robust enough. As will be discussed in the next paragraph a method was used to add some extra values of X_{mp} in the tail of the curve.

In the (MDCDAT pre-processed) storm file a number of storms do not have data on current during the entire storm period. Some of them lack data on current only in the records with a low significant wave height, compared to the maximum significant wave height in that storm. These storms can therefore not be used directly in calculations of total horizontal force and overturning moment, but only via the correlation rule. However, it has been shown that sea states with H_s lower than 0.8 times the maximum H_s in that storm interval will not contribute significantly to the probability distribution of the maximum wave height within a storm [2,8]. Therefore the records for these sea states can be left out of the calculations, without significantly influencing the probability distributions of extreme values of X. Omitting these records allows a few extra storms, which now do have records on current during the entire storm interval, to be used directly in the calculations rather than via the correlation rule (2.19).

Some changes were made in the MDCDAT code to omit the parts of the storm records with a H_s below 0.8 times the maximum H_s in that storm. In this way eleven extra "complete" storms were found. A few of these storms which are now complete are amongst the most severe storms. These storms will therefore be in the "tail" of the 1-$P(X_{mp})$ graph, and are significant in the fitting. Figure 6.2 gives an example of the fitting of the probability distribution function for the most probable maximum value of total horizontal force (including the extra complete storms). New MDC calculations with the new storm data file were performed. Return values for wave height remain, within a few percent, the same. The total number of storms found in the wide sector is, obviously, unchanged. However, instead of about 100, in this case 90 "bogus" values are used in the calculations for the variables total horizontal force and overturning moment. The new calculations turned out to be more stable in the fitting process. The small differences in return values for the different narrow sectors could now be captured. The similarity of the fittings over the different narrow sectors gives confidence in the stability of the fitting process. The maximum return values for both total horizontal force and overturning moment are now found in the directions where they are expected to be, in the direction of the narrow sector where the maximum current speeds occurs (sector 4). Table 6.2 gives the results for the 100 and 1,000 year return values for total horizontal force derived from the procedure, for the seven narrow sectors and for a "normal" run. The return values calculated for the narrow sectors are derived by putting all storms from the wide sector in the narrow sector, thus for an artificially increased arrival rate (see section 3.3).

Table 6.2; Total horizontal force return values.

sector *n*	Return values	
	BSR-100 (kN)	BSR-1000 (kN)
1	296.59	360.79
2	318.06	386.79
3	318.23	385.39
4	327.47	397.62
5	326.39	396.55
6	316.35	385.18
7	314.42	385.35
"normal"	317.81	386.85

In the runs of the integrated MDC procedure for the seven narrow sectors, again, some problems are encountered in the fitting of the long time scale distributions. The fitting procedure is not as stable as it was expected to be. For sector number 7 the procedure gives return values for total horizontal force which are higher than expected on grounds of the trend showed over all the sectors.

The problem shows that the differences of interest to us in this project are really at the limit of (or even smaller than) what the procedure, and the met-ocean data base, can be used for. However, one should consider the fact that the MDC procedure is designed to derive return values associated with rare events, by extrapolating (load) statistics beyond the limited duration of data gathering of a data base. In this perspective, differences of a few percent are of minor importance, and the procedure works rather well.

The procedure involves an extrapolation of 25 year data to a 100 year level. The differences derived in this report for the return values between adjacent sectors are really marginal. When using the results as design conditions one would loose the differences as found in this report in a rounding process, e.g. after assumptions made and extrapolation a total horizontal force return value as derived from the MDC procedure should really not be interpreted as having 5 significant figures. They are presented to such an accuracy in this report because the differences in the results between two adjacent sectors are so small.

Comparing the fits for different narrow sectors showed that the fitted curve for sector 7 has a somewhat different shape. As discussed in section 2.5 the number of data points used in the fitting procedure selected is based on minimising the mean square error (MSE) in the fitted parameter. The differences found from the MDC procedure between the lowest MSE and the MSE associated with a fit which is using one extra data point is very small. Using an extra data point makes the shape of the fitted curve similar with the fits for other sectors and gives return values which follow the trend over the wide sector. The results of a fitting procedure using one extra data point are used in the table above (table 6.2).

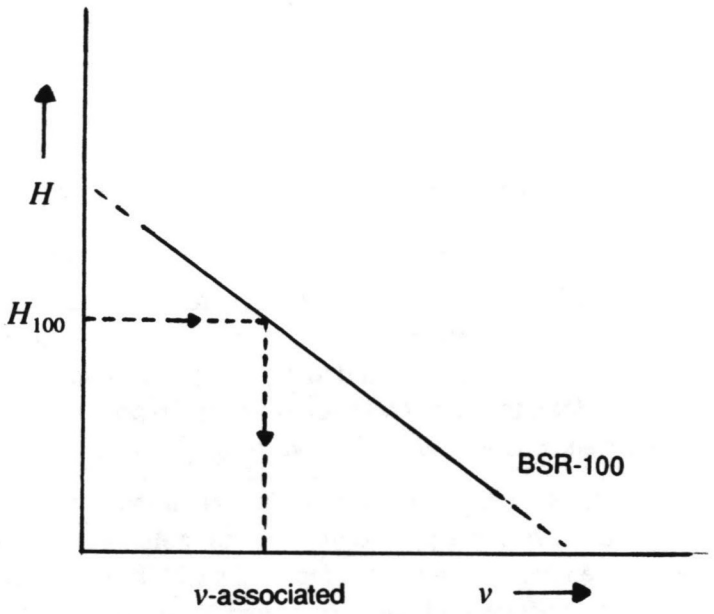

Fig. 6.3; Joint met-ocean conditions.

The difference in the 100 year return values of total horizontal force for the least (1) and most (4) severe sector in table 6.2 is about 11%. Considering the difference of 16 % found between the results when including and omitting current, this difference is significant.

6.2. Joint conditions

Omitting the influence of wind, some back calculations for joint-met ocean conditions are carried out. The current speed associated with the 100 year return value for wave height is calculated (fig. 6.3). The associated current speed is the in-line current speed that in combination with the 100 year individual wave height, produces the 100 year return value for total horizontal force (table 6.3 shows the results for the narrow sectors and for a "normal" run).

Representative values are used in the back calculations for the peak period, T_p, and for the reduction factor used in the generic load model to account for the reduction of wave loads due to directional spreading, φ:

T_p = 11.5 s
φ = 0.88

Calculating the current speeds associated with total horizontal force and overturning moment for the different sectors, the highest associated current speeds are found (as expected) in the sectors containing the highest current speeds and significantly (up to 40%) lower values in the less severe sectors.

Table 6.3; 100 year joint met-ocean conditions (calculated from the return values of wave height and total horizontal force).

	Joint Met-ocean Conditions	
sector n	H (m)	v (m/s)
1	15.6	0.30
2	15.6	0.43
3	15.6	0.43
4	15.6	0.48
5	15.6	0.47
6	15.6	0.42
7	15.6	0.40
"Normal" run	15.6	0.42

The in-line current speed of 0.48 m/s associated with a wave height of 15.6 metre may not seem very high. But compared with the northern North Sea (with a water depth of about 170 metres) where 100 year joint met-ocean conditions are found of a wave height of about 27.5 metre and an in-line current speed of about 0.25 to 0.30

m/s [1], the current speed in the southern North Sea is, relatively speaking, significantly higher.

Table 6.4 gives as an example the results (for total horizontal force, BSR, and overturning moment, OMT) in case a single pile with a diameter of 1 metre from the LOAD program (see appendix C)is considered in the above given joint met-ocean conditions. From this table it can be seen that the contribution of the current to the global loads in the southern North Sea (SNS) is considerably higher than in the northern North Sea (NNS). In the southern North Sea the current speed in this case contributes to the total horizontal force for about 24%, and in the northern North Sea for about 15%.

Table 6.4; Contribution of the current speed to the global loads on a single pile, 1 metre diameter, in joint met-ocean conditions in the southern and the northern North Sea.

SNS, water depth 30 m, H_{100} = 15.6 m and T_z = 9 s		
current speed (m/s)	BSR (kN)	OMT (kNm)
0.48	325	7,216
0	247	5,724
NNS, water depth 170 m, H_{100} = 27.5 m and T_z = 12 s		
current speed (m/s)	BSR (kN)	OMT (kNm)
0.25	671	100,438
0	566	87,152

6.3. Combined statistics over the sectors

As discussed in section 3.4 the load statistics of the narrow sectors can be combined to derive load statistics for the wide sector. These load statistics derived from combining the results of the seven narrow sectors can deviate from the results derived from the " normal" MDC procedure.

In table 6.5 the narrow sectors are given and the distribution of the number of storms used in the fitting of the long time scale distribution of X_{mp} over the narrow sectors. Table 6.6 gives some results for a uniform distribution of storms over the wide sector and a distribution as found in the NESS data base for this location.

Table 6.5; The sector numbers, directions and the distribution, over the narrow sectors, of the number of storms used in the fitting procedure.

sector number n	bearings (degrees)	middle of sector (degrees)	number of storms
1	270-285	277.5	16
2	285-300	292.5	30
3	300-315	307.5	26
4	315-330	322.5	24
5	330-345	337.5	50
6	345-360	352.5	32
7	360-15	7.5	8
Total number of storms in the wide sector:			186

Table 6.6; Comparison of total horizontal force return values, derived from combining sectors.

Return values	"normal" run	Uniform distribution.		Distribution as in NESS.	
		combined	Δ% to "normal"	combined	Δ% to "normal"
BSR-100 (kN)	317.81	317.78	-0.007	319.97	0.68
BSR-1000 (kN)	386.85	387.29	0.11	389.87	0.78

The distribution of the number of storms over the wide sector clearly influences the return values derived for combining the statistics of the narrow sectors. An extreme distribution, with little physical meaning, is obtained when all storms are put in the narrow sector with the lowest current speeds, i.e. the fraction in that sector is one and the other sectors are empty. A difference in that case is found with the "normal" run of about 7%. However if such a high fraction of the storms was found in this narrow sector, the wide sector would not have been chosen in the first place.

For the location of INDE-K the direction of the most severe storms does not differ that much from the direction of the strongest current speeds (see fig. 4.2 and 4.3). This explains the small difference found between the return values for the combined sectors and from a "normal" run.

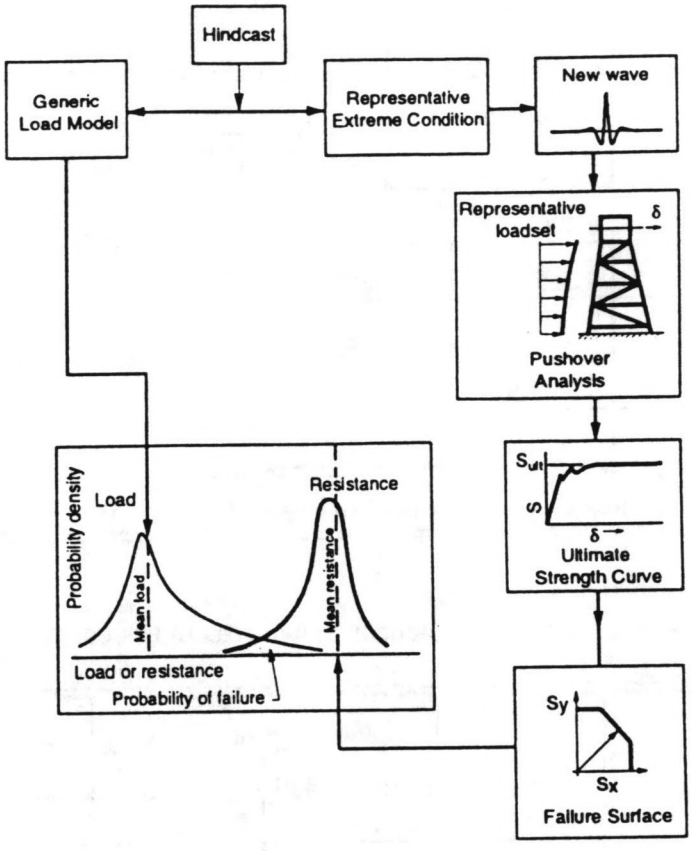

Fig. 7.1; Structural reliability assessment procedure.

7. STRUCTURAL RELIABILITY ANALYSIS OF OFFSHORE STRUCTURES

7.1. Introduction

Oil companies, when operating offshore hydrocarbon fields, have to satisfy two general objectives. On one hand they have duty to themselves, their shareholders and society to produce oil and gas as economically as possible. Low oil prices, as in the recent past, make profits in the offshore oil industry marginal. New production plans, e.g. involving the design of new structures or satellite fields developments, should therefore be designed as cost effectively as possible. On the other hand oil companies must ensure an acceptable level of safety for employees, society and the environment. The required level of safety is not solely determined by the companies' own standards but also by those imposed by government agencies and certifiers. Achieving a higher level of safety will, in general, require higher investments. Therefore the two objectives do interact, safety issues will involve economic considerations. They should not be considered as purely in conflict, since money saved on one project can be used to make another safer.

In order to be able to make rational decisions it is necessary to quantify the reliability of offshore structures during extreme conditions, to optimise the factors in design codes and evaluate these risks against those prescribed (e.g. by design codes), the risks of other hazards and what is regarded acceptable. Risk is in general defined as probability of an accident multiplied by the consequences. When comparing risks in economical terms, it is not always easy to estimate the financial consequences of all kinds of accidents, e.g. the loss of human lives or environmental damage are not easy to express in terms of money. The likelihood of structural failure is predicted by calculating the probability of environmental load exceeding the resistance of the structure.

Calculations of the extreme environment(al conditions), such as carried out in the previous sections of this report can be used as input for reliability analyses for offshore structures, as shown in figure 7.1 [10]. As explained before, the extreme environmental conditions can be derived, via back calculations from the extreme global loads. That is, the 100 year wave and associated in-line current which, in combination, generate the 100 year level of total horizontal force can be calculated from the 100 year return value of total horizontal force. Accounting for the phenomenon of strongly directional currents, as discussed in previous sections, changes the distribution of the extreme environmental conditions. Here, we investigate the influence of these changes on the results of a structural reliability analysis for an offshore structure.

This section will outline the theory of structural reliability analysis. First it will be outlined in general terms after which it will be used, in the next section, to estimate the probabilities of failure for a construction with a failure surface comparable to that derived for a space frame structure, such as INDE-K, with and without accounting for the phenomenon of a strongly directional current.

7.2. Outline of a structural reliability analysis

Although some of the theory discussed in this section will in principle be applicable to any kind of (offshore) structure, again it will be explained for space frame structures. This will be most evident in the shape of the failure surface used in section 8.1, which is typical for a jacket type of space frame structure, as well as the drag dominated loading. The methodology as discussed in this section and following sections is developed at KSEPL. It therefore may include some advanced methods and procedures developed in the past few years at KSEPL which are different from those used traditionally in the offshore industry, e.g. the New Wave model (Tromans et al., see appendix C) is used in the prediction of the shape of the extreme wave and its associated water kinematics.

A reliability analysis for a structure can be performed only after one has determined the global resistance to its loading. The collapse of an offshore structure can result from a number of mechanisms, such as member failure due to member buckling or tensile failure, foundation failure or a combination of these. Which failure mechanism dominates depends on the design of the structure, the load distribution, the materials, water depth, soil conditions etc. To determine the resistance to global load, one first needs to know the loads exerted on a given structure at different points, from sea bed to topsides, when it is exposed to "representative" extreme environmental conditions. The level of global load exerted on the structure in these representative environmental conditions is called the reference load set. The behaviour of the loaded structure and its ultimate strength is then determined by multiplying this "reference load set" by a stepwise increased "load factor" and computing the product's effect on the structure up to the point of total collapse. This collapse analysis is repeated for several directions to produce a failure surface, i.e. a boundary that marks the maximum load that the structure can sustain from all directions. The probability of failure within a given time period (typically one year, then expressed as the annual failure rate) is then finally obtained by combining the probability distribution of resistance to load with those of long term extreme loads, taking account of the distributions' directionality. The following paragraphs will discuss the steps in a structural reliability analysis in more detail. More details and background information will be given in appendix F.

Once one knows the environmental parameters (e.g. wave height and current speed) at the (future) location of an offshore structure, as derived from the MDC procedure, one can calculate the hydrodynamic forces exerted by the flows of the water around the structure using Morison's equation (see section 2.2.1). The reference load set for use in ultimate strength computations would thus consist of the hydrodynamic forces derived for the water kinematics associated with the representative environmental conditions (e.g. corresponding to say, the 100 year level of a global load such as total horizontal force).

An assessment of how safe an offshore platform really is should be based on a determination of how much load it can sustain before collapsing. In particular, it should quantify the "reserve" strength of the structure beyond its design load, up to the point where it totally collapses. The standard procedure by which this ultimate strength is investigated is known as a static pushover analysis. Such an analysis essentially tests a structure's capability of resisting the forces exerted on it due to the

passage of one extremely large wave and its associated current, together with the smaller force contribution of the wind that would occur simultaneously. In most instances a pushover analysis will not consider the effect of such loading on the structure's foundation, since the foundations of fixed structures tend to be stronger than their supporting members.

In a static pushover analysis the reference load is stepwise increased, starting from zero, by multiplying it with a so called load factor. For each load step a static analysis is performed of the structural deformations.

Eventually, when several supporting members have undergone plastic deformations the structure will start to collapse progressively. The load factor at the point where the structure's deflections start to increase without any further increase in the applied load, characterises the ultimate strength of the structure.

When carrying out a series of pushover analyses, one can get insight into how the structure under consideration is most likely to fail, and upon which global loading variable that depends (i.e. total horizontal force or overturning moment).

If the pushover analysis is repeated for several wave attack directions, one can plot the ultimate strength load factors and their respective directions as vectors based at the origin of a coordinate system centred on a plan view of the structure. Drawing a line through the vector tips for all the directions outlines a surface, the failure surface, that reveals the ultimate strength of the structure in all loading directions.

The next step in the reliability analysis will then be to investigate how likely it is that the global loading variable of interest will exceed the ultimate strength of the structure. This can be derived from the probability distribution of long term extreme global loading. This distribution of the extreme global loads can be expressed by a simple line if the loading is re-plotted as a logarithmic function of return period (i.e. the inverse of its probability), as shown in section 2.8. Again it is emphasised that the long term global loading statistics depend strongly on the geographical location.

7.3. Calculation of the probabilities of survival and failure

The prediction of the probability of failure begins with the calculation of the probability of survival, P_θ, under extreme loading in a very narrow sector centred on the wave attack direction, θ. This is the probability that the load does not exceed the value required to cause structural failure, i.e. does not fall outside the failure surface, in that direction:

$$P_\theta(\text{survival}) = P_\theta\left(L_\theta < \lambda_\theta \cdot S_{\text{ref}}\right) \tag{7.1}$$

where:

L_θ = environmental load in the direction θ
λ_θ = collapse load factor in the direction θ
S_{ref} = reference level of the global load

Once the failure modes are known then the type of global load (i.e. total horizontal force or overturning moment) causing failure is known. The load factor λ is the length of the vector determining the failure surface as derived from the pushover analysis

(see appendix F). It represents the ratio between the ultimate strength of the structure in a direction and the reference load level:

$$\lambda = \frac{S}{S_{ref}} \tag{7.2}$$

in which

S = ultimate strength of the structure
S_{ref} = reference level of the global load of interest.

For the reference load level the 100 year level of the global load could be chosen as derived (from the environmental conditions) from the MDC procedure:

$$\lambda = \frac{S}{S_{100}} \tag{7.3}$$

S_{100} = 100 year return value of the global load of interest

When the uncertainty in system strength is included in the calculation, the above equation (7.1) becomes a convolution of the probability density of system collapse strength and the cumulative distribution of extreme loading, both for the direction θ.

Assuming independence of rare events, i.e. the characteristics of a given extreme load are not in any way influenced by the characteristics of preceding extremes, we can write the probability of long-term survival under extreme loading as the product of the probabilities of surviving the extreme loading predicted for each separate wave attack direction:

$$P(\text{survival}) = \prod_{\text{all } \theta} P_\theta\left(L_\theta < \lambda_\theta \cdot S_{ref}\right) \tag{7.4}$$

The probability calculations are not necessarily performed over all possible directions. The directions from which the most severe storms, and thus the highest global loads, are coming will, in general, suffice. The wide sector is chosen on the basis of extreme wave heights in storms. The storms from directions outside the wide sector are therefore assumed to be significantly less severe. Since the probability of survival will be determined only by severe storms, thus from the wide sector, the probability of survival over the directions outside this wide sector will be so close to one that they will hardly influence the global probability of survival.

Finally, the probability of failure is obtained as one minus the probability of survival:

$$P(\text{failure}) = 1 - P(\text{survival}) \tag{7.5}$$

The probability of failure is usually expressed as an annual failure rate, Q, representing the probability of failure in one year, which is more amenable to risk analysis and decision making:

$$P(\text{failure per year}) = Q \tag{7.6}$$

8. STRUCTURAL RELIABILITY CALCULATIONS FOR (THE LOCATION OF) INDE-K

8.1. Introduction

The supporting space frame structure of INDE-K is of the jacket type. This implies that the foundation piles are driven through the legs of the structure and welded off at the top of the structure. This in contrast with a tower type of structure which has its foundation piles connected at the bottom of the structure, i.e. at the sea bed. The structure was designed in 1971 and consists of two jackets, one with four legs and one with six. The plan view of the structure has a rectangular shape. The topsides consist of a production module, living quarters for 17 men and a helideck.

The collapse of this jacket structure involves shearing of the bottom bays. Therefore, total horizontal force is an appropriate global load variable to use in the structural reliability calculations. At KSEPL ultimate strength calculations as outlined in section 7.2 and appendix F were performed, for the structure of INDE-K. There are two directions in which the bottom bays may fail, i.e. the end-on and broadside direction. See reference 10 for a more detailed description of the failure modes. Figure 8.1 shows, as an example, contour lines of the cumulant of extreme loads superimposed on the failure surface ranging from west to north, as derived for INDE-K at KSEPL [10]. The relationship between these contours and the failure surface shows that only the broadside collapse mode will contribute to the calculated failure rate. The elliptical form of extreme load distribution reflects the influence of phasing effects. When a wave passes the structure it will not exert the same level of global load on all members in a horizontal plane at the same moment in time, thus causing phasing effects. This phasing effect will be the strongest in the direction with the greatest length dimensions of the structure, i.e. in the end-on direction. In this report, for reasons of simplicity, a single pile is considered, in which case phasing effects do not occur. Therefore, phasing effects in wave loading will not be taken in account in this report.

The structural reliability calculations are performed here using the results of the MDC procedure derived in this report for a single pile, 1 meter diameter, erected in the sea at the location of INDE-K. The value of the collapse load factor used in this project is 2.2, this a realistic value for the construction of INDE-K. It represents the lowest load factor in a rectangular failure surface as derived at KSEPL for the structure of INDE-K [10]. That is, it represents the ultimate collapse strength of the structure in the end-on direction. In this project we are more interested in the influence of a strongly directional current on the load statistics and thus on the results of a structural reliability analysis than the exact values of the load factors and the derived failure rates. The differences should show the influence of the changes made on the results of a structural reliability analysis. And thus whether the additional efforts required, to account for the phenomenon of a strongly directional current, are worth while.

8.2. Outline of the calculations

For the long term distribution of global loads the formula given section 2.8 is used.

$$Q_{rp} = A \cdot e^{\left(\frac{-L}{\delta}\right)} \tag{2.20}$$

in which L is:

$$L = \frac{L_{rp}}{L_{100}} \tag{2.20a}$$

In this project a failure surface is chosen, based on a failure surface as calculated at KSEPL. In these calculations the structure failed due to shearing of the bottom bay. The shear force at the mud-line (base shear) equals the total applied horizontal environmental load on the structure. Therefore, as reference load sets can be used the 100 year return values of total horizontal force as derived from the MDC procedure.

The 100 year return value of total horizontal force and the collapse load factor are assumed to be constant within a narrow sector. Since the narrow sectors are 15 degrees wide this assumption seems to be sensible.

The 105° wide sector (270°-15°) has been divided into 7 narrower (15° wide) sectors. Return values for total horizontal force (100 and 1,000 year values) are calculated by the MDC procedure. The constants, i.e. A and δ, in the failure rate versus normalised load relation are derived from these return values.

The value of the collapse load factor in the sector n, λ_n, is substituted for L (in 2.20), the Q_{rp} thus represents the annual failure rate in the sector n, Q_n. The direction of a narrow sector n is represented by the direction of the middle of that sector.

Again we should account for the fraction of the storms in the narrow sectors, see section 6.3,

$$Q_n = f_n \cdot A \cdot e^{\left(\frac{-\lambda_n}{\delta}\right)} \tag{8.1}$$

in which f_n represents the fraction of the total number of storms used in the fitting procedure for a long time scale distribution of X_{mp} of which the (true) directions fall in a narrow sector n.

The collapse load factor for the sectors are calculated accounting for the effect of different 100 year return values of total horizontal force for different narrow sectors. Structural strength remains at the same level, 2.2 times the 100 year return value of total horizontal force as derived from a "normal" MDC procedure. "Normal" in this section refers again to the met-ocean design conditions procedure as developed at KSEPL without any of the changes proposed in this project.

Failure occurs at a load of $\lambda \cdot S_{100}$ (for the normal procedure) and at $\lambda_n \cdot S_{100,n}$ (for the revised procedure per sector). Since the structural strength remains unchanged these two collapse loads are equal:

$$\lambda_n \cdot S_{100,n} = \lambda \cdot S_{100} \tag{8.2}$$

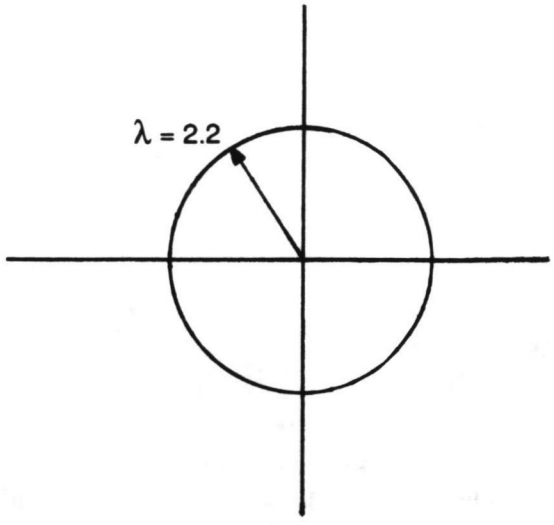

Fig. 8.2; A circular failure surface.

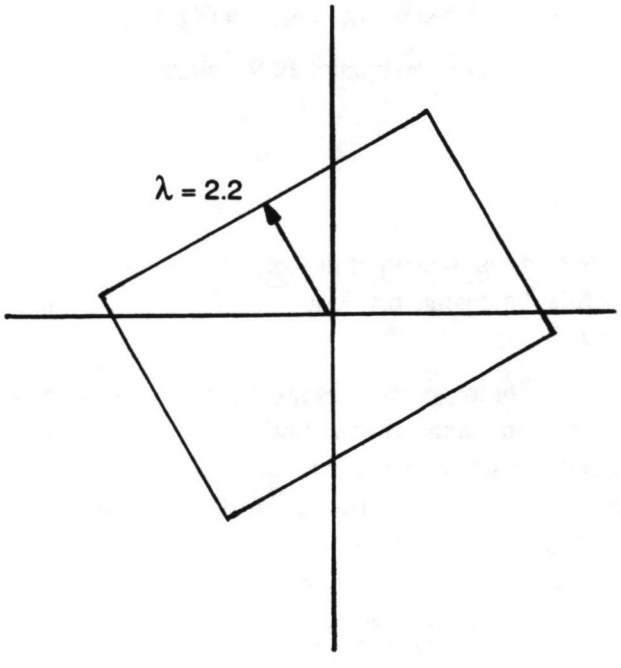

Fig. 8.3; A rectangular failure surface.

in which:
λ = 2.2, the collapse load factor, in the end on direction, as derived earlier at KSEPL for INDE-K
λ_n = the collapse load factor for the sector n
S_{100}= reference load, i.e. 100 year return value of total horizontal force, derived from the "normal" MDC procedure
$S_{100,n}$ = reference load for a directional sector, i.e. 100 year return value for total horizontal force derived for a sector n

For a circular failure surface (fig. 8.2), the following formula for the collapse load factor for the revised procedure in a sector n is derived from (8.2):

$$\lambda_n = \lambda \cdot \frac{S_{100}}{S_{100,n}} \tag{8.3}$$

In case a rectangular failure surface (fig. 8.3) is considered the collapse load factors in the different directions will not only be influenced by the changes in return values derived for different narrow sectors but also by the shape of the failure surface. Accounting only for the influence of the shape of the failure surface; the collapse load factors for one side of the rectangular failure surface can be calculated from the different angles of the direction of the sector considered an the direction of the smallest load factor.

$$\lambda_n = \frac{\lambda}{\cos(\alpha_n)} \tag{8.4}$$

in which:
α_n = angle between the middle of the sector n and the direction of the vector of the smallest value of the collapse load factor.

Combining the influence of different return values (8.3) and the shape of the failure surface (8.4), the collapse load factors for (one side of) a rectangular failure surface can then be derived from:

$$\lambda_n = \lambda \cdot \frac{S_{100}}{S_{100,n}} \cdot \frac{1}{\cos(\alpha_n)} \tag{8.5}$$

The annual failure rate over the entire wide sector can be derived easily from combining the failure rates in the narrow sectors. Since the annual failure rates, Q_n, will be small the following simplification can be used:

$$1 - Q = \prod_{n=1}^{N} (1 - Q_n) \approx 1 - \sum_{n=1}^{N} (Q_n) \tag{8.6}$$

or:

$$Q = \sum_{n=1}^{N} Q_n \tag{8.7}$$

in which N represents the total number of narrow sectors.

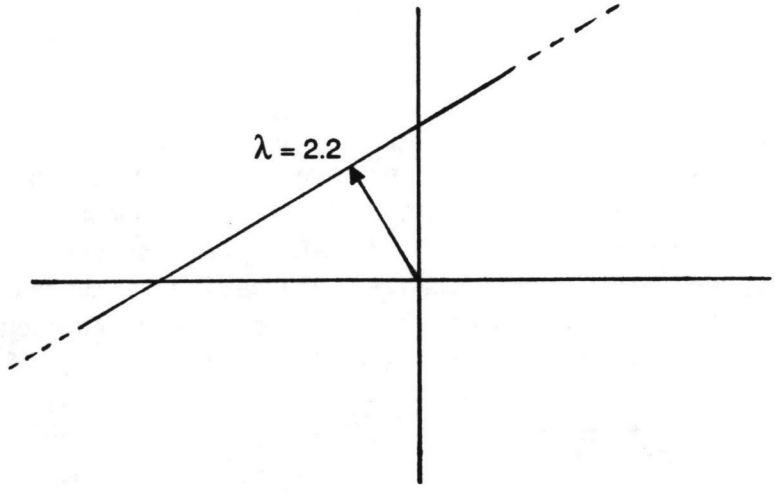

Fig. 8.4; One side of a rectangular failure surface represented by a single line.

8.3. The derived annual failure rates

Calculations have been performed for a circular (fig. 8.2) and rectangular (fig. 8.3) failure surface both for the results of a "normal" MDC procedure and for the changed procedure which accounts for strongly directional currents.

In the structural reliability calculations, as discussed in the previous sections, the rectangular failure surface can be represented by a single straight line (fig. 8.4). This can be done when one failure mode is considered to be dominant, i.e. will have a major influence on the annual failure rate, and all the storms contributing to the failure rate are coming from one wide sector coinciding with this side of the failure surface.

For the rectangular failure surface the direction where the collapse load factor has a length of 2.2 is from a wave direction 315°, which is slightly off the direction from which the highest loads are expected to occur.

When examining the results one should be aware of the fact that the difference in (total horizontal force) return values found for the sectors may be about 10% between the minimum and maximum values, but in the order of a few percent between the adjacent narrow sectors. Since the procedure involves an extrapolation of 25 year data to a 100 year level, the proposed differences are really marginal. When using the results as design conditions one would loose the differences as found in this report in a rounding process, e.g. after assumptions made and extrapolation a total horizontal force return value as derived from the MDC procedure should really not be interpreted as having 5 significant figures. They are presented to such an accuracy in this report because the differences in the results between two adjacent sectors are so small.

Table 6.5 gives the distribution of the unchanged storm directions over the seven narrow sectors.

Table 6.5; The sector numbers, directions and the distribution, over the narrow sectors, of the number of storms used in the fitting procedure.

sector number n	bearings (degrees)	middle of sector (degrees)	number of storms
1	270-285	277.5	16
2	285-300	292.5	30
3	300-315	307.5	26
4	315-330	322.5	24
5	330-345	337.5	50
6	345360	352.5	32
7	360-15	7.5	8
Total number of storms in the wide sector:			186

The annual failure rates for the 7 narrow sectors are given in table 8.1 and table 8.2. Table 8.1 gives the annual failure rates using the results of the changed MDC procedure, i.e. accounting for the effects of a strongly directional current, while table 8.2 gives those using the results from the "normal" procedure. The tables give also the combined annual failure rate, which is the sum of the annual failure rates derived for the narrow sectors.

Table 8.1; Annual failure rates derived accounting for the effects of a strongly directional current.

		Circular failure surface		Rectangular failure surface	
sector number	BSR-100 (kN)	load factor	Q_n	load factor	Q_n
1	296.59	2.36	4.61E-10	2.97	6.71E-13
2	318.06	2.20	4.6E-9	2.38	6.68E-10
3	318.23	2.20	2.97E-9	2.22	2.42E-9
4	327.47	2.14	6.49E-9	2.15	5.32E-9
5	326.39	2.14	1.31E-8	2.32	1.97E-9
6	316.35	2.21	4.72E-9	2.79	1.07E-11
7	314.42	2.22	1.62E-9	3.65	7.48E-16
Combined annual failure rate, Q:			3.39E-8		1.04E-8

Table 8.2; Annual failure rates using the results from a "normal" MDC procedure.

		Circular failure surface		Rectangular failure surface	
sector number	BSR-100 (kN)	load factor	Q_n	load factor	Q_n
1	317.81	2.2	2.58E-9	2.77	5.94E-12
2	317.81	2.2	4.83E-9	2.38	7.08E-10
3	317.81	2.2	4.19E-9	2.22	3.43E-9
4	317.81	2.2	3.87E-9	2.22	3.16E-9
5	317.81	2.2	8.06E-9	2.38	1.18E-9
6	317.81	2.2	5.19E-9	2.77	1.19E-11
7	317.81	2.2	1.29E-9	3.61	4.0E-16
Combined annual failure rate, Q:			3.0E-8		8.49E-9

8.4. Discussion of the derived failure rates

In the previous section the annual failure rates for two types of failure surfaces have been calculated, both for the results of a normal MDC procedure, i.e. a wide sector over which the load statistics are assumed to be constant, and in case all the storms were put in narrow sectors. The differences found between the annual failure rates are small, considering that at failure rates this low only the exponents are significant. For the location of INDE-K it seems as if the phenomenon of a strongly directional current has no significant influence on the structural reliability. This may again be explained by the small difference in direction between the most severe storms and the highest current speeds in the wide sector and by the fact that the largest contribution to the failure rate comes from the directions close to the lowest collapse load factor.

The results from the MDC procedure without any of the suggested changes predicts annual failure rates with the same order of magnitude as the procedure in which the effects of strongly directional currents are taken in account. The (results of the) procedure does not seem to be very sensitive to the effects of a strongly directional current. Therefore, based on the calculations as carried out in this report, the extra effort necessary to account for the effect of those strongly directional currents does not seem to be justified. Moreover, since the southern North Sea is the sector of the North Sea with the strongest and most directional currents, it is likely that this result pertains to the whole of the North Sea. However, in the data base used in this project the directions from which highest current speeds are coming from differs not much from those of the highest waves, a larger angle between wave and currents may influence the results.

The failure rates derived here should not be interpreted as exact values, but are, however, indicative of the reliability levels of southern North Sea offshore structures, designed to joint met-ocean conditions and achieving a load factor of 2.2. Collapse load factors of this level are likely to be achieved by applying design codes as API-RP 2A-LRFD (i.e. the, by the American Petroleum Institute, recommended design practice for steel space frame structures) [6,18]. At failure rates this low, other causes of collapse, loss of lives or production and damage to the environment may have much higher probabilities of occurrence (see also section 9). E.g., ship collisions, blow outs, fires, helicopter accidents or even earthquakes may be more likely to occur than platform collapse due to severe sea.

For storms with long return periods, the present calculations involve an enormous extrapolation of the met-ocean data and models. Such extremely rare events, however are likely to be subject to physical limitations on wave height, wave steepness and fetch length. Consequently, the low failure rates predicted may still be conservative. The accuracy of the extrapolation itself may also be subject to question, the fitted curve can influence the results both in a conservative as in an unconservative way.

9. PERSPECTIVE

In this section an attempt is made to put the work and its results in a somewhat broader perspective. This involves discussing:

- Some results of the procedures for met-ocean design conditions and structural reliability analysis in a few different situations, as derived at KSEPL.
- Some of the limitations of the procedures.
- Comparison of calculated structural failure rates with the probabilities of other hazards.
- In which perspective this student thesis work should be seen, and suggestions for further work in this area.

9.1. The MDC procedure and the reliability analysis

9.1.1. Practical applications

At KSEPL the methods for deriving met-ocean design conditions and performing a structural reliability analysis have been used to re-asses several structures in the Gulf of Mexico and the North Sea.

The first generation Gulf of Mexico (GoM) platforms designed in the 1950s proved to have insufficient reliability mainly because the magnitude of the environmental loading likely experienced by a platform was underestimated. Some of these early platforms collapsed during hurricanes and therefore early design practice was quickly superseded. Since hurricanes in this area can be very well forecast, the platforms were de-manned and fatalities avoided. The magnitude of the design loads tended to drift upwards through the 1960s and 1970s. Nowadays, conventional design practice uses extreme environmental design loads which are about 2.5-3 times higher than those used in the early 1950s for nominally identical structures in the same geographical area. Data on platform failures are limited. The availability of data on platform failure provides an opportunity to test the procedures and the theories involved for determining the extreme loads and associated structural behaviour up to the point of collapse and validate the results against the data. The failures of relatively old Gulf of Mexico platforms in hurricanes were analysed and correctly predicted from historical data [1].

Structural reliability analyses performed for offshore structures in the North Sea built from the 70's onwards showed that their designs are highly conservative, although conventional re-assessment procedures predicted a very low margin of safety in extreme conditions for one of them: Accounting for the non-coincidence of extreme waves and currents, design loads were largely reduced (up to 40%). Possible de-manning when severe environmental conditions are forecast seems therefore unnecessary. In fact the derived probabilities of structural failure where so low that a helicopter flight (especially in deteriorating weather) is likely to involve more risk to personnel than remaining onboard the offshore platform [10].

The methods for deriving met-ocean design conditions and performing a structural reliability analysis have not only been applied to re-assess fixed space frame structures, but also to support the decision making on the selection of a jack-up drilling rig for a certain location [19]. A jack-up was submitted to a re-assessment of the 100 year load and a pushover analysis. Existing site-assessment practices for jack-up rigs are based on conventional design methods for fixed steel structures. Although they provide criteria for acceptance or rejection, they do not quantify safety under extreme environmental loading. Conventional site assessments indicated that a financially attractive jack-up rig would not satisfy the criteria for the central North Sea. Re-assessment showed that the structural failure rates were low, compared to other hazards to which personnel is exposed. This supported the decision to use this jack-up, and saved the operator the costs of a higher capacity drilling rig [19].

As stated in the introduction the procedures can be used to re-assess existing structures in order to make rational decisions on the possibilities of keeping them operational beyond their original planned service life. The development of marginal fields as satellite fields and an extended recovery period of existing fields due to new production techniques, may make a longer service life desirable.

Although in this report the emphasis lies on loading, the met-ocean design conditions procedure is also amenable to determine a design elevation of the deck above mean sea level, when the calculations are performed for total surface elevation. This so-called air-gap should prevent the topside from being hit by crests of large waves. These can exert large loads on the topside and thus cause damage to the deck and the equipment on it, as well as to the substructure.

9.1.2 Limitations

The methods for deriving met-ocean design conditions and performing a structural reliability analysis demand an extensive data base including joint directional wave, wind and current data and a non-linear structural analysis package. The quality of the derived met-ocean conditions and the results of structural reliability analysis are highly dependent on the quality of the met-ocean data base. The validity of the long term statistics depends on the adequacy of the met-ocean data base, whether measured, or as in this report hindcast. In the case of NESS this was and is the subject of research at KSEPL. So far the conclusion is that the (environmental) variables based on NESS are adequately estimated [10].

There are, at the moment, two major areas for which extensive met-ocean data bases are available for use in the met-ocean design condition procedure. These are the Gulf of Mexico and the North Sea. When one wants to use the procedure in other areas, such as offshore West Africa, one obviously should acquire data bases for these areas. One should keep in mind that obtaining hindcast data bases, such as NESS, involves a huge amount of work and is therefore time consuming and expensive.

The models as used in this project in the reliability analysis do not cover all aspects of an offshore platform's structural integrity. Further refinement of the model is called for, together with careful validation. The scope of structural reliability analysis should also be widened to include other features of offshore platforms. Although the foundations of space-frame structures have by and large been found to be more

resistant to environmental loading than the structures themselves, models of pile-soil systems, for instance, will be crucial if they strongly influence the structural reliability in particular cases. The described procedure far a structural reliability analysis also does not incorporate the effect of cyclic degradation, i.e. the cumulative effect of a number of large waves on structural integrity, even as it does not account for the joint occurrence of failure modes (see appendix F). The applicability of the whole procedure should also be generalised beyond the fixed, space frame type, such as floating or deep water compliant structures.

In this thesis work only a sub-class of offshore platforms is studied. This is the type of fixed steel platforms whose response to environmental loading can be described as quasi static and which comprise a space frame of slender members which do not influence the gross characteristics of incident waves (i.e. negligible scattering of waves occurs). The majority of installed offshore platforms falls in this category. If one wants to extend the procedures to other types of structure a number of difficulties can arise [11]:

- Around large concrete structures the waves are known to be scattered and incompletely diffracted by the structures and thus will have different wave kinematics.
- In the case of dynamically responding structures, the maximum response may be associated with sea states less severe than those in the design conditions.
- The true interaction between the structure and the fluid motion, for instance vortex induced vibration of a member where the motion of the member influences the vortex shedding pattern.

The procedure for a structural reliability analysis involves a considerable amount of work generating the input for a specific structure for the pushover analysis and the determination of a collapse load factor and a failure surface. Thus though the procedure is highly applicable for re-assessment of existing structures and the assessment of already detailed designs, it is less applicable to assess a series of preliminary designs.

9.2. The derived failure rates

In section 8.3 the annual failure rates for two types of failure surfaces have been calculated, both using the results of a normal MDC procedure, i.e. a wide sector over which the load statistics are assumed to be constant, and the results of the procedure which accounts for the phenomenon of a strongly directional current. The differences found between the annual failure rates are small.

The failure rates derived in this report should not be interpreted as exact values, but are, however, indicative of the reliability levels of North Sea offshore structures. At failure rates this low, other causes of collapse, loss of lives or productivity and damage to the environment may have much higher probabilities of occurrence. E.g. ship collisions, blow outs, fires, helicopter accidents or even earthquakes and war may be more likely to occur than platform collapse due to severe storm generated seas.

In order to put the derived failure rate, of the order 10^{-8}, into perspective, this section gives some figures for other causes of platform loss and hazards threatening human lives.

Table 9.1 gives the number of the total losses (including constructive total losses from an insurance point of view in which case the offshore structure might be repaired) and severe damage of fixed offshore platforms caused by several types of accidents as found in the World-wide Offshore Accident Databank (WOAD) [12]. The table covers the world wide accidents in the period 1970-79.

Table 9.1; Different types of accident which have led to total loss or severe structural damage, and the number of occurrences, for fixed offshore structures world wide in the period 1970-79.

type of accident	total losses	severe damage
Blow out	7	5
Collision	2	8
Explosion	4	1
Fire	7	10
Structural failure	3	2

One should be careful in drawing conclusions from tables like the above. However it shows that there are other types of accident, apart from structural failure, contributing significantly to the risks of loss of an offshore platform.

If one considers only the structures designed after 1970, the number of failures between 1970 and 1989 is zero [11], however world wide six platforms collapsed in this period due to environmental overloading. The platforms which collapsed in this period were all designed prior to 1970 and were located in the Gulf of Mexico.

In table 9.2 some probabilities of accidents are given for reason of comparison. One should however keep in mind that involuntary risks, such as the risk of death due to the collapse of an office building, have a lower level of acceptance than voluntary risks, such as occur during mountaineering.

Table 9.2; Approximate annual probability of death for the UK. in the period 1970-73, taking into account the normal hours of exposure to the risk in the course of a year [13].

Activity or cause	Approx. annual risk per person
Mountaineering (international)	10^{-2}
Air travel (crew)	10^{-3}
Coal mining	$3 \cdot 10^{-4}$
Car travel	$2 \cdot 10^{-4}$
Construction site	$2 \cdot 10^{-4}$
Air travel (passenger)	10^{-4}
Home accidents (all persons)	10^{-4}
Manufacturing	$4 \cdot 10^{-5}$
Structural failure (all buildings)	10^{-6}

Recent re-assessment of North-Sea offshore platforms at KSEPL showed that indeed the derived failure rates are extremely small, even smaller than the order of 10^{-8} found in this report, thus suggesting that their designs might be considered to be excessively conservative. At KSEPL it is suggested that the offshore design procedures could be modified such that the resulting storm risk will be more in balance with other hazards threatening the structure and the people on it, thus leading to more cost effective designs of new structures. For geographical areas where platforms are either unmanned or can be evacuated prior to the arrival of severe storms, lower levels of reliability might be considered acceptable. Target reliabilities, which might be in the order of 10^{-5}, would need to be discussed and agreed on in industry and authority forums.

In some occasions the structural strength required of offshore structures or member size might not be governed by the loads on the structure after it has been erected on location in the sea, but by construction or transportation requirements. In those cases the additional steel cannot be eliminated from the design.

9.3. Where this project stands

After gaining experience from the results of re-assessments, the methods for deriving met-ocean design conditions and performing a structural reliability analysis will not only be applied to evaluate existing structures but also to design new structures. Unnecessary conservatism, both in loading and structural strength, can then be eliminated, thus leading to cost reductions, without compromising the integrity of the structure.

The student thesis work as presented in this report should be seen in this perspective. It reflects a small part of research in the total development and testing of a procedure including met-ocean design conditions and structural reliability analysis for the design and re-assessment of offshore structures. The effect of a phenomenon which is not

incorporated in the MDC procedure has been investigated. Eventually, after studies similar to the one presented here and re-assessments, as discussed earlier in this section, enough experience and confidence in the procedures should be gained, thus resulting in a "new" package for analysing structural reliability of offshore structures, without unnecessary conservatism, which is accepted by the offshore industry at large and (certifying) authorities.

Although it appears from the calculations as performed in this student thesis work that the results from the MDC procedure are not very sensitive to the effects of strongly directional currents, further work may be needed to generalise this conclusion. This can be done by means of performing similar calculations for other grid points in the NESS data base, where the angle between the main current axis and the direction of the highest waves is higher than in this report. The grid points should be selected based on expected strongly directional currents with relatively high speeds. These points are, therefore, most likely to be chosen also in the southern North Sea.

In case data bases for other grid points are used it may well be worth while to investigate again the directional properties of tidal and residual current separately. Since the residual current is believed to be related to the wind and waves, and thus may be similar over the wide sector, like the waves, only the directional properties of tidal current in that case will influence the distribution of the load statistics over the wide sector. If the residual current is resolved properly in the data base, the relations between waves and residual current could be determined from the data. The ellipse described by the tidal current may well be narrower than the ellipse for total current as used in this thesis work, thus increasing the directional effects.

LIST OF SYMBOLS

a	crest height	[m]
A_n	constant	[-]
A_ζ	inertia factor at a certain water depth ζ	[kg/m]
A	projected area	[m^2]
A_c	area normal to flow direction	[m^2]
B	drag factor, below mean sea level	[kg/m^2]
B_ζ	drag factor at a certain water depth ζ	[kg/m^2]
B_s	drag factor, above mean sea level	[kg/m^2]
C_D	drag coefficient	[-]
C_m	inertia coefficient	[-]
C_w	wind drag coefficient	[-]
d	depth	[m]
D	diameter of cylindrical member	[m]
D_s	stretching depth	[m]
F	force	[N]
f_n	fraction	[-]
g	gravitational acceleration	[m/s^2]
H_s	significant wave height	[m]
k	wave number	[1/m]
L	wave length	[m]
L_{rp}	return value of a global load	[N or Nm]
L_θ	return value of a global load for the direction θ	[N or Nm]
n	number of exceedances	[-]
n	sector number	[-]
N	number of sectors	[-]
N	sample size	[-]
$P(f)$	probability of non-exceeding f	[-]
$Q(f)$	probability of exceeding f	[-]
Q	(annual) probability of exceeding	[1/year]
Q_c	combined probability of exceeding for a number of sectors	[1/year]
Q	annual failure rate, i.e. one over return period ($1/R$)	[1/year]
Q_n	annual failure rate for a sector n	[1/year]

R	return period	[year]
R	residual current speed	[m/s]
S	ultimate structural strength	[N or Nm]
S_{100}	100 year level of a global load	[N or Nm]
$S_{100,n}$	100 year level of a global for a sector n	[N or Nm]
S_{ref}	reference level of a global load	[N or Nm]
t	depth mean tidal current velocity	[m/s]
T	(life)-time	[years]
T_p	peak period	[s]
T_z	zero-up crossing period	[s]
u_ζ	amplitude of particle velocity at a certain water depth	[m/s]
u_0	amplitude of vertical particle velocity at mean sea level	[m/s]
$\dot{u}_\zeta$	amplitude of particle acceleration at a certain water depth	[m/s^2]
$\dot{u}_0$	amplitude of vertical particle acceleration at mean sea level	[m/s^2]
v	depth mean total current speed	[m/s]
v_s	depth mean reduced current speed due to current blockage	[m/s]
v_0	current speed at mean sea level	[m/s]
W	wind speed	[m/s]
X	variable	[unit of X]
X_{mp}	most probable extreme value of variable X	[unit of X]
X_T	T-year return value of variable X	[unit of X]

α_n	angle between the middle of sector n and the direction of the smallest collapse load factor	[deg]
β	time scale parameter of storms	[-]
γ	estimate of the index of variation, in the fitting of a p.d.f. for the most probable extremes.	[-]
δ	constant in load versus return period relation	[-]
ζ	vertical coordinate, origin at mean sea level	[m]
ζ_s	substitute vertical coordinate from delta stretching	[m]
η	instantaneous water level	[m]
θ	angle	[deg]
θ_d	angle of direction of the middle of a sector, clockwise from North	[deg]
θ_H	angle of direction of wave propagation, relative to the waves	[deg]

θ_t	angle of direction of the tidal current, relative to the waves	[deg]
θ_R	angle of direction of the residual current, clockwise from North	[deg]
θ_v	angle of direction of the total current, relative to the waves	[deg]
θ_w	angle of direction of the wind, relative to the waves	[deg]
λ	collapse load factor	[-]
λ_n	collapse load factor in a narrow sector n	[-]
λ_θ	collapse load factor in a direction θ	[-]
μ	expected number of exceedances	[-]
ν	arrival rate, average number of storms per year	[1/year]
ξ	parameter in the fitting of the p.d.f. of X_{mp}	[1/unit of X]
ρ	density	[kg/m^3]
σ_θ	root mean square directional spreading	[rad]
φ	reduction factor in the GLM due to the directional spreading of the waves	[-]
ω	angular frequency	[rad/s]
∇	stretching parameter	[-]

BSR	total horizontal force	[kN]
GLM	Generic Load Model	
KSEPL	Koninklijke/Shell Exploratie en Produktie Laboratorium	
MDC	Met-ocean Design Conditions	
NNS	northern North Sea	
NESS	Northern European Storm Study	
OMT	overturning moment	[kNm]
SNS	southern North Sea	
WHT	wave height	[m]

REFERENCES

1. Extreme storm loading on fixed offshore platforms, P.S. Tromans, M. Efthymiou, J.W. van de Graaf, L. Vanderschuren and P.H. Taylor, April 1992, KSEPL publication no.1102.
2. Application of the random storm method to global structural loading on fixed offshore structures, KSEPL Student Report, July 1991, Maarten R. Kraneveld.
3. The statistics of the extreme response of offshore structures, P.S. Tromans, P.M. Hagemeijer and H.R. Wassink, Ocean Engineering, Vol. 19 No 2, pp. 161-181, 1992.
4. Waves in Ocean Engineering, M.J. Tucker, 1991, ISBN 0-13-932955-2.
5. An empirical model for random directional wave kinematics near the free surface, G. Rodenbusch and G.Z. Forristal, 1986, proceedings of the 18th Annual Offshore Technology Conference, OTC 5097.
6. Current blockage, reduced forces on offshore space frame structures, Taylor, P.H., 1991, Offshore Technology Conference Paper, OTC 6519.
7. Modelling the North Sea Through the North European Storm Study, D.J. Peters, Conoco Inc.; C.J. Shaw, SIPM bv.; C.K. Grant, BP Exploration; J.C. Heideman, Exxon Production Research Co.; and D. Szabo, Mobil R&D Corp., 1993 Offshore Technology Conference, OTC 7130.
8. Application of the random storm method to the air gap problem, KSEPL Student Report 91.070, May 1991, Bart H. Heijermans.
9. On the estimation of the index of variation, Wolf, P.P. de, KSEPL Student Report. 91.116.
10. Failure probability of southern North Sea platform under environmental loading, M. Si Boon-Ing, L. Vanderschuren, J.W. van de Graaf and P.S. Tromans, March 1993, KSEPL publication no. 1158.
11. Environmental Loading on Fixed Offshore Platforms, Efthymiou, M. and Graham, C.G., Shell U.K. Exploration and Production, Society of Underwater Technology (SUT) conference, November 1990.
12. World-wide Offshore Accident Databank, WOAD statistical report 1988, Statistics on Accidents to Offshore Structures Engaged in Oil and Gas Activities in the Period 1970 -87, Veritas Offshore Technology and Services A/S, Norway, ISSN 0801-5929.
13. Rationalisation of safety and serviceability factors in structural codes, CIRIA, Construction Industry Research and Information Association, London, U.K., 1977, ISBN 0-86017-017-9, ISSN 0305-408X
14. Forces on large cylinders in a random directional flow, Rodenbusch, G. and Kallstrom, C., 1986, Offshore Technology Conference, OTC 5096.
15. Directional wave forces on template offshore platforms, Rodenbusch, G., 1986, Offshore Technology Conference, OTC 5098.

16. Measured and predicted wave forces on offshore platforms, Bea, R.G., Pawsey, S.F. and Litton, R.W., 1988, Offshore Technology Conference, Houston, OTC 5787.

17. A new model for the kinematics of large ocean waves - application as design wave, Tromans, P.S., Anaturk, A.R. and Hagemeijer, P., 1991, ISOPE Conference, Edinburgh.

18. Recommended Practice for Planning, Designing and Constructing Fixed Offshore Platforms - Load and Resistance Factor Design, API recommended practice 2A-LRFD (RP 2A-LRFD), first edition, July 1, 1993, American Petroleum Institute, Washington DC, USA.

19. Failure probability of a jack-up under environmental loading in the central North Sea, van de Graaf, J.W., Tromans, P.S., Vanderschuren, L. and Jukui, B.H., August 1993, KSEPL publication number 1181.

GENERAL REFERENCES

- The Sea, volume 9 part a, Ocean Engineering Science, Bernard Le Méhauté and Daniel M. Hanes, ISBN 0-471-52856-0 (part a).
- Tides, Surges and Mean-Sea-Level, D.T. Pugh, 1987, ISBN 0-471-91505-X.
- Mechanics of wave forces on offshore structures, T. Sarpkaya and M. Isaacson, 1981, ISBN: 0-442-25402-4.

APPENDIX A

Contribution of inertia to extreme loads

Morison's equation for calculating the fluid load, on a structural member, due to wave and current can be written as:

$$F_\zeta = A_\zeta \cdot \dot{u}_\zeta + B_\zeta \cdot (v + u_\zeta) \cdot |(v + u_\zeta)| \tag{2.1}$$

in which:

$$A_\zeta = \left(C_m \cdot \rho \cdot \frac{\pi}{4} \cdot D^2 \right)_\zeta \tag{2.1a}$$

$$B_\zeta = \left(C_D \cdot \rho \cdot \frac{1}{2} \cdot D \right)_\zeta \tag{2.1b}$$

The first term r.h.s. of equation 2.1 represents the contribution of inertia to the load and the second term the contribution of drag. Since the fluid loads, on slender members, in extreme waves are drag dominated, extreme total horizontal force and overturning moment (the main extreme loads of interest) tend to be drag dominated for steel space frame structures. In this student thesis work the inertia term, in Morison's equation (2.1), is omitted. A justification for this omission of inertia will be given in this appendix.

For this purpose a computer program, LOAD, is used. LOAD numerically integrates the fluid forces on a structure over the submerged depth at a number of time steps and derives the maximum values of the global loads during the passage of the wave. The LOAD program is developed at KSEPL, and is also used in the calibration of generic load models. The features of the LOAD program are discussed in more detail in appendix C. To investigate the influence of the inertia term on the global load, several runs of LOAD were made.

Different values for the inertia coefficient, C_m (0 and 1.5), are used in different environmental conditions, i.e. significant wave height, H_s, zero-up-crossing period, T_z and current speed at mean sea level, v_0, are changed.

The calculations are performed for a single pile, diameter 1 metre, in 30.0 metres of water. The diameter of the legs of INDE-K is 1 metre. The inertia and drag coefficients used in the calculations are representative values for the type of space frame structures. Different values for the drag coefficient, C_D, have been used above and below mean water level (0.63 and 1.2), to account for the effect of marine growth. Results are given in table A.

As can be read from table A, the contribution of the inertia to the global load decreases from around 20% in a moderate sea to 1.5% during severe seas. Although the global load increases when the environmental conditions get more severe the contribution of the inertia term to the global load stays more or less the same, i.e. about 8 kN for total horizontal force. When extrapolating to rare (i.e. extreme) events of global load the influence of inertia on the global load will decrease rapidly and will

be negligible compared to the influences caused by other uncertainties, such as in the fittings of probability distribution functions.

In case extreme environmental loads on a single pile 1 metre diameter are considered, as in this student thesis work, the omission of inertia seems reasonable.

Table A; The influence of the inertia term on the global loads.

C_m	H_s (m)	T_z (s)	U_s (m/s)	BSR (kN)	Δ%	OMT (kNm)	Δ%
1.5	3.5	6	0	33.12		852	
0	3.5	6	0	42.11	21	1056	19
1.5	3.5	6	0.3	54.04		1296	
0	3.5	6	0.3	46.55	14	1132	13
1.5	5	7	0.3	103.46		2424	
0	5	7	0.3	94.52	8.6	2220	8.4
1.5	8	9	0	222.20		5087	
0	8	9	0	229.98	3.4	5258	3.2
1.5	8	9	0.5	295.24		6519.88	
0	8	9	0.5	288.24	2.4	6379.61	2.2
1.5	8	9	0.7	324.05		7073.81	
0	8	9	0.7	317.91	1.9	6943.94	1.8
1.5	9.5	10	0	341.3		7666	
0	9.5	10	0	334.2	2.1	7509	2.1
1.5	9.5	10	0.8	476.12		10284.1	
0	9.5	10	0.8	470.63	1.2	10166.9	1.6

Due to the effect of inertia the maximum wave load occurring on a structure during the passage of a wave precedes the maximum in surface elevation. When extreme loads are considered, generated by waves with extreme wave heights, the loads are drag dominated and the maxima in wave loading and surface elevation almost exactly coincide.

However, one should keep in mind that inertia effects cannot always be omitted from the load calculations, i.e. in case of large member diameters or calculations for not so severe environmental conditions, inertia can contribute significantly to the global loads. Members of constructions designed for deeper water can have significantly larger diameters than 1 metre, but not necessarily in the top bays where the largest

wave loads (and thus inertia effects) occur. For constructions in water depths of about 170 metre leg diameters may vary between about 6 metres at the sea bed to about 1.5 meter at mean sea level.

APPENDIX B

Example of the integration procedure in the derivation of the load model

As an example of the integration of the fluid loads (see section 2.2 and 3.2) over the entire submerged length of a column, the global (horizontal) drag force due to the orbital wave velocity under a wave crest is derived here.

$$F_1 = \int_{-d}^{\eta} B_\zeta \cdot u_\zeta^2 \cdot d\zeta \tag{3.3a}$$

The vertical coordinate, ζ, has its origin at mean sea level. To account for the effect of marine growth, different values for the drag coefficient are used above and below mean sea level:

$$\zeta \le 0 \quad \Rightarrow B_\zeta = B$$
$$\zeta > 0 \quad \Rightarrow B_\zeta = B_s$$

Assuming deep-water conditions, the amplitude of the (orbital) particle velocity, u_ζ, at a certain level ζ is;

$$u_\zeta = u_0 \cdot e^{k\cdot\zeta} \tag{2.7a}$$

And therefore the velocity squared:

$$u_\zeta^2 = u_0^2 \cdot e^{2\cdot k\cdot\zeta} \tag{B.1}$$

Delta stretching is introduced to account for the effect of overprediction of particle velocities under the crest of large waves by formula 2.7a.

$$\zeta > -D_s \;\Rightarrow\; \zeta_s = (\zeta + D_s)\cdot\frac{\eta\cdot\nabla + D_s}{\eta + D_s} - D_s \tag{2.5}$$

Substituting the formulas for the drag coefficients, the particle velocities and delta stretching in the integral result in:

$$\begin{aligned} F_1 = &\int_{-d}^{-D_s} B\cdot u_0^2\cdot e^{2\cdot k\cdot\zeta}\cdot d\zeta + \int_{-D_s}^{0} B\cdot u_0^2\cdot e^{2\cdot k\left((\zeta+D_s)\frac{\eta\cdot\nabla+D_s}{\eta+D_s}-D_s\right)}\cdot d\zeta \\ &+\int_{0}^{\eta} B_s\cdot u_0^2\cdot e^{2\cdot k\left((\zeta+D_s)\frac{\eta\cdot\nabla+D_s}{\eta+D_s}-D_s\right)}\cdot d\zeta \end{aligned} \tag{B.2}$$

Solving the first of the three integrals on the right hand side of equation B.2.

$$\begin{aligned} \int_{-d}^{-D_s} B\cdot u_0^2\cdot e^{2\cdot k\cdot\zeta} &= \left[\frac{B}{2\cdot k}\cdot u_0^2\cdot e^{2\cdot k\cdot\zeta}\right]_{-d}^{D_s} = \frac{B}{2\cdot k}\cdot u_0^2\cdot\left(e^{-2\cdot k\cdot D_s} - e^{-2\cdot k\cdot d}\right) \\ &\approx \frac{B}{2\cdot k}\cdot u_0^2\left(1-2\cdot k\cdot D_s\right) \end{aligned} \tag{B.3}$$

Since only deep water conditions are considered, terms with $e^{-k \cdot d}$ can be neglected. Exponential terms (e^x) can be approximated by a Taylor series:

$$e^x = 1 + x + \frac{x^2}{2!} + \ldots\ldots\ldots + \frac{x^n}{n!} + O\left(x^{n+1}\right) \tag{B.4}$$

When $x << 1$, a first order approximation suffices:

$$e^x \approx 1 + x \tag{B.5}$$

Therefore the following approximation is used in (B.3):

$$e^{-2 \cdot k \cdot D_s} \approx 1 - 2 \cdot k \cdot D_s \tag{B.6}$$

The same approximation method is used at similar occasions in the other integrals. The linearisation of the exponential terms near mean sea level eliminates the delta stretching parameters so that they do not appear in the approximations. The linearisation of the exponential terms is almost exactly equivalent to delta stretching [3].

Solving the second integral:

$$\int_{-D_s}^{0} B \cdot u_0^2 \cdot e^{2 \cdot k \left((\zeta + D_s) \frac{\eta \cdot \nabla + D_s}{\eta + D_s} - D_s \right)} \cdot d\zeta$$

$$= \left[u_0^2 \cdot \frac{B}{2 \cdot k} \cdot \frac{\eta + D_s}{\eta \cdot \nabla + D_s} \cdot e^{2 \cdot k \left\{ (\zeta + D_s) \frac{\eta \cdot \nabla + D_s}{\eta + D_s} - 2 \cdot k \cdot D_s \right.} \right]_{-D_s}^{0}$$

$$= u_0^2 \cdot \frac{B}{2 \cdot k} \cdot \frac{\eta + D_s}{\eta \cdot \nabla + D_s} \cdot \left(e^{2 \cdot k \cdot D_s \frac{\eta \cdot \nabla + D_s}{\eta + D_s} - 2 \cdot k \cdot D_s} - e^{-2 \cdot k \cdot D_s} \right)$$

$$\approx u_0^2 \cdot \frac{B}{2 \cdot k} \cdot \frac{\eta + D_s}{\eta \cdot \nabla + D_s} \cdot \left(\left(1 + 2 \cdot k \cdot D_s \cdot \frac{\eta \cdot \nabla + D_s}{\eta + D_s} - 2 \cdot k \cdot D_s \right) - \left(1 - 2 \cdot k \cdot D_s \right) \right)$$

$$= u_0^2 \cdot \frac{B}{2 \cdot k} \cdot \frac{\eta + D_s}{\eta \cdot \nabla + D_s} \cdot 2 \cdot k \cdot D_s \cdot \frac{\eta \cdot \nabla + D_s}{\eta + D_s}$$

$$= u_0^2 \cdot B \cdot D_s \tag{B.7}$$

And the third:

$$\int_{0}^{\eta} B_s \cdot u_0^2 \cdot e^{2 \cdot k \left((\zeta + D_s) \frac{\eta \cdot \nabla + D_s}{\eta + D_s} - D_s \right)} \cdot d\zeta$$

$$= \left[u_0^2 \cdot \frac{B_s}{2 \cdot k} \cdot \frac{\eta + D_s}{\eta \cdot \nabla + D_s} \cdot e^{2 \cdot k \cdot (\zeta + D_s) \frac{\eta \cdot \nabla + D_s}{\eta + D_s} - 2 \cdot k \cdot D_s} \right]_0^{\eta}$$

$$= u_0^2 \cdot \frac{B_s}{2 \cdot k} \cdot \frac{\eta + D_s}{\eta \cdot \nabla + D_s} \cdot \left(e^{2 \cdot k \cdot (\eta + D_s) \frac{\eta \cdot \nabla + D_s}{\eta + D_s} - 2 \cdot k \cdot D_s} - e^{2 \cdot k \cdot D_s \frac{\eta \cdot \nabla + D_s}{\eta + D_s} - 2 \cdot k \cdot D_s} \right)$$

$$\approx u_0^2 \cdot \frac{B_s}{2 \cdot k} \cdot \frac{\eta + D_s}{\eta \cdot \nabla + D_s}$$

$$\cdot \left(\left(1 + 2 \cdot k \cdot (\eta + D_s) \cdot \frac{\eta \cdot \nabla + D_s}{\eta + D_s} - 2 \cdot k \cdot D_s \right) - \left(1 + 2 \cdot k \cdot D_s \cdot \frac{\eta \cdot \nabla + D_s}{\eta + D_s} - 2 \cdot k \cdot D_s \right) \right)$$

$$= u_0^2 \cdot \frac{B_s}{2 \cdot k} \cdot 2 \cdot k \cdot \eta = u_0^2 \cdot B_s \cdot \eta \qquad \text{(B.8)}$$

Combining the results of the three integrals derived above:

$$F_1 = \int_{-d}^{\eta} B_n \cdot u_n^2 \cdot d\zeta \approx \frac{B}{2 \cdot k} \left(1 + 2 \cdot k \cdot \frac{B_s}{B} \cdot \eta \right) \cdot u_0^2 \qquad \text{(B.9)}$$

Assuming deep water conditions (i.e. $k \cdot d$ large), the wave number, k, can be replaced by:

$$k = \frac{2 \cdot \pi}{L} = \frac{\omega^2}{g} \qquad \text{(B.10)}$$

Assuming the maximum force on the column will occur during the passage of the crest of the wave, η can be replaced by a. Further can u_0 and ω be replaced by respectively:

$$u_0 = a \cdot \omega \qquad \text{(B.11)}$$

and:

$$\omega = \frac{2 \cdot \pi}{T} \qquad \text{(B.12)}$$

The global load due to the particle velocities under a wave crest can now be expressed in terms of crest height, a, and wave period, T.

$$F_1 = \int_{-d}^{\eta} B_\zeta \cdot u_\zeta^2 \cdot d\zeta \approx \frac{B}{2 \cdot k} \left(1 + 2 \cdot k \cdot \frac{B_s}{B} \cdot \eta \right) \cdot u_0^2$$

$$= \frac{B \cdot g}{2} \cdot a^2 + 4 \cdot \pi^2 \cdot B_s \cdot \frac{a^3}{T^2} = A_* \cdot a^2 + A_* \cdot \frac{a^3}{T^2} \qquad \text{(B.13)}$$

These terms can easily be identified in the load models used in this report in sections 2.2, 3.2 and 4.2. A_* and $A_\bullet$ are constants, depending on the parameters of the structure (e.g. drag coefficients).

Including the effect of directional spreading, which only influences the velocities and not the crest height, can be done by multiplying both terms with φ^2.

The same procedure as used above can be used for integrating the other terms in the derivation of the load models, and for moments instead of horizontal forces.

APPENDIX C

The LOAD program and the calibration of the load model

As discussed in section 2.2.4 a computer program called LOAD is used in the calibration of the constants in the load model. This appendix will discuss the LOAD program and its use in more detail.

The computer program "LOAD"

The LOAD program essentially calculates the total applied horizontal hydrodynamic force on vertical columns by numerical integrating Morison's equation over depth. It does this at a number of time steps and derives the maximum values of the global loads during the passage of the wave. The LOAD program was developed at KSEPL, and is used in the calibration of the constants in generic load models. Wave kinematics are calculated using "New Wave" theory and accounting for delta stretching, the particle velocity and acceleration profile over (a finite) water depth and directional spreading.

The computer program does not include wind induced forces and does not automatically reduce current speeds due to the presence of the structure (i.e. current blockage). The space frame structure can be modelled as a single pile, as in this project, or as a group of closely spaced columns. In the latter case the LOAD program accounts for the phasing effects in the wave load. Phasing effects arise because different members will experience their maximum wave loading at a different moment in time, as the wave passes the construction.

An extreme wave and its kinematics, "New Wave"

The load program incorporates "New Wave" theory (Tromans et al. [17]) to predict the shape and the kinematics of an extreme wave. The following paragraphs will outline the logic of "New Wave" theory and it's advantages above time domain simulations.

The ocean surface is a random process: it comprises a complex superposition of components of different wave lengths, amplitudes and periods, travelling at different speeds and in different directions. Large waves occur when, by chance, many of these components come into phase. The resultant water particle motion is a similar random process. Such processes cannot be accurately described by regular, periodic wave theories (such as Stokes V, which essentially is a non-linear periodic wave derived from correcting a sinusoidal wave for non-linearities in the shape of an extreme wave). In spite of this, in conventional design and re-assessment practices wave loads on fixed offshore structures are calculated using wave theories similar to Stokes V. The height and period of the wave are chosen to correspond to some extreme condition. Typically this extreme will be the most probable highest wave to occur in the once in 100 year sea state.

To simulate the sea realistically, it is necessary to capture its random, broad-banded nature. The most direct way to accomplish this is by time domain simulations, which accurately model the random and directional characteristics of waves. The history of surface elevation of the sea in a storm can be modelled by doing time domain simulations for a single sea state. This involves programming a computer to sum

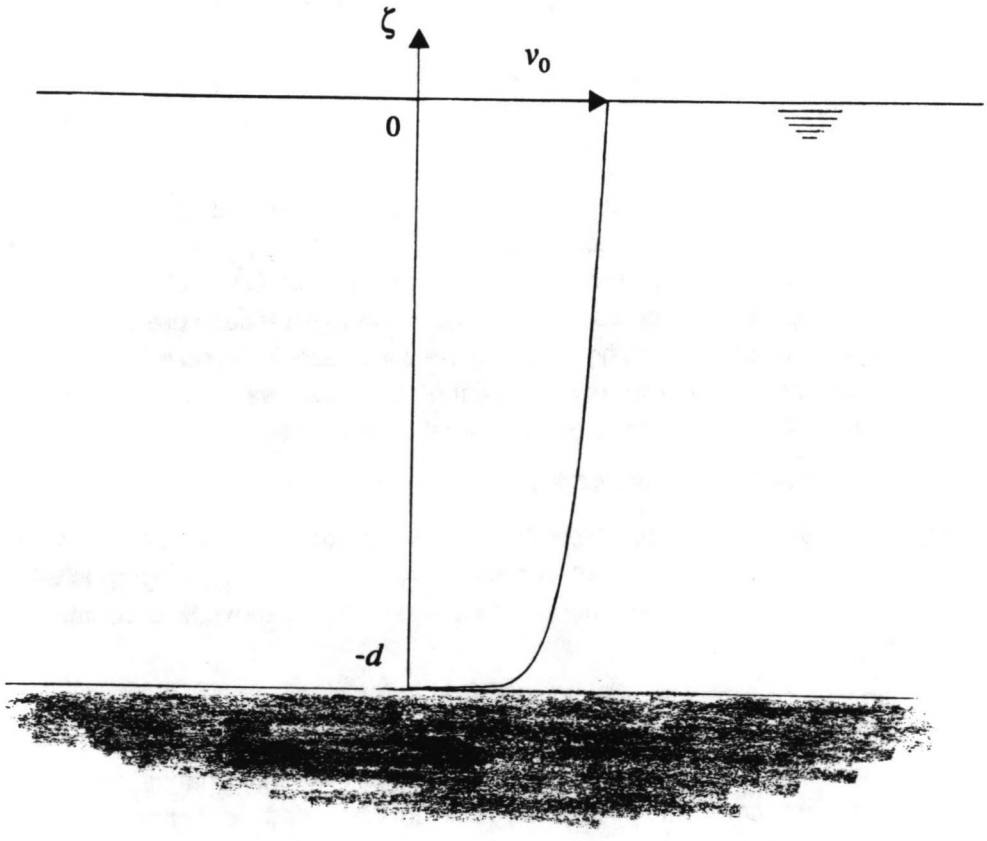

Fig. C.1; Relative depth to the power 1/7 current profile.

randomly selected values of wave amplitude and phase angle, much as in a real sea. However, large waves appear infrequently in such simulations. If one wants to capture the characteristics of extreme waves, these simulations involve much computer processing time and human time required for the subsequent statistical analysis. Computer software packages for time domain simulations are available. The kinematics and loads predicted by such programs have been extensively validated against offshore measurements in various water depths. Application of time domain simulation programmes involves the simulation of many hours of a single sea state to generate a statistical estimate of the most probable extreme wave. Therefore time domain simulations are very costly, both in man hours as in computer time.

Tromans developed a new theory [17], to calculate the shape of the extreme wave, the particle velocities and accelerations around a structure. This theory describes the extreme event occurring when dispersed wave energy focuses at a single point in space and time such that component frequencies come into phase. It is this process which generates the extreme waves in a real storm sea. The theory involves superposition of directional, linear wave components, as in time domain simulation. However their phases and amplitudes are selected according to statistical theory. The most probable extreme wave and its water particle kinematics are captured explicitly. Thus, the realism of time domain simulation is achieved with the economy and convenience of a deterministic wave analysis.

Since, like a time domain simulation, New Wave is a linear wave theory, it does not predict correctly the kinematics at and above mean sea level in extreme waves . This is easily dealt with by the delta stretching method as discussed in section 2.2.2.

There is much evidence supporting this theory. It is completely consistent with the well validated random direction time-domain wave simulations as performed at KSEPL and successfully predicts the loads generated on the Tern platform by very high crests.

In applications of New Wave theory a reduction factor for the kinematics is used to account for directional spreading of wave energy. Spreading, see also section 2.2.3, reduces the in-line wave kinematics and decreases the loading on the structure. Data on spreading are provided in the NESS data base, and are also taken in account in the load model.

Wave spectra

The LOAD program has the option to choose between two kinds of wave spectra, i.e. the Pierson-Moskowitz and the JONSWAP spectrum. The JONSWAP spectrum is selected for the calculations as carried out in this report.

Current profile

Different types of current speed profiles can be chosen; a constant or profile with the relative depth to the power 1/7th (fig C.1). The latter profile is used in the calibration of the load model, as used in this report. Formula (C.1) gives the current speed at a vertical coordinate ζ as a function of the current speed at mean sea level, v_0, coordinate ζ and the water depth, d.

$$v(\zeta) = v_0 \cdot \left(\frac{\zeta + d}{d}\right)^{\frac{1}{7}} \qquad \text{(C.1)}$$

The current speed at mean sea level, v_0, can be calculated from the depth averaged current as given in the NESS data base.

Inertia and drag coefficients

Realistic values for the drag and inertia coefficients are used in Morison's equation, for the tubular members of space frame structures. For the drag coefficient, C_D, different values are used below and above mean sea level, 1.2 and 0.63, to account for the effect of roughening of the members due to fouling by marine life. The inertia coefficient, C_m, is set to 1.5. [14,15,16]

Calculations, i.e. numerical integration of the fluid load, are performed for a number of time steps during the passage of a wave. The program outputs the maximum loads, i.e. the maximum total horizontal force and overturning moment at the mud line, occurring during the passage of the extreme wave. Because of inertia, (for a single pile) the maximum force occurs before the maximum in surface elevation. However, in case of a drag dominated load, the maximum load on the structure will be only slightly in advance of the maximum surface elevation at the column.

Calibration of the constants in generic load models

The generic load model is an approximate analytical relationship derived via integration, over the submerged depth, of the applied environmental loads on an offshore structure. The load model is used to transform statistics of extreme surface elevation into statistics of extreme load. It should, therefore, give accurate results for the loads within the range of interest. The constants in the load model are calibrated against the results from the LOAD program, according to the following method.

Representative sea state conditions are selected from the NESS data base. For these conditions the loads are calculated numerically with the LOAD program on a single column (or a set of columns) with constant diameter submerged in a mean water depth, d. A least square method is then used to fit the constants of the generic load model. The relative difference between the load values as calculated with the generic load model and the LOAD program is typically less then a few percent.

For the generic load model for intermediate water depth, the relative differences (in shallow water) are significantly smaller (less than a percent).

Since LOAD does not include wind induced forces and reduced current speeds due to the presence of the structure, these effects are incorporated in the load model afterwards.

The load model for shallow water

In the derivation of the load model (section 2.2) in this report, only the case of waves in deep water is considered. In fact by using approximations which are based on the

assumption of the water depth to be relatively large compared to the wave height, the integrating of Morison's equation over the submerged depth is facilitated.

$$X = A_1 \cdot v^2 + A_2 \cdot v \cdot \phi \cdot a \cdot T \cdot \cos(\theta_d - \theta_v) + A_3 \cdot \phi^2 \cdot a^2 + A_4 \cdot \frac{v \cdot a^2}{T} \cdot \phi \cdot \cos(\theta_d - \theta_v) + A_5 \cdot \frac{\phi^2 \cdot a^3}{T^2} + A_6 \cdot W^2 \cdot \cos\theta_w \tag{3.5}$$

It is assumed that in intermediate water depths, i.e. where the assumptions made for deep water are no longer valid, inadequacies in the model can be corrected for simply by adjusting the constants in the load model. The differences between the results derived using the calibrated load model and the LOAD program can be further improved for shallower water conditions. In section 5 a load model is introduced with a somewhat modified functional form, i.e. some extra terms are introduced. This model (5.1) is not derived completely theoretical. It represents the model as derived for deep water conditions with some, empirical, extra terms to make it better applicable to waves in shallower water.

$$\begin{aligned} X = {} & A_1 \cdot v^2 + A_2 \cdot v \cdot \phi \cdot a \cdot T \cdot \cos(\theta_d - \theta_v) + A_3 \cdot \phi^2 \cdot a^2 \\ & + A_4 \cdot \frac{v \cdot a^2}{T} \cdot \phi \cdot \cos(\theta_d - \theta_v) + A_5 \cdot \frac{\phi^2 \cdot a^3}{T^2} + A_6 \cdot v \cdot \phi \cdot a \cdot T^2 \cdot \cos(\theta_d - \theta_v) \\ & + A_7 \cdot \phi^2 \cdot a^2 \cdot T + A_8 \cdot v \cdot a^2 \cdot \phi \cdot \cos(\theta_d - \theta_v) + A_9 \cdot \frac{\phi^2 \cdot a^3}{T} \\ & + A_{10} \cdot W^2 \cdot \cos\theta_w \end{aligned} \tag{5.1}$$

the terms with constants A_6 to A_9 arise from a linearisation of the terms including wave influences, according to a Taylor series. In the calculations in this report, this model has been applied. The modified load model is known to give good results, as will be shown later. In fact the results are of such high quality that at KSEPL the idea exists that it might be possible to derive a similar model for shallow water conditions theoretically. This is the subject of investigation at KSEPL.

The distinction between water depth regimes is normally made based on the ratio of wave length to water depth. The dispersion relation (C.2) is valid in any arbitrary water depth.

$$\omega^2 = g \cdot k \cdot \tanh(k \cdot d) \tag{C.2}$$

in which ω, g, d, represent the angular wave frequency, the gravitational acceleration and the water depth. The wave number, k, is defined as:

$$k = \frac{2 \cdot \pi}{L} \tag{2.6}$$

in which L represents the wave length. Considering $k \cdot d$ to be either large (i.e. greater than 3) or small (i.e. smaller than 1/3) the $\tanh(k \cdot d)$, in the dispersion relation, can be approximated by respectively 1 and $k \cdot d$. Therefore the following distinctions are made in the water depth, d, to wave length, L, ratio;

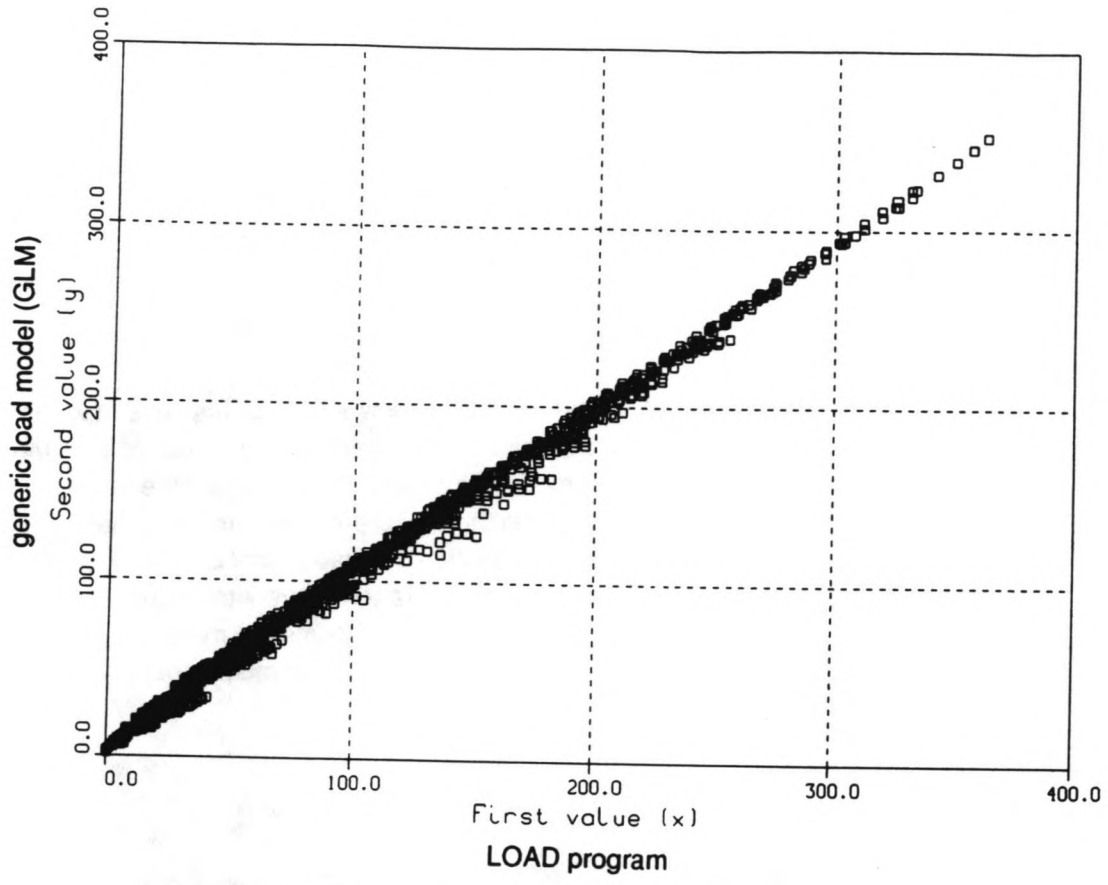

Fig. C.2; Results for total horizontal force from the LOAD program versus the results of the GLM as derived for deep water conditions.

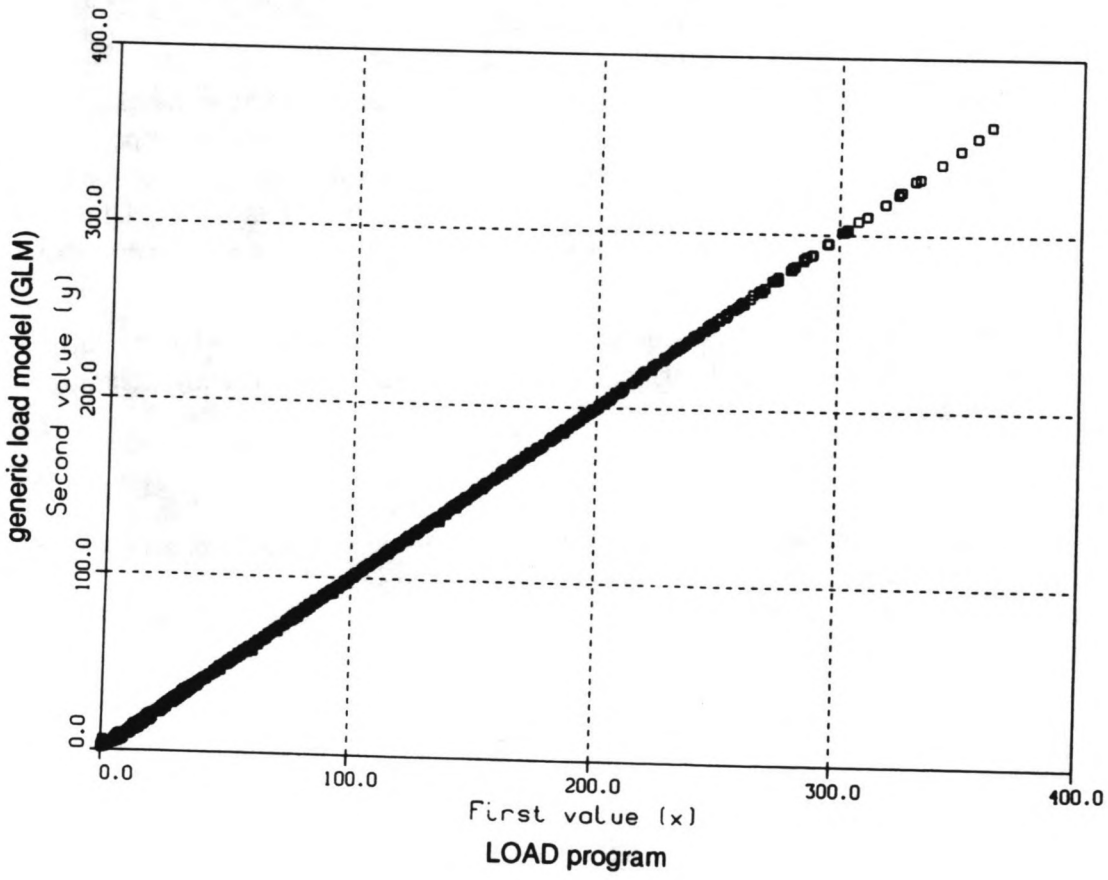

Fig. C.3; Results for total horizontal force from the LOAD program versus the results of the GLM for intermediate water depth.

$\frac{d}{L} < \frac{1}{20}$;shallow water wave

$\frac{1}{20} < \frac{d}{L} < \frac{1}{2}$;intermediate water depth wave

$\frac{d}{L} > \frac{1}{2}$;deep water wave

INDE-K stands in approximately 30 metres of water, considering the wave lengths associated with the extreme waves of about 100 metres, this in the region of intermediate water depth. Comparing the two load models, i.e. the one with the extra terms against the one without showed that the load model including the extra terms gives the best results. The two load models are compared by means of scatter plots of the results for representative sets of environmental conditions obtained by calculating total horizontal force using both the models against the results derived using the LOAD program. If the load model gives exactly the same results as the load program, against which its constant are calibrated, the points in the scatter plot for all the sets of environmental conditions should lie on one straight line, with a slope of 1.

The generic load models are first calibrated against loads derived by using a series of sea state parameters (i.e. significant wave height, (peak) period, current speed , etc.), next the results of the load models with their derived constants are plotted for each set of environmental parameters against the results from the LOAD program in the same conditions, i.e. on the horizontal axis the results from the LOAD program are given and on the vertical axis those from the load model. Figure C.2 shows the results for the load model without the extra terms and figure C.3 for the load model including the extra terms. The plots are made using about 1,000 sets of sea state conditions. Although the results for the normal load model are quite good, the results using the modified model are much better. The differences between the results of the load program and the load model are for the latter smaller, i.e. all the points fall almost exactly on the same straight line with a slope 1.

APPENDIX D

Poisson distribution

In this report:

$Q(f)$ = probability of exceeding f.

$P(f)$ =1-$Q(f)$ = probability of non-exceeding f.

Probability of n exceedances in N independent, random samples can be expressed as a binomial distribution:

$$\Pr(\underline{n} = n) = \binom{N}{n} \cdot (Q(f))^n \cdot (1 - Q(f))^{N-n} \tag{D.1}$$

If $\begin{cases} Q(f) \to 0 \\ N \to \infty \end{cases} \wedge \; N \cdot Q(f) = \text{constant} = \mu$, a binomial distribution can be approximated by a Poisson distribution.

$$\Rightarrow \Pr(\underline{n} = n) = \frac{\mu^n}{n!} \cdot e^{(-\mu)} \quad , n = 0,1,2,3..... \tag{D.2}$$

in which μ represents the expected number of exceedances,

$$\mu = E\{\underline{n}\} = N \cdot Q(f) \tag{D.3}$$

Probability of non-exceeding is then:

$$\Pr(\underline{n} = 0) = e^{-\mu} \tag{D.4}$$

The T year return value of X, X_T, can be defined as the most probable maximum value of X from the T year distribution. This almost exactly equals the value of X corresponding to a probability of non-exceeding of e^{-1}. This value of X will be exceeded on the average once in T years.

When the arrival rate, the return period T and probability distribution of extremes in a random storm are known, the T-year return value can be derived from the random storm distribution.

$$P(X|\nu \cdot T) = \left[P(X|r.s.)\right]^{\nu \cdot T} \tag{2.16}$$

The distribution of 2.16 can be approximated by a Poisson distribution. When $Q(X|r.s.)$ represents the probability of exceeding a value of X in a random storm and ν the arrival rate of the storms, the expected number of exceedances in T years is $\nu \cdot T \cdot Q(X|r.s.)$. In which case the probability distribution 2.6 can be written as:

$$P(X|\nu \cdot T) = e^{-\nu \cdot T \cdot Q(X|r.s.)} \tag{D.5}$$

The T-year return value of X, X_T, can then be determined from:

$$-\nu \cdot T : Q\left(X_T \middle| r.s.\right) = -1 \tag{D.6}$$

$$\Rightarrow \ \nu \cdot T \cdot \left(1 - P\left(X_T \middle| r.s.\right)\right) = 1 \tag{D.7}$$

$$\Rightarrow \ P\left(X_T \middle| r.s.\right) = 1 - \frac{1}{\nu \cdot T} \tag{D.8}$$

in which $P\left(X_T \middle| r.s.\right)$ represent the probability of the T-year return value of X given the probability distribution of X in a random storm (see fig. 2.5).

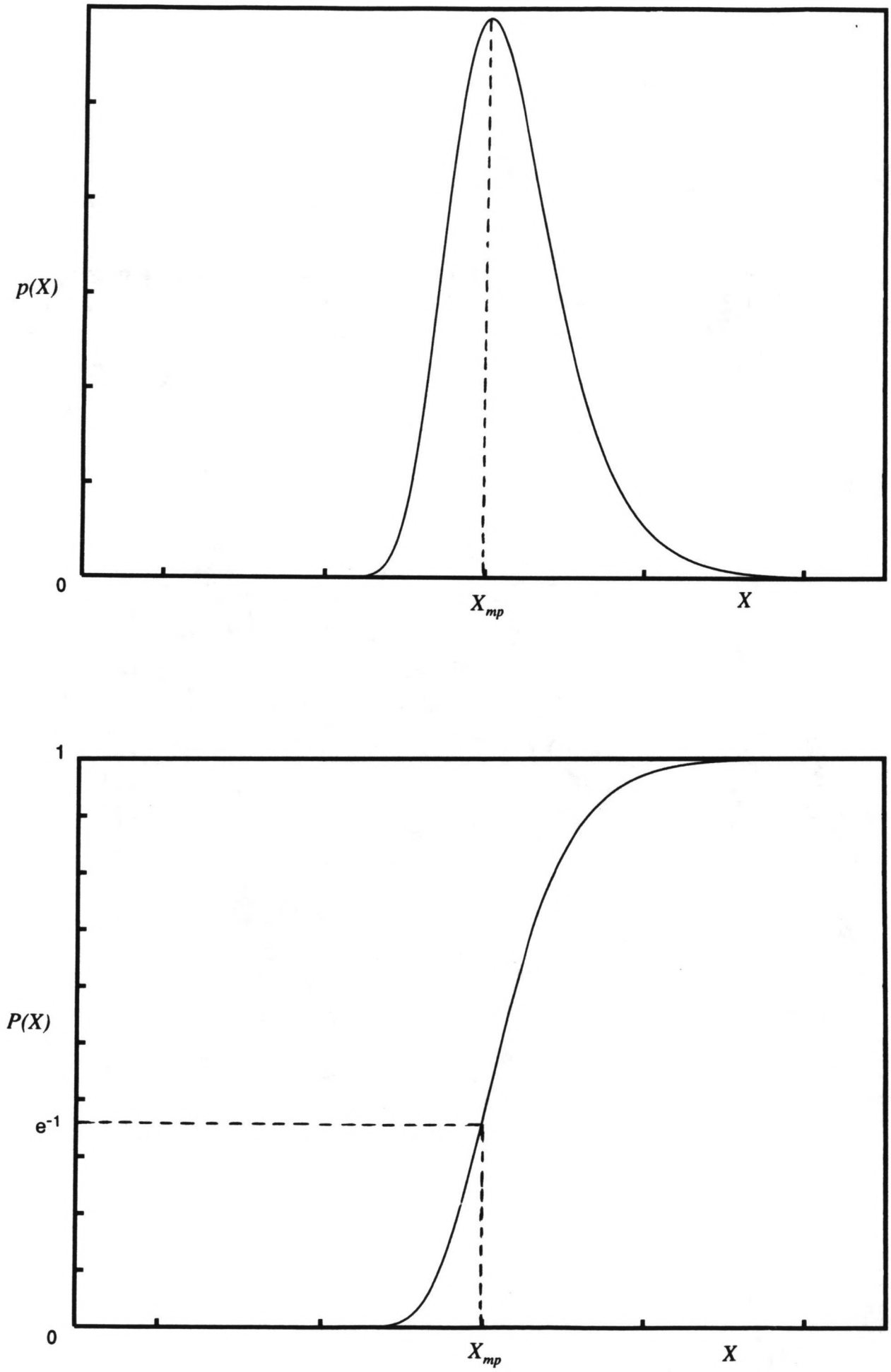

Fig E-1; The probability density function, $p(X)$, and the probabilty distribution function, $P(X)$, of X.

APPENDIX E

Short and long time scale probability distributions

Short time scale probability distribution

In the procedure as described in this report the short time scale statistics represent the statistics within storms. The variable of interest is X. The probability distribution functions of X in all the storms are re-scaled (normalised) by dividing the X values in a storm by the most probable maximum value, X_{mp}, in that particular storm. The value of X_{mp} represents here the value of X associated with the top of the probability density (or the point of inflection in the probability distribution) function (fig. E.1). The most probable extreme value of X can be calculated as the value of X which has a probability of not being exceeded of e^{-1} (≈0.37) [2]. After scaling, the probability distribution functions for different storms appear to fall on one curve. This reflects the storm similarity. A "model curve" is fitted to the scaled probability distribution functions of X. This "model curve" can be represented by a Fisher Tippett FT-1 distribution function [4], which is a double exponential function:

$$F(x) = e^{-e^{\left(\frac{x-a}{b}\right)}} \tag{E.1}$$

The functional form of the fitted curve derived for wave height can be written as:

$$P\left(H|H_{mp}\right) = e^{-e^{\left(\beta\left(1-\left(\frac{H}{H_{mp}}\right)^2\right)\right)}} \tag{E.2}$$

in which β:

$$\beta = \ln N \tag{E.3}$$

is a parameter describing the time scale of the storm. N represents the number of samples used, essentially the number of waves in the storm interval. Let T_s represent the duration of the storm period, typically around 10 hours, and T_z the zero-up crossing period, typically 10 or 11 seconds. The value of β is given as the natural logarithm of the ratio of T_s and T_z, N. Typical values of N and β are:

$$N = \frac{T_s}{T_z} \approx 3{,}000 \Rightarrow \beta = \ln N \approx 8 \tag{E.4}$$

When N is rather large, the exact value of N will hardly influence the value of ln(N). Thus, when somewhat different values for T_s and T_z are used the value of β will not change significantly. Therefore assuming a value for β of 8 gives a good estimation for the fitted curve.

Since the global loads are assumed to be dominated by the drag force, and thus be proportional to the wave height squared, the probability distribution function for a global load can be represented by;

$$P\left(X|X_{mp}\right) = e^{-e^{\left(\beta\left(1-\left(\frac{X}{X_{mp}}\right)\right)\right)}} \tag{2.17}$$

Again the value of β is assumed to be 8, which is known to give a good fit. The short term (i.e. short time scale) variability can now be represented for all storms by a similar probability distribution function, $P(X \mid X_{mp})$, being conditional on the X_{mp} in a storm.

The long time scale distribution of X_{mp}

The probability density function of the X_{mp} values, $p(X_{mp})$, represents the long time scale statistics. The probability density function, $p(X_{mp})$, is necessary in extrapolating the extreme values beyond the 25 year of hindcasting. Assumptions are made on the behaviour of the upper tail of the distribution function, $P(X_{mp})$, where $P(X_{mp})$ approaches the value one, to be able to predict the behaviour of $P(X_{mp})$ beyond the 25 year of hindcasting. A semi-parametric method [9] is used. This method uses an optimum number of the largest samples, determined by minimising the mean square error of the estimate of the index of variation, γ, between a fitted curve and the data points derived for the variable of interest from the data base. The optimum, i.e. the number of storms used in the fitting, can be used to derive an arrival rate, ν, associated with this fitting, as the number of storms used in the fitting divided by the length of the hindcasting period. Since only an optimum number of the largest samples are used in the fitting, the fitted curve should only be used for values larger than the lowest sample used in the fitting, X_0. A semi-parametric method is used to estimate the (fitting) parameters in a probability distribution function with the following functional form:

$$P(X_{mp}) = 1 - \left(1 + \xi \cdot (X_{mp} - X_0)\right)^{-\frac{1}{\gamma}} \qquad \text{(E.5)}$$

in which ξ and γ represent fitting parameters and X_0 the lowest value for the variable of interest (e.g. total horizontal force) used in the fitting procedure.

The associated probability density function is the first derivative of this probability distribution function:

$$p(X_{mp}) = \frac{\xi}{\gamma} \cdot \left(1 + \xi \cdot (X_{mp} - X_0)\right)^{-\frac{1}{\gamma}-1} \qquad \text{(2.18)}$$

APPENDIX F

Structural reliability analysis

The reference load set

Once one knows the environmental parameters (e.g. wave height and current speed) at the (future) location of an offshore structure, as derived from the MDC procedure, one can calculate the hydrodynamic forces exerted by the flows of the water around the structure using Morison's equation (see section 2.1). The reference load set for use in ultimate strength computations would thus consist of the hydrodynamic forces derived for the water kinematics associated with the representative environmental conditions (e.g. corresponding to say, the 100 year level of a global load such as total horizontal force).

"New Wave" theory (as developed by Tromans et al., 1991, see appendix C) is applied to calculate the shape of the extreme wave, the particle velocities and accelerations, at KSEPL. This theory describes the extreme event occurring when dispersed wave energy focuses in space and time such that component wavelets come into phase. It is this process which generates the extreme waves in a real storm sea.

The forces include the non-linearities of wave crests as well as different roughness of the members below and above mean sea level due to marine fouling and current blockage of the structure (see section 2). The force due to wind, which is usually minor in comparison to that of the wave and current, can easily be added to the top of the load set at the location of the topside.

The ultimate strength of structures under extreme loads

An assessment of how safe an offshore platform really is should be based on a determination of how much load it can sustain before collapsing. In particular, it should quantify the "reserve" strength of the structure beyond its design load, up to the point where it totally collapses. The standard procedure by which this ultimate strength is investigated is known as a static pushover analysis. Such an analysis essentially tests a structure's capability of resisting the forces exerted on it due to the passage of one extremely large wave and its associated current, together with the smaller force contribution of the wind that would occur simultaneously. In most instances a pushover analysis will not consider the effect of such loading on the structure's foundation, since the foundations of fixed structures tend to be stronger than their supporting members.

The procedure involves multiplying a reference load set by a load factor that is increased stepwise, starting at zero. Each time the load factor is incremented the static, or equilibrium, global deflection is calculated using a computer programs. At KSEPL the computer program USFOS is used for this purpose. USFOS is an abbreviation of Ultimate Strength For Offshore Structures and is a non-linear finite element computer program developed in a Norway based (at the SINTEF Group, a large Norwegian research institute) joint industry project. The deflections of the structure increase with an increasing load factor, at first linearly, but then non-linearly. The transition from linear to non-linear behaviour marks a member's transition from

the elastic regime (in which deformations are reversible) to the plastic (in which deformations become increasingly irreversible). The computer program takes in account how permanently deformed members can still contribute to the total strength of the structure and the ability of the structure to redistribute loads after first member failure.

Eventually, when several supporting members have undergone plastic deformations the structure will start to collapse progressively. The load factor at the point where the structure's deflections start to increase without any further increase in the applied load characterises the ultimate strength of the structure.

If the pushover analysis is repeated for several wave attack directions, one can plot the ultimate strength load factors and their respective directions as vectors based at the origin of a coordinate system centred on a plan view of the structure. Drawing a line through the vector tips for all the directions outlines a surface, the failure surface, that reveals the ultimate strength of the structure in all loading directions.

A pushover analysis considers the effect of only one large wave at a time. But several large waves are generated by a storm, and so each does not exist in isolation. It might well be possible that a series of large waves will cause damage to the structure cumulatively, leading to a decrease of its overall strength relative to the results derived via a pushover analysis. Based on the loading sequences developed by KSEPL, studies on cyclic loading were undertaken. These led to the conclusion that structures capable of surviving the passage of one wave of exceedingly rare height in an extreme storm are very likely to survive all the waves encountered in that storm.

Despite this, it is suggested at KSEPL that further work is needed to generalise the above mentioned methods and conclusions, e.g. including the effects of the inertia of the structural members at or near the point failure. At present a quasi-static analysis, as discussed in this appendix, is believed to be sufficient to test a structure's integrity.

Uncertainty in resistance

The failure surface is the result of a deterministic analysis in which parameters, such as the yield strength of the steel, are taken at their nominal value. Such an analysis does therefore not explicitly allow the parameter values to vary according a statistical distribution. To account for this kind of variability at the structural component level, one can assume, for instance, a normal distribution in the material (i.e. steel tubes) properties of the members participating in the failure mechanism that leads to the structure's ultimate collapse. For structural members in offshore design, even when buckling, the yield strength of the steel is the main source of variability in the strength of the member. As examples of other influences one can think of the effects on buckling of forces not acting along the centre line of the members, i.e. eccentric loading. Lateral loading on members will also influence the resistance of the members against buckling. However, in the push-over analysis the nominal value for yield strength is normally used. This is effectively a lower bound on the true yield strength. The materials used in offshore structures are closely monitored from the first production at the mill to the final application in the fabrication of the structure. Material that does not fulfil the required specifications (e.g. strength) is generally

rejected in routine tests during the fabrication of the structure. One can, therefore, sensible truncate the "below average" tail end of a normal distribution.

If the behaviour of only one supporting member is determining whether or not a structure collapses, then the uncertainty in the entire structure's strength is obviously the same as that of the critical member. Failure modes, however, usually involve several members. As a consequence, the uncertainty in the ultimate strength of a structure can be assumed to be less than that of the participating members, since the weakness of some members is generally compensated for by the strength of others, confining the strength of the complete structure closer about an average value.

The distribution of an entire structure's strength can be obtained by performing (several) thousands of collapse simulations, arbitrarily assigning parameter values to the individual structural members. The results of these simulations can then be compiled into a probability density function of ultimate strength. Such probability density functions commonly will have narrow peaks and stunted tail ends (especially on the left side), suggesting that the influence of structural uncertainty is of minor importance compared with the uncertainty in environmental loading, whose probability density functions have much broader peaks and long, drawn out tails. This was investigated at KSEPL by Tromans and van de Graaf, in 1991.

Although the occurrence of multiple failure mechanisms may increase a structure's probability of failure, the most likely ones can generally be narrowed down to one or two.